

# Climate vulnerability assessment for habitat and associated fisheries in the inland waters of northern Washington State

Eric Beamer<sup>1</sup>, Courtney M. Greiner<sup>2</sup>, Julie S. Barber<sup>2</sup>, Casey P. Ruff<sup>1</sup>, and Karen Wolf<sup>1</sup>

August 2020



<sup>1</sup>Skagit River System Cooperative

<sup>2</sup>Swinomish Indian Tribal Community Fisheries Department

### **Recommended citation:**

Beamer, EM, CM Greiner, JS Barber, CP Ruff, and K Wolf. 2020. Climate vulnerability assessment for habitat and associated fisheries in the inland waters of northern Washington State. Skagit River System Cooperative, La Conner, WA. 105 pp.

### **Title page photos:**

- Top row: Skagit River estuary near Fishtown (left) and Lone Tree Lagoon on Fidalgo Island (right); examples of two shore types biologically important to fisheries resources that are also sensitive to human and climate change pressures.
- Second row: Chinook salmon juveniles (left), Dungeness crab adults (middle) & cockle clam adults (right); examples of fisheries resources dependent on healthy nearshore habitat.
- Third row: Swantown area on Whidbey Island; example of a complex shore type area where natural processes intersect with human development and where climate change pressures will further exacerbate the intersection.
- Bottom row: SneeOosh Beach on Fidalgo Island; example of an armored barrier beach after a wind wave storm event. Note the eroded rip rap pulled onto the gravelly beach face.
- Photo credits: The Skagit River Estuary aerial oblique is from <https://fortress.wa.gov/ecy/shorephotoviewer/>. All other photos are from Eric Beamer and Swinomish Fisheries.

### **Acknowledgements**

E. Beamer, C. Ruff, and K. Wolf were partially supported by an EPA Puget Sound Partnership Implementation fund PA-00J276-01. Special thanks to L. Hunter, J. Jannetta, and M. Nelson for reviewing drafts of this paper. C. Cook, S. Grossman, J. McArdle, and A. McBride also assisted with aspects of this project. Funding for C. Greiner was provided by EPA Puget Sound Tribal Capacity Program PA-00J99101 and Bureau of Indian Affairs (BIA) Rights Protection Implementation, Climate Change Program. We thank L. Loomis and the Swinomish Senate for the continued support.

# Table of contents

Table captions	5
Figure captions	6
Abbreviations	9
Executive summary	10
Chapter 1. Introduction	12
Chapter 2. Description of study area, spatial unit of analysis, and GIS layer development	17
Study area	17
Spatial unit of analysis	18
Attribute data used	20
Shore type	24
Barrier beach	26
Estuary, large river type	27
Estuary, pocket estuary type	28
Human-modified beach	29
Pocket beach	30
Rocky beach	31
Sediment source beach	32
Landscape characteristics	33
Fetch	33
Depth of adjacent marine water	34
Distance from nearest large river	34
Distance from entrance of the Strait of Juan de Fuca	34
Land use	35
Discussion	35
Size of spatial units for analysis	35
Shore type GIS arcs	35
Age of land use and shoreline armoring data	36
Chapter 3. Shore type resilience to wave energy and sea level rise	36
Methods	36
Results	38
Discussion	45
Utility of WSLRR framework	45
Limitations of current data and suggested improvements	45

Chapter 4. Nearshore surface water characteristics	46
Methods	46
GIS datasets	47
Sea surface temperature and salinity observations	47
Analytical methods	48
Data transformation	48
ANOVA models	48
Model Results	48
Mean July – August sea surface temperature ( <i>Tmean</i> )	48
Additional sea surface temperature and salinity results	53
Application of prediction results to biotic thresholds	54
Climate change scenarios for sea surface temperature	57
Vulnerability results for sea surface temperature	57
Predictions of mean sea surface temperature	59
Juvenile Chinook salmon growth under current and future sea surface temperature regimes	62
Cockle larvae survival under current and future sea surface temperature regimes	67
Postlarval and juvenile Dungeness crab survival under current and future sea surface temperature regimes	70
Discussion	74
Utility of framework	74
Oversimplified relationships between biota and environmental thresholds	74
Gaps between climate change predictions and biotic environmental thresholds	75
Accuracy and precision in model predictions	76
References	78
Appendix A. Geographic distribution of common shore types throughout the study area	84
Appendix B. Geographic distribution of landscape characteristics assessed throughout the study area	91
Appendix C. Additional temperature and salinity models	98
Maximum July – August sea surface temperature ( <i>Tmax</i> )	98
Mean salinity ( <i>Smean</i> )	98
Maximum seasonal salinity ( <i>Smax</i> )	103
Minimum seasonal salinity ( <i>Smin</i> )	104
Limitations in sea surface salinity predictions	104
Future model applications	105

## Table captions

Table 1. Environmental indicators considered to directly impact salmon and shellfish species throughout the geographic range covered in this study. Future end of century projections for each indicator are provided. Associated environmental metrics (see abbreviations) covered by the models developed in this study that may be influenced by the projected change are listed. ....	15
Table 2. Target fish and shellfish species distributed throughout the study area (see Figure 2). For each species, seasonal and life stage specific associations with dominant habitats and shore types throughout the tidal continuum are depicted. ....	21
Table 3. Summary of geomorphic, landscape, and human land use attributes quantified as data layers with generalized responses. Mechanistic models developed for this study, including sea surface temperature (SST) and salinity (TempSal) and wave and sea level rise resilience (WSLRR), are indicated in terms of their application to each attribute and generalized response combination.....	23
Table 4. The total “wet” area in hectares by dominant shore type for each of the 1,742 spatial units included in the study. ....	26
Table 5. Summary of windy months and dominant wind direction during the annual windy period for six cities within the study area. The dominant wind direction for each city was defined arbitrarily as the predominant wind direction encompassing $\geq 20\%$ of the time during windy months over the weather station’s period of record.....	34
Table 6. Assigned response scores of each shore type to wave energy. Values indicate either high (0) or low (1) resistance to wave energy.....	37
Table 7. Performance of nearshore mean sea surface temperature models. All models shown, along with the included factors and/or covariates, are significant ( $p < 0.05$ ). The presence of an ‘x, t, or u’ means that a factor or covariate was included in the model. The presence of a ‘t’ or ‘u’ denotes the covariate was natural log-transformed or untransformed, respectively. The best model has the lowest AICc value and is in bold font.....	50
Table 8. Pairwise testing of mean sea surface temperature by shore type using Tukey's Honestly-Significant-Difference Test using least squares means from the model results with a MSE of 4.446 with 161 df. Pairs with p-values $< 0.05$ are bolded. ....	51
Table 9. Summary of landscape coefficients estimated from the ANOVA model for mean sea surface temperature (Tmean) for all shore types. P-values significant at the 0.05 level are bolded. ....	51
Table 10. Generalized threshold relationships for specific physical environmental parameters for selected fish and shellfish species utilizing nearshore habitats in the study area. ND = no known data source or thresholds not well understood relative to our predictive models, SST = sea surface temperature. ....	55

## Figure captions

- Figure 1. Conceptual study framework. The framework depicts how environmental response variables considered in this study may be influenced by the synergistic effects of landscape factors and climate change. Results may be used to further refine hypotheses about species-specific risk to climate change and other anthropogenic stressors. SLR = sea level rise. .... 17
- Figure 2. Map depicting the geographic extent of the study area in inland waters of northern Washington. The thick black lines reflect the shoreline of the study area. .... 18
- Figure 3. Map of the basic spatial unit polygons in the study area..... 19
- Figure 4. Boxplot of polygon wet area (left panel) and shoreline length (right panel) by shore type for the 1,742 GSU\_ID polygons within the study. Shore type abbreviations are: BB = barrier beach; E-LR = estuary, large river type; E-PE = estuary, pocket estuary type; M = human-modified beach; PB = pocket beach; RB = rocky beach; SSB = sediment source beach..... 25
- Figure 5. Photo of Third Lagoon on San Juan Island, showing both barrier beach (seaward side) and pocket estuary (landward side) shore forms. Aerial oblique photo is from <https://fortress.wa.gov/ecy/shorephotoviewer/>. .... 26
- Figure 6. Photo of the Nooksack River tidal delta, showing three vegetated estuarine wetland zones (EEM, EFT, and FRT), unvegetated delta flats, and blind or distributary channels. Aerial oblique photo is from <https://fortress.wa.gov/ecy/shorephotoviewer/>..... 27
- Figure 7. Photo of Race Lagoon on Whidbey Island, showing both barrier beach (seaward side) and pocket estuary (landward side) shore forms. Aerial oblique photo is from <https://fortress.wa.gov/ecy/shorephotoviewer/>. .... 28
- Figure 8. Photo of Cap Sante Marina in Anacortes on Fidalgo Island. Aerial oblique photo is from <https://fortress.wa.gov/ecy/shorephotoviewer/>. .... 29
- Figure 9. Photo of pocket beach on Waldron Island (Mail Bay). Aerial oblique photo is from <https://fortress.wa.gov/ecy/shorephotoviewer/>. .... 30
- Figure 10. Photo of rocky beach on Orcas Island (within East Sound). Aerial oblique photo is from <https://fortress.wa.gov/ecy/shorephotoviewer/>. .... 31
- Figure 11. Photo of sediment source beach on Waldron Island (Little Hammond). Aerial oblique photo is from <https://fortress.wa.gov/ecy/shorephotoviewer/>..... 32
- Figure 12. Boxplots of wave and sea level rise resilience (WSLRR) predictions, percent forested habitat, percent armored, and fetch score by shore type. Shore type abbreviations are: BB = barrier beach; E-LR = estuary, large river type; E-PE = estuary, pocket estuary type; PB = pocket beach; RB = rocky beach; SSB = sediment source beach. The resilience score is a qualitative metric with a possible range between -1 and +1 where the most resilient areas have positive scores (but not >1) and the least resilient areas have negative scores (but not <-1) ..... 39
- Figure 13. Map of wave and sea level rise resilience (WSLRR) predictions for each GSU in the study area where a value of 1 indicates a highly resilient GSU..... 40
- Figure 14. Map of maximum fetch values used for the wave and sea level rise resilience predictions. Values incorporate the maximum distance (km) from four possible wind directions including northeast, east, southeast, and south (see Chapter 2 for detailed information) where a more negative value equals a high maximum fetch..... 41
- Figure 15. Map of maximum geomorphic response scores (*G*) used for the wave and sea level rise resilience predictions. Values are based on projected geomorphic resistance to wave energy where a value of zero indicates high resistance to erosion..... 42

Figure 16. Map of maximum existing human scores used for the wave and sea level rise resilience predictions. Values are based on the percentage of armored shoreline present in each GSU in the 1990s where a score of -1 indicates a high percentage of armored shoreline.....	43
Figure 17. Map of maximum future human scores values based on percent forested area used for the wave and sea level rise resilience predictions. A score of zero equates to lower percentage of forested area in the 1990s. ....	44
Figure 18. Boxplots of sea surface temperature (C°) by month and geomorphic shore type (excluding human-modified beaches). Data are from 6,872 observation collected at 173 sites across Whidbey Basin, Bellingham and Samish Bays, and the San Juan Islands. Shore type abbreviations are: BB = barrier beach; E-LR = estuary, large river type; E-PE = estuary, pocket estuary type; PB = pocket beach; RB = rocky beach; SSB = sediment source beach. Boxes show median, 25th and 75th percentiles. Whiskers show the 5th and 95th percentiles, circles are outliers. ....	49
Figure 19. Relationships between observed mean sea surface temperature and salinity and three continuous landscape variables including mean geomorphic scaling unit depth ( <i>MeanGSU_Depth</i> ), distance from the nearest large river ( <i>N_LgRivKm</i> ), and distance from the entrance to the Strait of Juan de Fuca ( <i>DistSjfKm</i> ). Lines depict smoothed linear relationships estimated separately for each shore type. ....	52
Figure 20. Boxplot showing the distribution nearshore sea surface temperature (°C) in July/August in pocket estuaries with (n = 21) or without (n = 5) direct freshwater sources. Boxes show median, 25th and 75th percentiles. Whiskers show the 5th and 95th percentiles and circles are outliers. ....	58
Figure 21. Spatial distribution of mean July/August sea surface temperature under existing conditions.....	60
Figure 22. Spatial distribution of mean July/August sea surface temperature under a future climate change scenario of a 2.2°C rise in sea surface temperature.....	61
Figure 23. Percent distribution of each shore type across the study area overlapping sea surface temperature (SST)-dependent growth categories for juvenile Chinook salmon based on mean SST in July/August under existing conditions and a future climate change scenario of a 2.2°C increase in SST. BB = barrier beach, E-LR = large river estuary, E-PE = pocket estuary, M = modified, PB = pocket beach, RB = rocky beach, SSB = sediment source beach.....	63
Figure 24. Spatial distribution of optimal growth ranges for juvenile Chinook based on mean water temperature in July/August under existing conditions. Optimal growth = 11°C – 14°C; < optimal =14.1°C – 16°C; stressful = 16.1°C – 20°C; negative growth is ≥ 20.1°C. ....	64
Figure 25. Mean density of marked (hatchery origin) and unmarked (natural origin) juvenile Chinook salmon by habitat type and month in the Skagit River estuary and Skagit Bay (Figure 2.1 from Beamer et al. 2005). ....	65
Figure 26. Spatial distribution of optimal growth ranges for juvenile Chinook based on mean water temperature in July/August under a climate change scenario where sea surface temperatures rise by 2.2°C. Optimal growth = 11°C – 14°C; < optimal =14.1°C – 16°C; stressful = 16.1°C – 20°C; negative growth is ≥ 20.1°C. ....	66
Figure 27. Spatial distribution of larval basket cockle, <i>Clinocardium nuttallii</i> , survival potential based on mean water temperature July/August under existing conditions. Optimal survival = 10-22°C; < optimal = 23-25°C.....	68
Figure 28. Spatial distribution of larval basket cockle, <i>Clinocardium nuttallii</i> , survival potential based on mean water temperature in July/August under a climate change scenario where sea surface temperatures rise by 2.2°C. Optimal survival = 10-22°C; < optimal = 23-25°C. ....	69

Figure 29. Percent distribution of each shore type across the study area and megalopae and juvenile Dungeness crab survival potential in July/August under existing sea surface temperature conditions and future climate change scenario of a 2.2°C increase in sea surface temperature. BB = barrier beach, E-LR = large river estuary, E-PE = pocket estuary, M = modified, PB = pocket beach, RB = rocky beach, SSB = sediment source beach.....	71
Figure 30. Spatial distribution of postlarval and juvenile Dungeness crab survival potential in July/August under existing conditions. Optimal survival = 10-14°C; < optimal = 15-21°C; extremely stressful = > 22°C. ....	72
Figure 31. Spatial distribution of postlarval and juvenile Dungeness crab survival potential in July/August under a climate change scenario where sea surface temperatures rise by 2.2°C. Optimal survival = 10-14°C; < optimal = 15-21°C; extremely stressful = > 22°C.....	73
Figure 32. Relationship between observed and predicted mean sea surface temperature for 169 nearshore surface water sites located throughout the Whidbey Basin, Bellingham and Samish Bays, and the San Juan Islands. ....	77

## Abbreviations

- BB = barrier beach
- DAU = delta accounting unit, from PSNERP
- DistSjfKm = distance to the entrance of the Strait of Juan de Fuca, in kilometers
- DU = delta unit, from PSNERP
- EH = existing human score
- E-LR = large river estuary
- E-PE = pocket estuary
- FW = freshwater
- GSU\_ID = geomorphic scaling unit, data field used for the unique ID of spatial units within the study, from PSNERP
- IPCC = Intergovernmental Panel on Climate Change
- M = human-modified
- MeanGSU\_Depth = mean water depth adjacent to the nearshore, in meters
- N\_LgRivKm = distance to the source of the nearest large river, in kilometers
- PB = pocket beach
- PH = predicted human score
- PSNERP = Puget Sound Nearshore Ecosystem Restoration Project
- RB = rocky beach
- RCP = representative concentration pathway
- SLR= sea level rise
- Smax = maximum annual salinity
- Smean = mean annual salinity
- Smin = minimum annual salinity
- SPU = shoreline process unit, from PSNERP
- SSB = sediment source beach
- SST = sea surface temperature
- TempSal = temperature and salinity model
- Tmax = maximum water temperature value during July and August
- Tmean = mean water temperature during July and August
- WSLRR = wave and sea level rise resilience score
- ZU = zone units, from PSNERP

## Executive summary

For the marine inland waters of northern Washington, the spatial extent of habitats of fish and shellfish has been reduced extensively over the last century by human land use actions such as shoreline armoring, pollution, agricultural practices, and urbanization. In addition to human impacts, ongoing and long-term climate change is thought to influence the suitability of marine habitats to support productive populations of fish and shellfish species. To better understand future habitat availability within the study area, we developed a framework to evaluate the vulnerability of certain fish and shellfish species and their associated habitats to future environmental change. Species included in the framework were selected for their cultural and commercial importance to the Swinomish Indian Tribal Community and other residents of the greater Puget Sound area. This framework paired spatially explicit measurements of landscape features (e.g., shore type) with environmental response metrics including erosion and sea surface temperature (SST). These landscape and environmental data were then combined with known physiological thresholds of the target fish and shellfish species to estimate environmental conditions experienced by individual species during specific life stages.

Specifically, we developed a qualitative tool for assessing habitat risk to wave energy and sea level rise (the “wave and sea level rise resilience” model). We then created predictive models for SST using landscape features and 6,672 *in situ* observations collected within the study area and applied these models to predict current SST (the “water temperature model”) conditions throughout the study area. Landscape-scale model predictions of SST under current conditions were compared with literature-based estimates of thermal tolerance for juvenile Chinook salmon (*Oncorhynchus tshawytscha*), cockle clam larvae (*Clinocardium nuttallii*), and postlarval and juvenile Dungeness crab (*Metacarcinus magister*) to estimate the percentage of habitat providing favorable metabolic conditions for each species under those current conditions. Finally, we assessed how habitat availability for the three species may change under future climate change by applying a 2.2°C increase in SST across the study area based on projections generated at the scale of the North Pacific Ocean.

The study area for this project encompasses inland waters throughout northern Washington including the majority of Whidbey Basin and Admiralty Inlet, the northern inland waters of Bellingham and Samish Bay, the eastern section of the Strait of Juan de Fuca, the southern section of the Strait of Georgia, and the San Juan Islands. We used the regionally accepted Puget Sound Nearshore Ecosystem Restoration Project Shoreline Process Units as the basic spatial unit for analysis. We associated shore type and landscape characteristics to each of the 1,742 spatial units within the study area. Shore types included barrier beaches, estuaries (large river estuaries and pocket estuaries), human-modified beaches, pocket beaches, rocky beaches, and sediment source beaches. Landscape characteristics were fetch, depth of adjacent marine water, distance from the nearest large river, and distance from entrance of the Strait of Juan de Fuca.

Wave and sea level rise resilience (WSLRR) model: We estimated considerable differences in resilience to wave energy and sea level rise across each shore type. These results were likely driven by spatial variability in fetch, geomorphic, and existing shoreline armored scores. In general, we found that large river estuaries and human-modified shore types were projected to be the least resilient to wave energy and sea level rise while barrier beaches, sediment source beaches, and rocky beaches were projected to be the most resilient.

Water temperature model: Our estimates of mean nearshore SST during the summer under current conditions ranged from 10.9 to 23.2°C throughout the study area with the coldest areas on the west side of San Juan Island and the warmest areas within isolated parts of large river estuaries and pocket estuaries. Categorically applying a 2.2°C increase in North Pacific Ocean SST to the study area resulted in mean summer nearshore SSTs ranging from 13.1 to 25.4°C. Using these SST data, we estimated the percent of habitat providing favorable conditions for three target species under current conditions and under a climate change scenario.

Juvenile Chinook salmon: Based on known thresholds for juvenile Chinook salmon growth, current conditions in most nearshore habitats within the study area provide optimal growth conditions, especially pocket and rocky beach shore types located farther from rivers. However, by July and August, SSTs within all the large river and pocket estuarine habitats exceed those that would be considered metabolically favorable for juvenile Chinook salmon, potentially explaining why juvenile Chinook leave estuaries for more marine waters at this time of year. Under a moderate climate change scenario (2.2°C increase in SST), we predicted a reduction in the average percent of optimal habitat across shore types from 16.5% to 0.3%. As the window for optimal growth potential in critical rearing habitats, such as estuaries, is constrained under future climate change, juvenile Chinook salmon may be forced to move prematurely to more favorable SSTs in nearshore habitats at the expense of increased predation risk.

Cockle larvae: Under current conditions, we predicted that habitat across all shore types within the study area has SSTs that are optimal for cockle larvae growth and survival with the exception of a small percentage of pocket estuaries that exceed 22°C. Under the climate change scenario of a 2.2°C increase in SST, we predicted all shore type habitat within the study area to remain within the optimal SST range except pocket estuaries where the percent under suboptimal conditions increased to 45%. Major data gaps including larval distribution within the study area need to be addressed before conclusions on future habitat conditions for cockle larvae should be drawn. Our modeling work on cockle larvae illustrates the importance of having a strong understanding of species life history traits and habitat requirements in order to provide robust results.

Dungeness crab postlarvae and juveniles: Most nearshore habitats currently preferred by early life stages of crab within the study area (sediment source beaches, barrier beaches, and estuaries) have SSTs that are less than optimal for postlarval and juvenile survival by July/August. Exceptions to this pattern are the pocket and rocky beach shore types (particularly those located further from rivers) which still provide optimal growth conditions for early life stages of Dungeness crab. Under a 2.2°C rise in SST, we predicted virtually all shore type habitats within the study area would have suboptimal temperatures for crab postlarvae and juveniles. The predicted spatial shift in optimal thermal habitats supporting postlarval and juvenile crab growth under climate change may not only result in reduced cohort survival due to thermal tolerance mismatch but may result in density dependent processes, such as increased cannibalism. Importantly, if the presumed Puget Sound postlarval/juvenile cohort is identified as a genetically-distinct population, this cohort is likely to be exposed to higher late summer SSTs during the critical time period

of larval settlement to the benthos. Differential impacts to cohorts could affect how this fishery needs to be managed in the future.

Our study is intended to provide an initial template for identifying and prioritizing work to better inform efforts focused on maximizing the viability of critical habitats and associated species under future environmental conditions impacted by climate change. This framework will be particularly helpful when we have a comprehensive understanding of species phenology (e.g., timing of specific life stages and habitat associations), habitat dependence, and physiological thresholds. Conversely, where significant data gaps remain for individual species, as is the case for many shellfish species, our framework can be used to identify future monitoring efforts or studies necessary to fill knowledge gaps.

The WSLRR model framework provides a tool to assess resilience of estuarine and nearshore habitats to erosional losses due to climate change. Although coarse in nature, this analysis illustrates how a landscape scale assessment of habitat characteristics can be combined with subjective information to provide a spatially-explicit projection of risk to habitats throughout the study area. This information can be used to inform prioritization of habitat protection measures while considering future climate change predictions.

Our water temperature model does not provide exhaustive fish and shellfish nearshore habitat vulnerability predictions, rather, the model presents a framework with which to conduct such analyses as part of an ongoing program. Here, we demonstrate how this model can be used to predict the vulnerability of target species under current SST regimes and a future climate change scenario. We proved that observations of nearshore SST with landscape and shore type data can predict spatially explicit means and extremes of nearshore SST. We also demonstrated how current and future climate change patterns of mean summer nearshore SST could affect juvenile Chinook salmon, cockle larvae, and postlarval and juvenile Dungeness crab. Specifically, we predicted that increases in SST are likely to expand areas with suboptimal rearing conditions for postlarval and juvenile Dungeness crab and juvenile Chinook salmon but not cockle larvae. However, these results should be interpreted with some caution due to several factors including: 1) oversimplified relationships between biota and environmental thresholds, 2) gaps between climate change predictions and biotic environmental thresholds, 3) lack of inclusion of adaptive responses by biota to compensate for environmental stress, and 4) accuracy and precision in model predictions due to the scale of shore type units and outdated land use and shoreline armoring data. Overall, this simplistic approach is a good starting point that elucidates deficiencies where new knowledge could fill gaps and thus improve analyses and resource management decisions. Model results can be utilized in conjunction with other prioritization tools to maximize the effectiveness of restoration and adaptation efforts aimed to promote species viability under changing ocean conditions.

## **Chapter 1. Introduction**

Over contemporary time scales, climate change is affecting the suitability of marine habitats to support productive populations of fish and shellfish species (Free et al. 2019). For example, as ocean temperatures have warmed considerably over the last century due to climate change (IPCC 2013), populations have declined for many marine fish species already experiencing water

temperatures at the warm end of their thermal tolerance range. Reduction in habitat suitability due to environmental conditions exceeding species' physiological constraints may lead to significant declines in viability, loss of those species that are unable to acclimate, and/or a northward shift in the overall range of a species (Deutsch et al. 2015, Molinos et al. 2015).

For urbanized marine inland waters such as Washington State's southern Salish Sea, the spatial extent of preferred habitats of culturally and commercially important fish and shellfish has been reduced extensively over the last century by human land use actions such as shoreline armoring, pollution, agricultural practices, and urbanization. Biotic and abiotic factors important to the stability of the marine ecosystem of these inland waters are projected to undergo significant changes between now and the end of the century (Table 1, Roop et al. 2020). The combined effects of habitat loss, ongoing threats due to urbanization and environmental change, and continued fisheries exploitation may further compromise the future resilience of individual species to climate change (Scavia et al. 2002, Doney et al. 2012). Therefore, a better understanding of habitat requirements of fish and shellfish species under current environmental conditions is required to develop more accurate projections of species-specific vulnerability to climate change. In turn, these projections may help inform necessary policy actions such as habitat protection strategies or fisheries management actions that are robust to climate change and can be implemented to increase the future viability of fish and shellfish species (e.g., Gaines et al. 2018).

Here we developed a framework to evaluate the vulnerability of certain fish and shellfish species and their associated habitats to future environmental change (Figure 1). Species included in the framework were selected for their cultural and commercial importance to the Swinomish Indian Tribal Community (SITC) and other residents of the greater Puget Sound area. This framework paired spatially explicit measurements of landscape features (e.g., habitat type) with environmental response metrics including erosion, sea surface temperature (SST), and salinity. These landscape and environmental data were then combined with known spatial distributions of the target fish and shellfish species to estimate environmental conditions experienced by individual species during specific life stages. Using these data, we first developed a qualitative tool for assessing habitat risk to wave energy and sea level rise. We then developed predictive models for SST and salinity using landscape features and applied these models to predict current SST and salinity conditions encountered by target fish and shellfish species throughout the study area. Landscape-scale model predictions of SST under current conditions were compared with literature-based estimates of thermal tolerance for each species to estimate the percentage of habitat providing favorable metabolic conditions for each species under current conditions. Finally, we assessed how habitat availability for each species may change under future climate change by applying a 2.2°C increase in SST across the study area based on climate change projections generated at the scale of the North Pacific Ocean (RCP 4.5 prediction; IPCC 2014). To illustrate the utility of this framework in assessing species-specific vulnerability to climate change we focused on juvenile Chinook salmon (*Oncorhynchus tshawytscha*), larval cockle clams (*Clinocardium nuttallii*), and postlarval and juvenile Dungeness crab (*Metacarcinus magister*<sup>1</sup>).

This study is intended to provide an initial template for identifying future work that can be used to better inform restoration and management actions. These actions should focus on maximizing the

---

<sup>1</sup> We recognize that the current scientific name for Dungeness crab is disputed. We have opted to utilize the accepted name, *Metacarcinus magister*, from the World Register of Marine Species (WoRMS) taxonomic database.

viability of critical habitats and associated species under future environmental conditions due to climate change. Our framework can be used to prioritize important habitat or fisheries management actions to augment species viability, particularly when we have a robust understanding of species phenology (e.g., timing of specific life stages and habitat associations), habitat dependence, and physiological thresholds. Conversely, where significant data gaps remain for individual species, our framework can be used to identify future monitoring efforts or studies necessary to fill these data gaps.

Table 1. Environmental indicators considered to directly impact salmon and shellfish species throughout the geographic range covered in this study. Future end of century projections for each indicator are provided. Associated environmental metrics (see abbreviations) covered by the models developed in this study that may be influenced by the projected change are listed.

Anthropogenic driver	Environmental parameter	General effect	Regional prediction (by end of century, based on RCP 4.5*)	Metric	Model
	Sea surface temperature	Increase of global mean sea surface temperature	+1.1°C to 2.6°C (IPCC 2014); mean. no. days above freezing +41.6 days (Abatzoglou & Brown 2012)	Tmean, Tmax	TempSal
	Sea level rise	Increase in intensity and frequency of winter storm events/surges	50% likelihood sea level will increase 0.52 m (Miller et al. 2018)	Fetch	WSLRR
		Increased/accelerated erosion, beach loss with sea level rise, storm events			No model
Climate change	Precipitation	Increase in winter precipitation	Total precipitation Jan-Dec +96.0 mm; Oct-March +118.9 mm (Abatzoglou & Brown 2012)	Smean, Smax, Smin	TempSal
		Decrease in summer precipitation	Total precipitation April-Sept -24.6 mm (Abatzoglou & Brown 2012)	Smean, Smax, Smin	TempSal
	Snowpack	Decrease in snow-water equivalent, snowpack/ glacial mass	Amount of water contained in snowpack 1 April and 1 May -249.0 mm and -270 mm respectively (Mote et al. 2014)	Tmean, Tmax	TempSal
		Upper elevation transition from snow-dominant to rain-dominant		Tmean, Tmax	TempSal
	Streamflow	Higher winter flows due to increased rainfall	Jan-Dec max daily flow on Skagit, north fork of Stillaguamish, and Snohomish rivers increase 2%, 72%, and 55% respectively (Mote et al. 2014)	Tmean, Tmax; Smean, Smax, Smin	TempSal
		Lower summer flows due to reduced snowpack	July-Sept min daily flow on Skagit, north fork of Stillaguamish, and Snohomish rivers decrease 34%, 28%, and 41% respectively (Mote et al. 2014)	Tmean, Tmax; Smean, Smax, Smin	TempSal
		pH	Global increase in ocean acidification	pH decrease additional 0.14-0.15 pH units (IPCC 2014)	Insufficient data

Table 1 continued

<b>Anthropogenic driver</b>	<b>Environmental parameter</b>	<b>General effect</b>	<b>Regional prediction (by end of century, based on RCP 4.5*)</b>	<b>Metric</b>	<b>Model</b>
Climate change/ Socioeconomic development	Dissolved oxygen	Decrease in O <sub>2</sub> levels due to reduced O <sub>2</sub> solubility as SST rises (Gruber 2011)	It is very likely that the dissolved oxygen content of the ocean will decrease by a few percent during the 21st century in response to surface warming (IPCC 2014)	Insufficient data	No model
		Decrease in O <sub>2</sub> levels due to eutrophication caused by increasing nutrient levels from run-off (Gruber 2011)		Insufficient data	No model
Socioeconomic development	No. of people and coastal infrastructure	Increase in coastward migration, industrialization, and urbanization	Exacerbate coastal squeeze, impair shoreline processes, and reduce capacity to adapt (Mauger et al. 2015)	EH, PH	WSLRR

\*Representative concentration pathway of radiative forcing stabilized without overshoot pathway to 4.5 W/m<sup>2</sup> (~650ppm CO<sub>2</sub> eq) at stabilization after 2100 (van Vuuren et al. 2011).

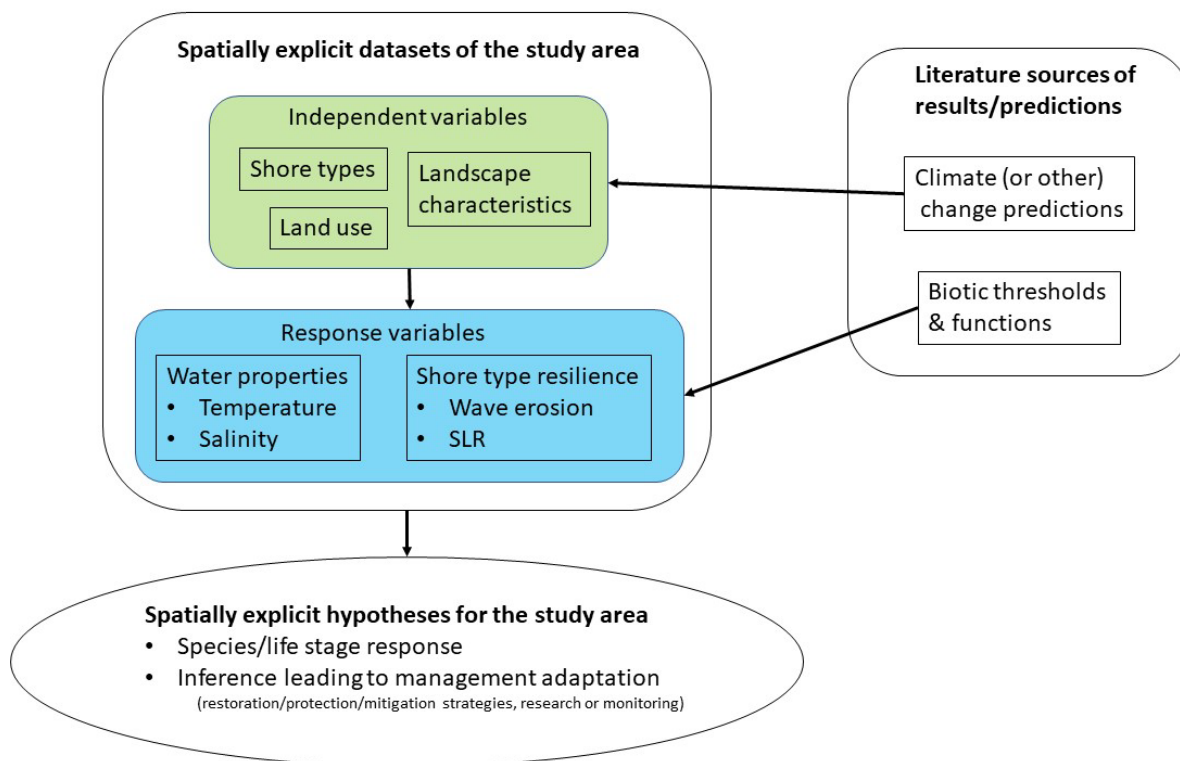


Figure 1. Conceptual study framework. The framework depicts how environmental response variables considered in this study may be influenced by the synergistic effects of landscape factors and climate change. Results may be used to further refine hypotheses about species-specific risk to climate change and other anthropogenic stressors. SLR = sea level rise.

## Chapter 2. Description of study area, spatial unit of analysis, and GIS layer development

### Study area

The geographic area for this project, herein 'study area', encompasses inland waters throughout northern Washington. It consists of nearshore areas within northern Puget Sound, including much of Whidbey Basin and Admiralty Inlet, in addition to Bellingham and Samish Bay, the eastern section of the Strait of Juan de Fuca, the southern section of the Strait of Georgia, and the San Juan Islands (Figure 2). Other regions of Washington's inland waterways were excluded from this analysis solely due to limited resources, as this model could and should eventually be expanded and applied to other regions.

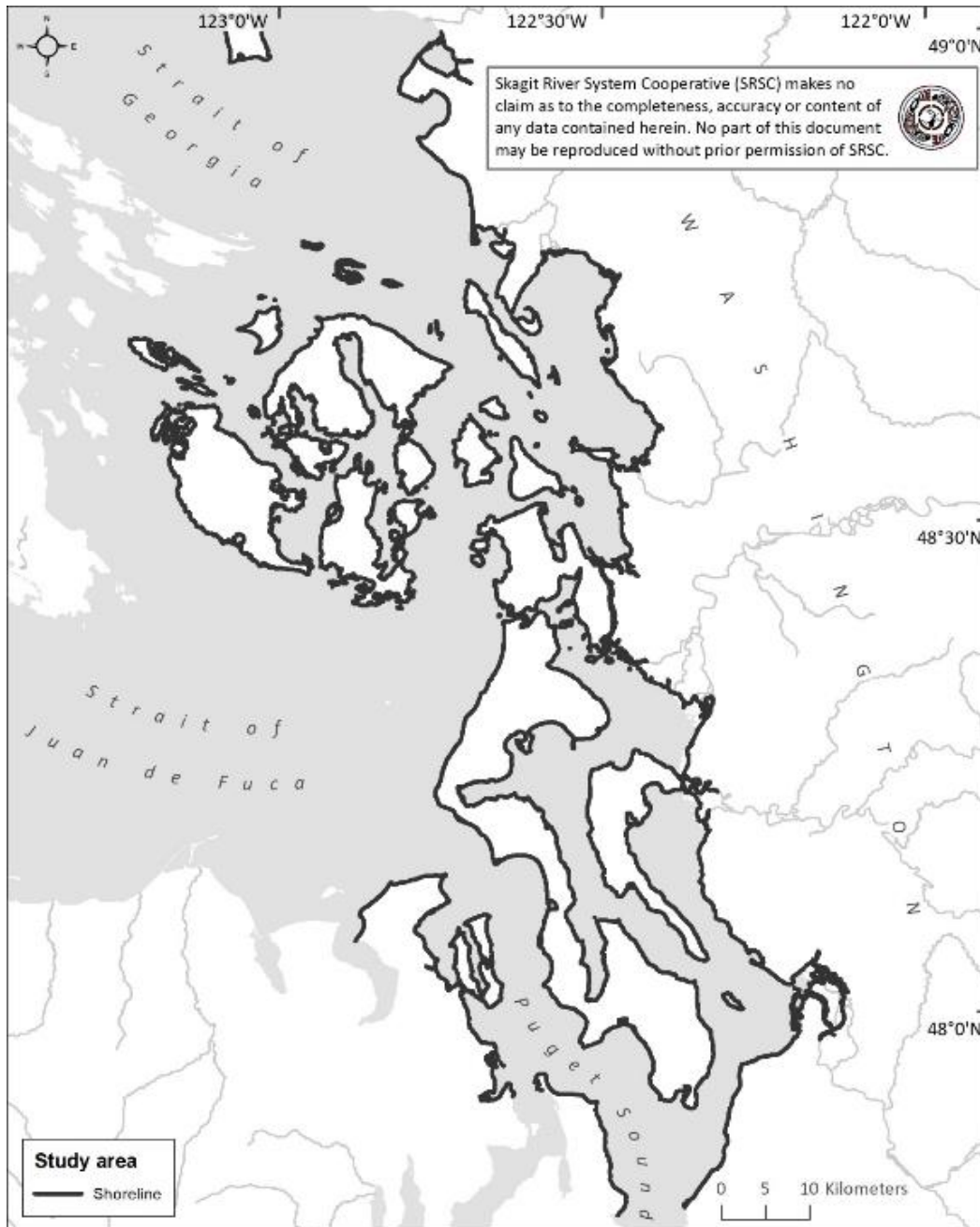


Figure 2. Map depicting the geographic extent of the study area in inland waters of northern Washington. The thick black lines reflect the shoreline of the study area.

### Spatial unit of analysis

We used the Puget Sound Nearshore Ecosystem Restoration Project (PSNERP) Shoreline Process Units (SPU) for the study area to create a polygon layer that spans the shoreline arcs and allows for attachment of attributes via geographic information systems (GIS) from the marine environment as well as the adjacent land (Simenstad et al. 2011). This data layer is regionally accepted and has a small enough spatial unit to reduce much of the heterogeneity within the study area for shoreline geomorphology, landscape, and land use characteristics. We only used zone units (ZU) assigned as 1 (landward areas, i.e., within 200 m of the shoreline) and 2

(waterward areas, extending to the 10- depth contour). The resulting GIS shapefile of the study area has 1,742 unique polygons identified by geomorphic scaling unit (GSU\_ID) and is our base map of the study area where we assigned each polygon with data attributes needed for analysis (Figure 3). GSU\_ID is a concatenation of the ID values within the PSNERP dataset for DU (delta unit), DAU (delta accounting unit), and the ZU. These terms are defined in the geospatial methodology published in the PSNERP dataset (Simenstad et al. 2011). For the purposes of visualizing landscape characteristics and the spatial distribution of model results, both the upland and aquatic portion of each spatial unit were incorporated to show enough useful detail about each spatial unit. However, only the wet (i.e., waterward) portions of each polygon were used for the analysis and are therefore incorporated in the results.

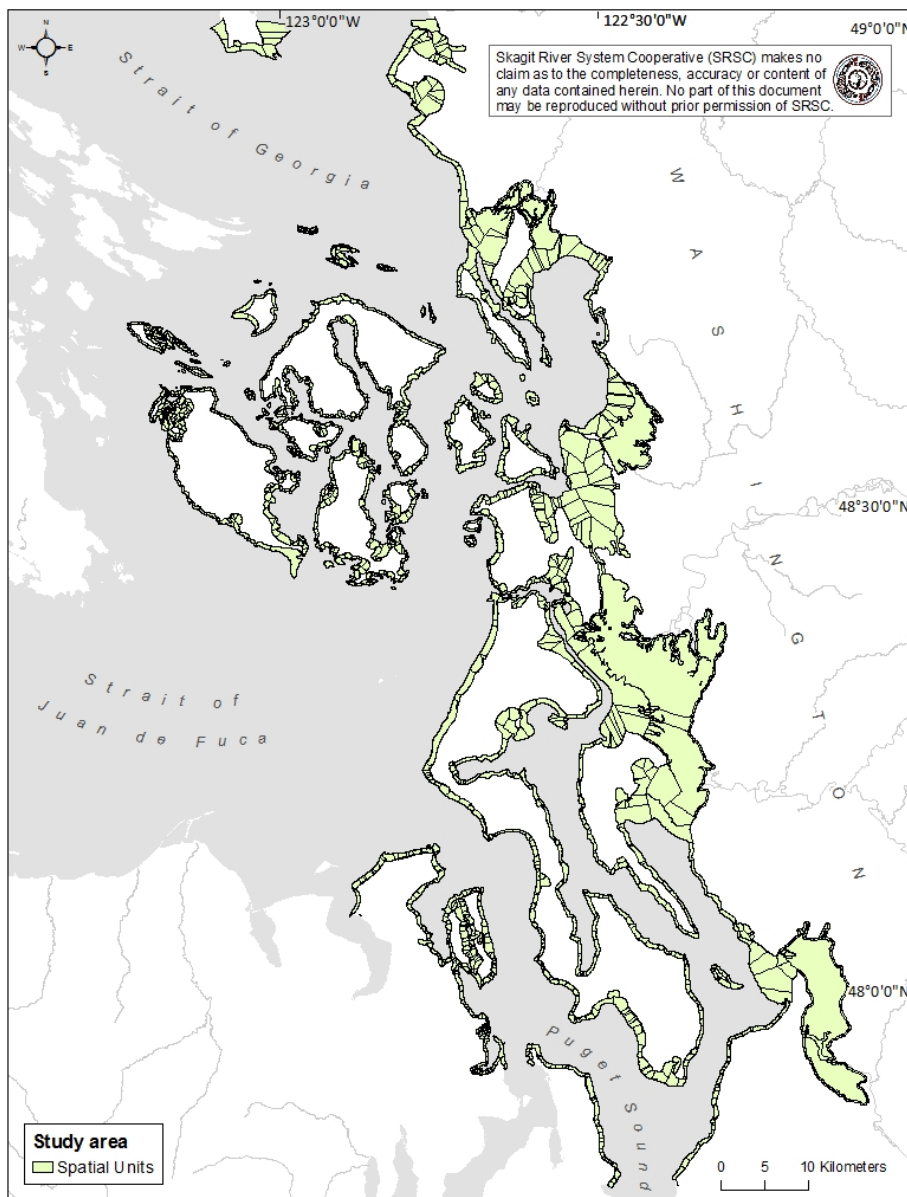


Figure 3. Map of the basic spatial unit polygons in the study area.

### **Attribute data used**

Our conceptual model of how habitat is formed, disturbed, and sustained shaped how we envisioned this project and the data types needed for analysis. It is well known that landscape controls and natural processes form habitat conditions that influence life history expression of biota (Beechie et al. 2003, Beechie et al. 2010). Thus, we expect habitat conditions to have a limit to their condition potential as a function of their geologic, geomorphic, and landscape context as well as to the extent natural or human processes can interact with the site. To evaluate this hypothesis, we assembled existing or newly created GIS data layers for 1) shore type geomorphology, 2) landscape characteristics related to natural processes, and 3) human land use for each polygon within the study area. We hypothesize that habitat conditions are dynamic with respect to the synergistic effects of localized pressures/stressors (e.g., land use change, localized natural disturbance) and large-scale environmental change. Specifically, differentiation of shore type and other landscape variables within the study area are an important component of our analysis because of their potential linkages to biota and differential expression to environmental variability which links to long-term climate change predictions (Table 1 – Table 3). In this study, we used climate change predictions of attributes known or hypothesized to influence the distribution and/or survival of selected fish and shellfish species/life stages. We developed a framework to conduct a vulnerability analysis for multiple species and habitat types and present results from a vulnerability assessment of juvenile Chinook salmon, larval cockle clams, and postlarval and juvenile Dungeness crab, to elucidate the value of such an approach in addition to its potential challenges and limitations.

Table 2. Target fish and shellfish species distributed throughout the study area (see Figure 2). For each species, seasonal and life stage specific associations with dominant habitats and shore types throughout the tidal continuum are depicted.

Species	Life stage	Tidal elevation/depth	Temporal/Seasonal use	Wave exposure	Shipman (2008) shore types	References	
<i>Oncorhynchus tshawytscha</i>	Chinook salmon	Fry (<60 mm)	Tidal delta/blind channel	7 months; Feb-Aug	Low	Large river estuaries, pocket estuaries	(Beamer et al. 2005, Fresh 2006, Rice et al. 2011, Beamer & Fresh 2012)
			Shallow intertidal	6 months; Feb-Jul	Moderate		
		Parr (60-150 mm)	Intertidal/subtidal	7 months; Feb-Aug	Moderate	All shore types	
			Surface waters	5 months; Apr-Aug	Moderate	Pocket beaches	
			6 months; Jun-Nov	Any	Neritic		
<i>Metacarcinus magister</i>	Dungeness crab	Larvae	Pelagic	3-5 months; ~Jan-Aug	N/A	Bluffs, barrier beaches, estuarine deltas, estuaries, low-energy bays	(Pauley et al. 1986, Jamieson & Phillips 1993, Holsman et al. 2003, Curtis & McGaw 2012, Rasmuson 2013)
		Juveniles	Upper subtidal to mid-intertidal	Summer-winter	Low-med		
		Adults	Low intertidal to > 100 m	Year round	Low-med		
<i>Panopea generosa</i>	Geoduck	Larvae	Pelagic	4-6 weeks; Mar-Aug	N/A	Bluffs, low-energy bays	(Goodwin & Pease 1989)
		Juveniles	Mostly subtidal	Year round	Moderate		
		Adults	Low intertidal to subtidal	Year round	Moderate		
<i>Leukoma staminea</i>	Native littleneck clam	Larvae	Pelagic	3 weeks; Apr-Aug	N/A	Bluffs, barrier beaches, estuarine deltas, estuaries	(Strathmann 1987)
		Juveniles	Low-mid intertidal to shallow subtidal	Year round	Moderate		
		Adults		Year round	Moderate		

Table 2 continued.

Species		Life stage	Tidal elevation/depth	Temporal/Seasonal use	Wave exposure	Shipman (2008) shore types	References
<i>Saxidomus gigantea</i>	Butter clam	Larvae	Pelagic	2 months; May-Aug	N/A	Bluffs, barrier beaches, estuarine deltas, estuaries	(Quayle & Bourne 1972, Gallucci & Gallucci 1982, Strathmann 1987, Liu et al. 2010, Hiebert 2015)
		Juveniles	Low-mid intertidal to shallow subtidal	Year round	Moderate		
		Adults		Year round	Moderate		
<i>Clinocardium nuttallii</i>	Cockle	Larvae	Pelagic	Apr-Nov	N/A	Bluffs, barrier beaches, estuarine deltas, estuaries, low-energy bays	(Gallucci & Gallucci 1982, Strathmann 1987, Liu et al. 2010, Hiebert 2015)
		Juveniles	Intertidal to subtidal	Year round	Low		
		Adults		Year round	Low		
<i>Tresus sp.</i>	Horse clam	Larvae	Pelagic	19-35 days; Mar-May	N/A	Bluffs, barrier beaches, estuarine deltas, estuaries, low-energy bays	(Bourne & Smith 1972, Strathmann 1987, Harbo 1997, Coan et al. 2000, Hiebert 2015 & 2016)
		Juveniles	Mid-intertidal to subtidal	Year round	Low		
		Adults		Year round	Low		
<i>Ruditapes philippinarum</i>	Manila clam	Larvae	Pelagic	3-4 weeks; Jun-Sep		Bluffs, barrier beaches, estuarine deltas, estuaries	(Bardach et al. 1972, Numaguchi 1998)
		Juveniles	Intertidal	Year round			
<i>Ostrea lurida</i>	Olympia oyster	Larvae	Pelagic	11-16 days; mid-May-July	N/A	Estuarine deltas, estuaries, low-energy bays	(Strathmann 1987, Hettinger et al. 2012, Hettinger et al. 2013, Barber et al. 2016, Cheng et al. 2015)
		Juveniles	Low intertidal to subtidal	Year round	Low		
		Adults	0-10 m deep	Year round	Low		
<i>Mytilus sp.</i>	Mussels	Larvae	Pelagic	Apr-May	N/A	Bluffs, barrier beaches, estuarine deltas, estuaries, low-energy bays	(Bayne 1965, Griffiths & Griffiths 1987, Strathmann 1987, Bamber 1990, Harbo 1997, Michaelidis et al. 2005, Gazeau et al. 2007)
		Juveniles		Year round	Low		
		Adults	Intertidal to shallow subtidal	Year round	Low		

Table 3. Summary of geomorphic, landscape, and human land use attributes quantified as data layers with generalized responses. Mechanistic models developed for this study, including sea surface temperature (SST) and salinity (TempSal) and wave and sea level rise resilience (WSLRR), are indicated in terms of their application to each attribute and generalized response combination.

<b>Data category</b>	<b>Attribute</b>	<b>Generalized responses</b>	<b>Model use</b>
Shore type geomorphology	Barrier beaches	Sensitive to changes in longshore sediment supply, sea level, and wave energy; susceptible to beach erosion and landward barrier migration or barrier breach	TempSal, WSLRR
	Large river estuaries	Sensitive to changes in fluvial sediment supply, sea level, and wave energy; susceptible to marsh erosion and landward migration.  Sensitive to hydrologic changes; susceptible to SST and salinity changes	TempSal, WSLRR
	Pocket estuaries	Sensitive to changes in local fluvial sediment supply, adjacent barrier beach changes, sea level, and wave energy; susceptible to marsh erosion, lagoon breach, and landward migration.  Sensitive to hydrologic changes; susceptible to SST and salinity changes	TempSal, WSLRR
	Pocket beaches	Sensitive to changes in local sediment supply, sea level, and wave energy; susceptible to beach erosion and landward migration	TempSal, WSLRR
	Sediment source beaches	Sensitive to changes in longshore sediment supply, sea level, and wave energy; susceptible to sediment bluff and beach erosion and landward migration	TempSal, WSLRR
	Rocky beaches	Naturally resistant to erosion processes	TempSal, WSLRR

Table 3 continued.

<b>Data category</b>	<b>Attribute</b>	<b>Generalized responses</b>	<b>Model use</b>
Landscape characteristics	Fetch	Key determinant of wave energy acting on drift cell and pocket beach sediment dynamics and storm surge; areas with larger fetch are more susceptible to erosion and storm surge flooding than areas with lower fetch	WSLRR
	Distance to nearest large river	Influences nearshore surface salinity and SST; shorelines more distant from their nearest large river are also saltier than shorelines closer to their nearest large river.	TempSal
	Distance to entrance of Strait of Juan de Fuca	Influences nearshore surface salinity and SST; deeper water adjacent to the shoreline yields colder and saltier nearshore surface water.	TempSal
	Depth	Influences nearshore surface salinity and SST; deeper water adjacent to the shoreline yields colder and saltier nearshore surface water.	TempSal
	Presence of local freshwater input	Influences pocket estuary salinity and SST; pocket estuaries with local freshwater inputs are warmer and less saline than those without.	TempSal
Human land use	Percent of shoreline armored	Disruptor of longshore sediment supply and transport; indicator of human disturbance (investment) in the water/land interface.	WSLRR
	Percent of adjacent upland in forest	An indicator of a lack of human disturbance along the shoreline; theoretical predictor of a site's potential human response to storm surge and sea level rise potential.  Areas more developed by humans are more likely to illicit a "fortify" response as opposed to a "retreat" response	WSLRR

### Shore type

We associated shore type to each GSU\_ID polygon in the study area to account for geomorphic constraints in the expression of habitat conditions. We utilized seven shore types based on their linkages to potential biota and potential sensitivity to environmental variability or long-term climate change: barrier beaches (BB); estuary, large river type (E-LR); estuary, pocket estuary type (E-PE); human-modified beaches (M); pocket beaches (PB); rocky beaches (RB); and

sediment source beaches (SSB). The groupings are a simplified geomorphic typology following classifications created for Puget Sound nearshore landforms (Shipman 2008, McBride et al. 2009). The seven shore types are described below with additional citations as necessary. The geographic distribution of shore types for the study area are shown in Appendix A. Shore type data were extracted from the shoreline arc layer developed for the Salmon and Steelhead Habitat Inventory and Assessment Program (SSHIAP) which includes a Puget Sound-wide GIS data layer (McBride et al. 2009).

The range in size of polygons by dominant shore type was mostly between 5 to 80 hectares (25-75 percentile) except for the large river estuaries which are much greater in scale (Figure 4). The study area includes five different large river estuaries (Nooksack, Samish, Skagit, Stillaguamish, and Snohomish). The total “wet” area in hectares for each of the 1,742 spatial units varies by dominant shore type such that of the 87,893 hectares of wetted area included in this study, large river estuaries make up the greatest wetted area (Table 4).

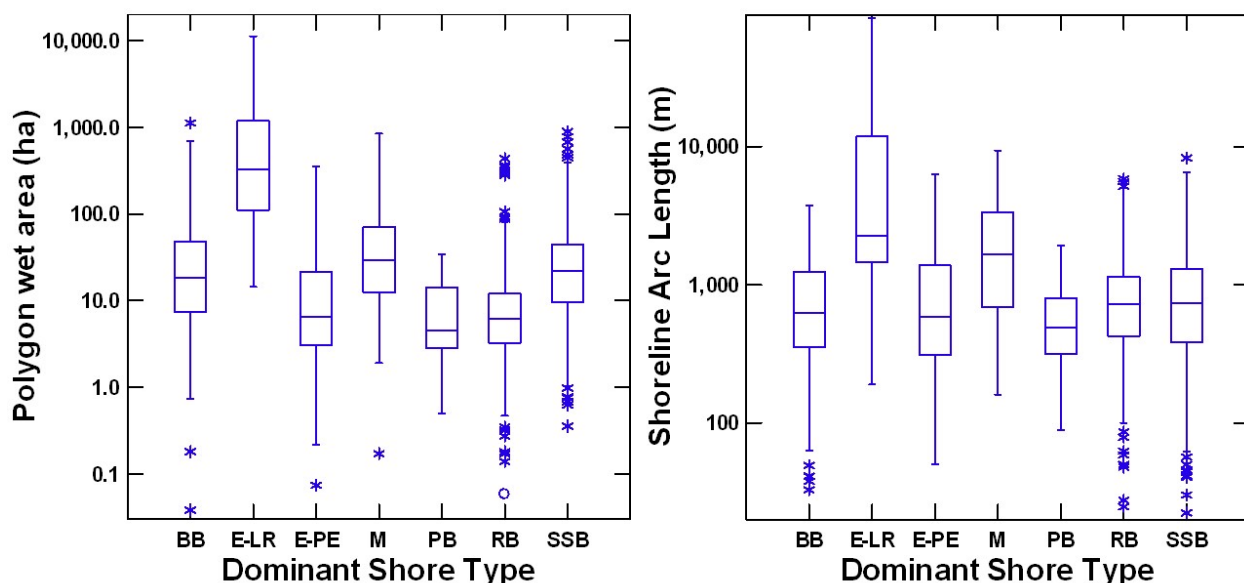


Figure 4. Boxplot of polygon wet area (left panel) and shoreline length (right panel) by shore type for the 1,742 GSU\_ID polygons within the study. Shore type abbreviations are: BB = barrier beach; E-LR = estuary, large river type; E-PE = estuary, pocket estuary type; M = human-modified beach; PB = pocket beach; RB = rocky beach; SSB = sediment source beach.

Table 4. The total “wet” area in hectares by dominant shore type for each of the 1,742 spatial units included in the study.

Shore type	Wet area (ha)
Barrier beach	11,873.8
Estuary, large river type	34,833.4
Estuary, pocket estuary type	2,966.5
Human-modified	3,409.0
Pocket beach	211.4
Rocky beach	10,142.1
Sediment source beach	24,456.7

### Barrier beach

The barrier beach group includes true barrier beaches, which are depositional landforms that often form connected or closed lagoon and marsh shore types on their landward side (Figure 5 & Figure A1). The barrier beach group is characterized by low relief beaches with well-developed backshore areas and leeward tidal and/or freshwater impoundments. The impoundments themselves are part of the pocket estuary group if there is a consistent surface connection to marine water.

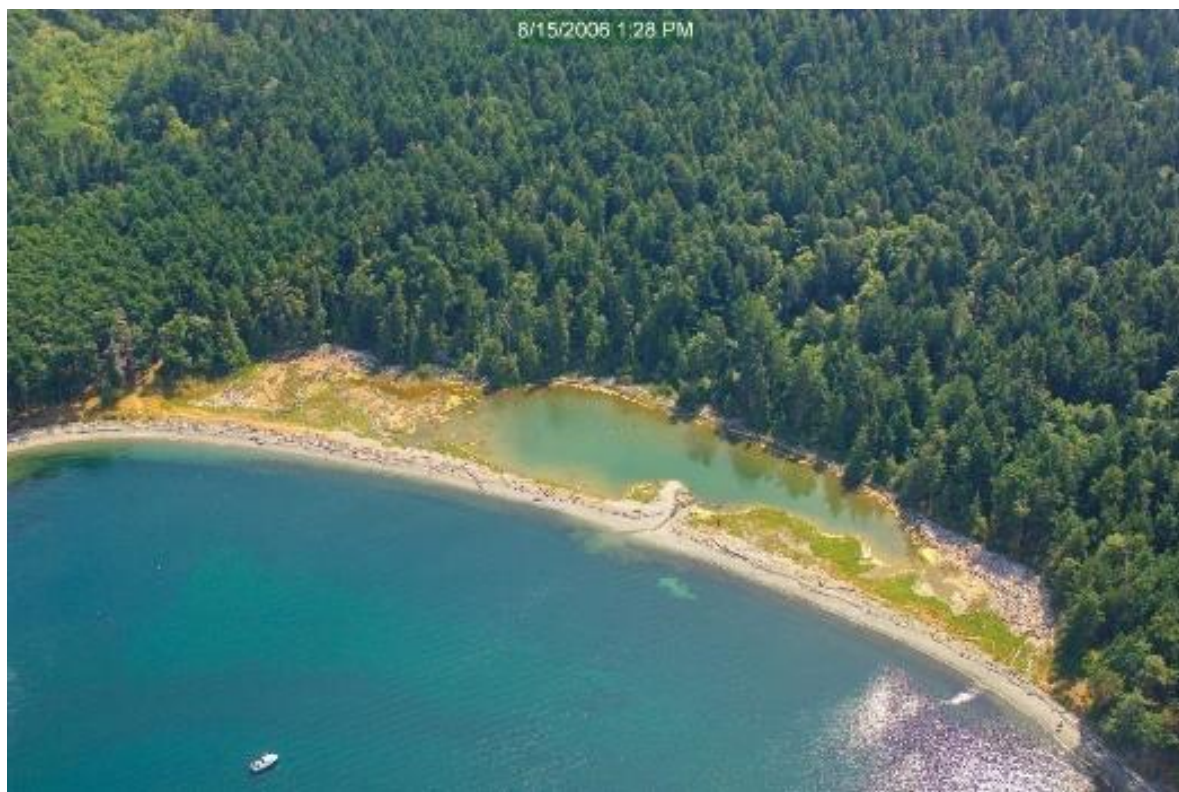


Figure 5. Photo of Third Lagoon on San Juan Island, showing both barrier beach (seaward side) and pocket estuary (landward side) shore forms. Aerial oblique photo is from <https://fortress.wa.gov/ecy/shorephotoviewer/>.

## Estuary, large river type

The study area is located within the larger footprint of a fjord estuary, containing many large river estuaries. Our study area includes the following five rivers: Nooksack, Samish, Skagit, Stillaguamish, and Snohomish. These large river estuaries are geomorphically tidal deltas or drowned channels with unvegetated flats and vegetated tidal wetland zones with varying amounts and types of channels, water salinity, and wetland plant communities ranging from salt tolerant emergent species to freshwater riparian forest species (Figure 6 & Figure A2). The riverine tidal zone is the area of river channels and wetlands where freshwater is tidally pushed but not mixed with marine water. The tidal estuarine zone includes the channeled emergent and scrub-shrub marshes where freshwater mixes with saltwater. Within functioning estuaries, a diverse network of habitats is formed and maintained by tidal and riverine processes, creating a mosaic of wetlands and channels (e.g., emergent or scrub-shrub wetlands, blind tidal, or open-ended distributary channels) (Cowardin 1979, Simenstad 1983).

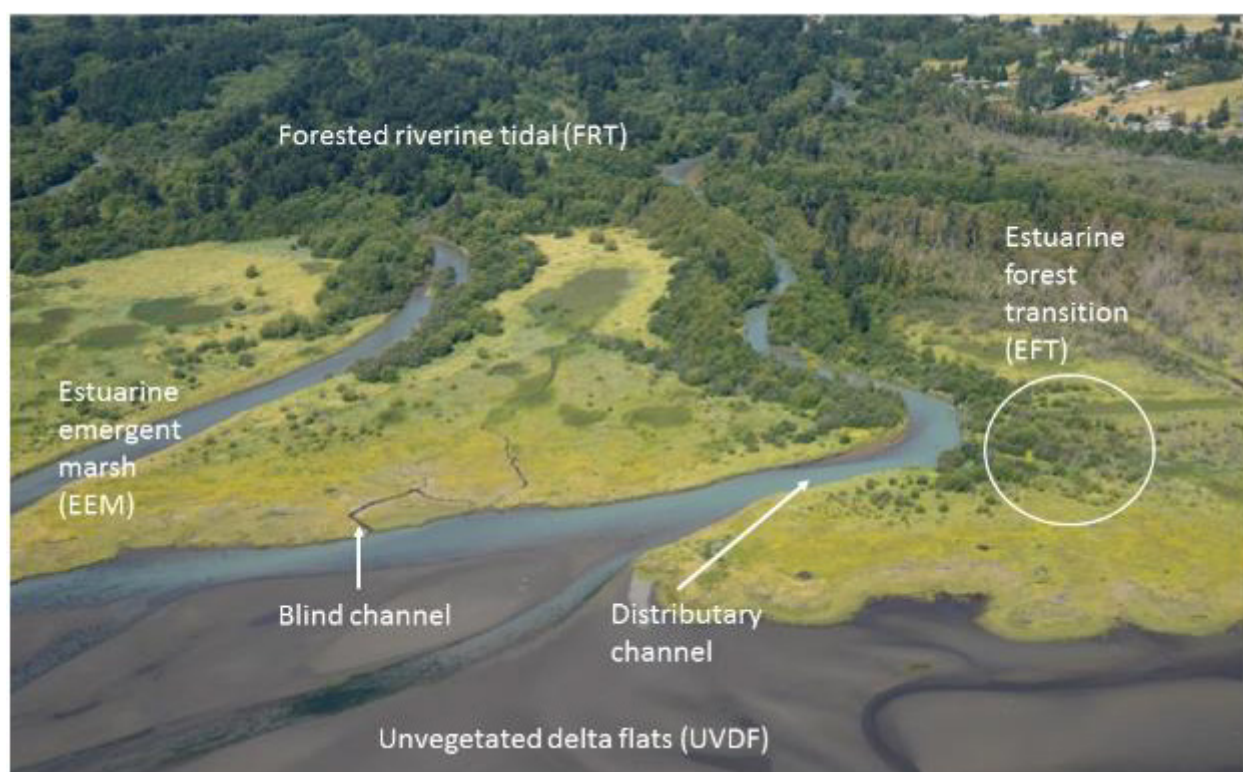


Figure 6. Photo of the Nooksack River tidal delta, showing three vegetated estuarine wetland zones (EEM, EFT, and FRT), unvegetated delta flats, and blind or distributary channels. Aerial oblique photo is from <https://fortress.wa.gov/ecy/shorephotoviewer/>.

### Estuary, pocket estuary type

The pocket estuary group includes all the impoundments behind spits or other barrier beaches and those habitats impounded behind pocket beaches (Figure 7 & Figure A2). They also include stream estuaries not partially enclosed by lagoons/barrier beaches (deltas, drowned channels and tidal deltas). Many pocket estuaries have freshwater inputs resulting from the intersection of the shoreline with a stream or glacial valley. The valley indentations formed by pocket estuaries are often crossed and then partially enclosed by beach sediments moving across the indentation opening thereby creating lagoons.

In special cases, pocket estuaries may form in the absence of a direct freshwater input. Specifically, where tidally inundated lagoons form parallel to bluffs, seasonal inundation of freshwater into lagoons from groundwater seeps or heavy rains can create temporary pocket estuaries. Specifically, pocket estuaries may form in the absence of a direct freshwater input when tides encroach into coastal lowlands thereby forming a tidal channel marsh. This shore type is also associated with abundant eelgrass or the potential to support eelgrass production. Aside from the large river estuary polygons, all other estuary polygons within the study area are considered pocket estuaries.



Figure 7. Photo of Race Lagoon on Whidbey Island, showing both barrier beach (seaward side) and pocket estuary (landward side) shore forms. Aerial oblique photo is from <https://fortress.wa.gov/ecy/shorephotoviewer/>.

### Human-modified beach

Some shorelines throughout the study area have been heavily modified relative to their baseline conditions as a result of human land use actions, thereby changing their geomorphic shore type. Modified areas typically have extensive tidal fills, shoreline armoring, and a high degree of development on or adjacent to the shoreline. These shorelines were by default classified as 'modified' and are usually in urbanized environments such as the City of Anacortes shoreline (Figure 8 & Figure A3).

It should be noted that the modified shore type is not defined by the presence of shoreline armoring alone. There are many shoreline areas with armoring where the historical shore type is still visible from aerial photos and are subsequently defined by their historical type, unlike modified areas where traces of the historical shore type are unrecognizable.

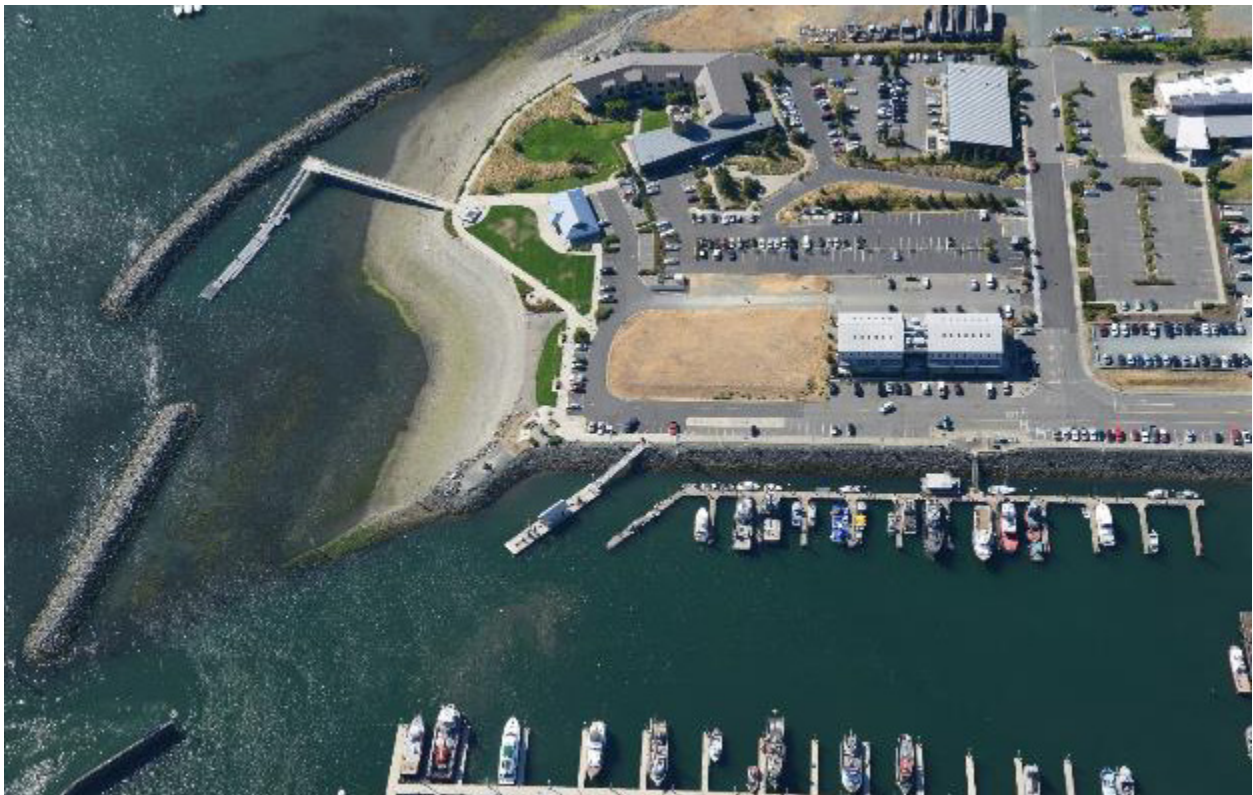


Figure 8. Photo of Cap Sante Marina in Anacortes on Fidalgo Island. Aerial oblique photo is from <https://fortress.wa.gov/ecy/shorephotoviewer/>.

## Pocket beach

Pocket beaches are a particular variation of a beach that can look like ‘bluff-backed beach’ at the base of rocky bluffs (Figure 9 & Figure A4). Unlike bluff-backed beaches, however, pocket beaches have no adjacent sediment source from drift cells and only derive sediments from local inputs.



Figure 9. Photo of pocket beach on Waldron Island (Mail Bay). Aerial oblique photo is from <https://fortress.wa.gov/ecy/shorephotoviewer/>.

## Rocky beach

Rocky beaches include both low to medium gradient rocky shorelines and plunging rock cliffs. Although this shore type is naturally resistant to wave energy erosion, the species occupying this shore type are vulnerable to wave energy (Figure 10 & Figure A5). Although rocky beaches are not associated with abundant eelgrass or the potential for its growth, these beaches are associated with abundant macroalgae, mainly kelp.

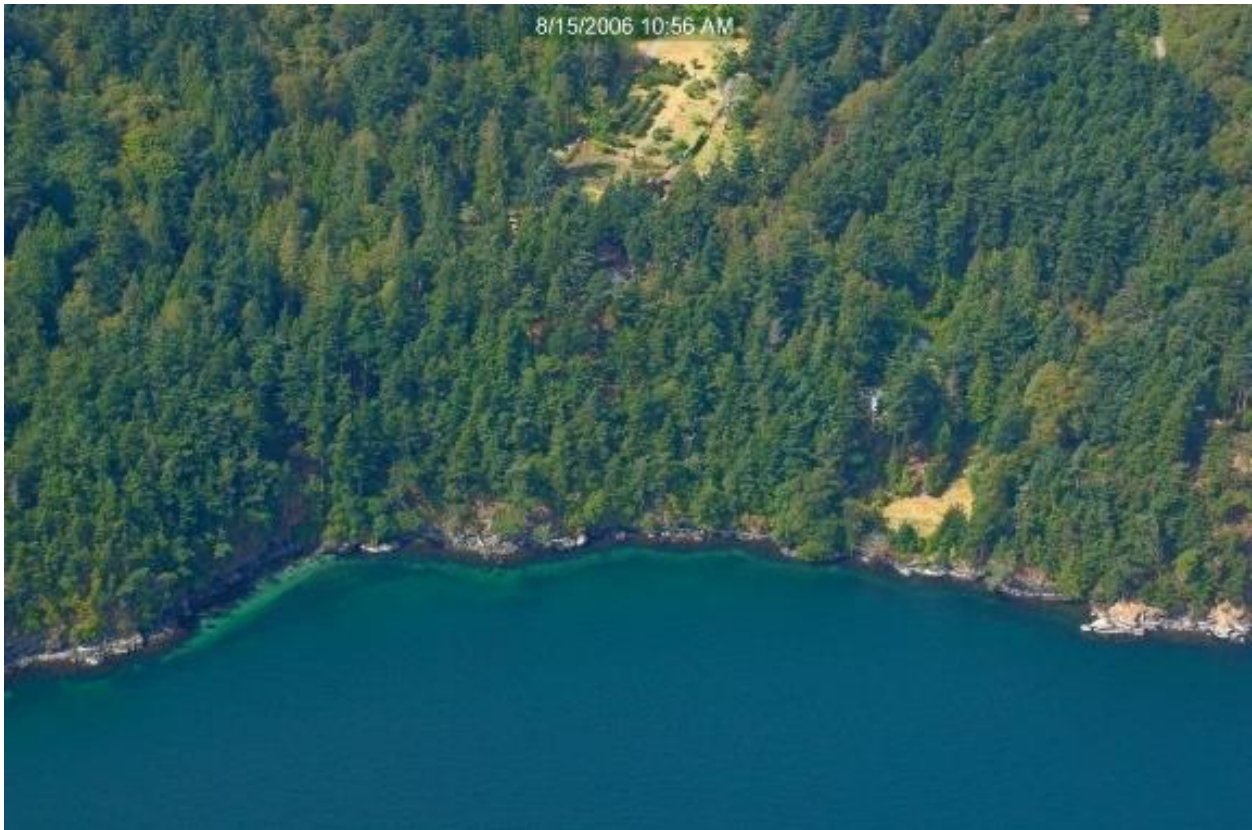


Figure 10. Photo of rocky beach on Orcas Island (within East Sound). Aerial oblique photo is from <https://fortress.wa.gov/ecy/shorephotoviewer/>.

### **Sediment source beach**

Sediment source beaches include erosional depositional beaches at the base of sediment bluffs. This group also includes sediment-covered rock beaches and seeps or small streams that enter the beach via the bluff rather than via a pronounced stream valley (Figure 11 & Figure A6). Sediment source beaches function to support the formation of lagoons at neighboring barrier beaches through longshore transport.



Figure 11. Photo of sediment source beach on Waldron Island (Little Hammond). Aerial oblique photo is from <https://fortress.wa.gov/ecy/shorephotoviewer/>.

## Landscape characteristics

Numerous landscape characteristics are known or hypothesized to influence local geomorphic and/or environmental conditions (e.g., SST, salinity, wave energy). We associated four landscape characteristic values to each GSU\_ID polygon in the study area to account for variation across the study area. The four selected landscape characteristics are: fetch, depth of adjacent marine water, distance from nearest large river, and distance from entrance of the Strait of Juan de Fuca. Each landscape characteristic is described below, and the geographic distribution of each characteristic assessed for the study area is shown in Appendix B.

### Fetch

Fetch is an important landscape characteristic that can influence habitat vulnerability by affecting longshore sediment transport, erosion, and storm surge.

To determine which fetch direction to use for this analysis, we summarized wind direction and magnitude information from six cities representing shoreline areas within the study area. This information was used to identify:

1. what months have high winds capable of generating waves large enough to initiate change in beach substrate and topography and,
2. dominant wind directions within those months.

Average wind direction results were summarized from weatherspark.com accessed on 2 October 2017 for the following six cities: Blaine, Bellingham, Oak Harbor, Friday Harbor, East Sound, and Everett (Table 5). We assumed most geomorphic change by waves on shorelines within the study area originated from storm events where winds were coming from the northeast (NE 45°), east (E 90°), southeast (SE 135°), and south (S 180°) directions during the annual windy period. Therefore, using area-specific predominant wind records from these four directions averaged over the October – March or April timeframe (Table 5) we calculated fetch results for each GSU\_ID (Figures B1– B4). All other fetch directions had infrequent or lower magnitude winds. Thus, the fetch (F) score used in our analysis of wave and sea level rise resilience (WSLRR) was the maximum distance from any of these four bearings.

Table 5. Summary of windy months and dominant wind direction during the annual windy period for six cities within the study area. The dominant wind direction for each city was defined arbitrarily as the predominant wind direction encompassing  $\geq 20\%$  of the time during windy months over the weather station's period of record.

City/weather station (period of record)	Windy months	Wind direction during windy months (percent of time)			
		NE	E	SE	S
Blaine/White Rock (1996 to present)	mid-October – mid-April	0.3	0.2	0.2	
Bellingham International Airport (1948 to present)	mid-October – mid-April		0.25	0.35	
Oak Harbor/Naval Air Station Whidbey (1945 to present)	mid-October – mid-April		0.2	0.4	
Friday Harbor Airport (1989 to present)	late-October – end of March		0.3	0.25	
East Sound/Orcas Island Airport (2004 to present)	mid-October – end of March		0.3	0.3	
Everett/Snohomish County Airport (1941 to present)	mid-October – mid-April		0.2	0.4	0.2

### Depth of adjacent marine water

Differential water depth adjacent to shorelines might influence nearshore habitat characteristics. To quantify adjacent water body depth for each GSU\_ID in the study area we calculated the mean depth of the waterward polygon ( $ZU = 2$ ) using bathymetry data within the PSNERP water polygon.

### Distance from nearest large river

We assumed that the distance between major freshwater sources and nearshore sites may influence the nearshore habitat characteristics of those sites. We expected the major sources of freshwater input to the study area to be the following large rivers: Fraser, Nooksack, Skagit, Stillaguamish, and Snohomish. To quantify distance from the nearest river for each GSU\_ID in the study area we calculated distance from each river mouth to the centroid of each GSU\_ID using the GIS cost-distance function (ESRI 2017).

### Distance from entrance of the Strait of Juan de Fuca

The proximity of nearshore sites to full strength seawater is likely to influence nearshore habitat characteristics. We assumed the entrance (i.e., the western end north of Cape Flattery) of the Strait of Juan de Fuca is a source of 100% seawater due to its proximity to the Pacific Ocean. To quantify

distance from the entrance of the Strait of Juan de Fuca for each GSU\_ID in the study area we calculated distance from the Strait's entrance to the centroid of each GSU\_ID using the GIS cost-distance function (ESRI 2017).

## **Land use**

As an index of the impact of human land use, we utilized the PSNERP dataset for percent forested (Figure B5) and percent shoreline armored (Figure B6) from the mid-1990s to each GSU\_ID within the study area. These indices represent a compilation of human land use metrics that may influence the overall resilience of a given shore type to environmental change (Simenstad et al. 2011).

## **Discussion**

### **Size of spatial units for analysis**

Because PSNERP has developed a commonly accepted spatial unit for Puget Sound and surrounding inland waters that is at a meaningful spatial scale for classifying geomorphic shore type difference, we selected this dataset as the basis for our study. We demonstrate that the combination of shore type and landscape characteristics will influence how the nearshore ecosystem may respond to natural processes and stressors via SST and salinity changes. However, the spatial unit of our analysis could be refined further to account for the diversity of habitats present within the spatial units of analysis used in the current study (see Chapter 4 Discussion). This would likely improve model predictions of SST and salinity throughout the study area and hence our inferences of how these habitats may be influenced by climate change.

### **Shore type GIS arcs**

The GIS shore type dataset used in this study developed by McBride et al. (2009) represents the best available spatial information for the overall study area with respect to shore type. In its development, McBride et al. (2009) performed steps of quality assurance and quality control (QA/QC) of their data for the shore type attributes using Washington State Department of Ecology 2006-07 oblique air photos. The QA/QC process found imperfections in locations of some ArcGIS lines. The ArcGIS lines originated from the Washington State Department of Natural Resources (DNR) shore zone ArcGIS lines. In some cases, the inherited DNR shore zone ArcGIS lines did not follow a true representation of the shoreline. A notable issue with the inaccurate ArcGIS shoreline was the potential for missing pocket estuaries. Specifically, for some smaller pocket estuaries, the shoreline ArcGIS line follows the barrier beach shoreline and cuts across the pocket estuary's outlet channel, thus omitting the shoreline of the pocket estuary in its GIS representation. Furthermore, the QA/QC process did not edit the location of ArcGIS lines, but did document pocket estuaries present on the landscape that were not accounted for in the original DNR shore zone ArcGIS lines by creating and populating a GIS attribute (field name: 'offline SZ') to flag the presence of unmapped pocket estuaries. For this study, we utilized the 'offline SZ' attribute results to account for 42 unmapped pocket estuaries. We recommend as a future effort that shoreline ArcGIS lines be edited throughout the study area where pocket estuaries are present but not identified. Additionally, the dataset does not accurately account for "modified" shore types present within the study area because most modified shore types were already changed from their historical type before the 2006-07 aerial photo time period used for data QA/QC of shore type.

## Age of land use and shoreline armoring data

We used land use and shoreline armoring results for the study area available from the PSNERP dataset (Simenstad et al. 2011). These were the best available data covering the entire study area at the time of this study's inception. However, many of the results for land use and shoreline armoring are over 20 years old and could bias model results that utilize them as inputs. We suggest future efforts to improve upon this study utilize two new datasets that are becoming available:

- ESRP shoreline armoring:
  - [https://salishsearestoration.org/wiki/Beach\\_Strategies\\_for\\_Nearshore\\_Restoration\\_and\\_Protection\\_in\\_Puget\\_Sound#Beach\\_Strategy\\_Geodatabase](https://salishsearestoration.org/wiki/Beach_Strategies_for_Nearshore_Restoration_and_Protection_in_Puget_Sound#Beach_Strategy_Geodatabase)
    - Data:
      - <https://wdfw.maps.arcgis.com/apps/webappviewer/index.html?id=2400779486234481ad56742b31eca519>
- WDFW land use data (see <http://www.pshrcd.com/#/intro>)
  - Data: <http://www.pshrcd.com/#/data>

## Chapter 3. Shore type resilience to wave energy and sea level rise

Sea level in Washington State waters is projected to increase due to climate change (Table 1; Miller et al. 2018). Understanding the susceptibility of different habitats to wave energy under current conditions could allow scientists to better predict how habitats supporting commercially and culturally important fish and shellfish may be affected by climate change. Under current conditions, shore types within our study area exhibit significant variability with respect to exposure to wave energy due to fetch (Figures B1 - B4), predominant wind direction (Table 5), and alteration due to human development (Figures B5 – B6). Therefore, each shore type included throughout the study area will vary in its susceptibility to erosion in response to projected sea level rise and increased wave energy due to climate change (Table 3). Here, we developed and applied an anecdotal framework to generate preliminary estimates of habitat resilience stratified by shore type to wave energy and sea level rise.

### Methods

To assess wave and sea level rise resilience (WSLRR) within the study area, we combined spatial data for fetch, shore type, and land use to calculate a resilience score for each GSU\_ID. For our purposes, the resilience score is a qualitative metric with a possible range between -1 and +1 where the most resilient areas have positive scores (but not >1) and the least resilient areas have negative scores (but not <-1). We used a unitless score because we currently do not have a way to accurately estimate appropriate wave energy or sea level rise metrics. The WSLRR score for each GSU\_ID  $i$  was calculated as:

$$WSLRR_i = (G_i \times F_i \times -(EH_i)) + PH_i ;$$

where  $G$  = geomorphic score,  $F$  = fetch score,  $EH$  = existing human score, and  $PH$  = predicted human score.

The fetch score ( $F$ ) for each site was set equal to a value ranging from 0 to -1 for sites exposed to a small fetch (less negative) versus those exposed to a large fetch (more negative). Specifically, the fetch score incorporates the maximum distance (km) from four possible wind directions including NE, E, SE, and S (see Chapter 2 for detailed information).

The geomorphic score ( $G$ ) was set equal to a value ranging from 0 to 1 and was calculated as:

$$G = \sum_s^n \%shoretype_s \times r_s;$$

Where  $r$  was the hypothesized response score of each shore type  $s$  (Table 6).

Table 6. Assigned response scores of each shore type to wave energy. Values indicate either high (0) or low (1) resistance to wave energy.

Grouped shore types ( $i$ )	Response score ( $r$ )	Explanation
Barrier beaches	1	Beach erosion and loss; landward barrier migration
Estuaries	1	Landward habitat migration, area and tidal prism loss
Human modified beaches	1	Artificially resistant, but our assumed human response to wave energy and SLR will be additional fortification because of a desire to protect the extensive existing human footprint
Pocket beaches	1	More and deeper sediments are mobilized; increased local sediment input; landward habitat migration; area and tidal prism loss
Rocky beaches	0	Naturally resistant
Sediment source beaches	1	More and deeper sediments are mobilized; bluff retreat; increased sediment input from bluffs

Human alteration scores incorporate the percent of armored shoreline ( $a$ ) and percent of forested habitat ( $f$ ) present within each GSU during the mid-1990s (Simenstad et al. 2011). Specifically, human alteration scores within each GSU include a metric for existing conditions ( $EH$ ) which was calculated as:

$$EH = -a/100;$$

and a metric for predicted future conditions ( $PH$ ):

$$PH = f/100$$

A theoretical “resilient” example of this calculation involves a shoreline area with a high percentage of sensitive shore types and a long fetch, but the shoreline is in good current condition from human impacts. Therefore, the area has a higher likelihood of future human ‘retreat’ response

because the land is less developed compared to land with a high level of capital improvements within the area. We would expect this area to score near +1.

$$WSLRR = (G \times F \times -(EH)) + PH;$$

$$WSLRR = (1 \times -1 \times -(0)) + 1 = 1$$

A theoretical “vulnerable” example of this calculation involves a shoreline area consisting of a high percentage of sensitive shore types combined with a long fetch, but the area is in poor current condition from human impacts. There is a high likelihood of a future human fortification response to increased wave energy and SLR pressure. We would expect this type of example to score near -1.

$$WSLRR = (G \times F \times -(EH)) + PH;$$

$$WSLRR = (1 \times -1 \times -(-1)) + 0 = -1$$

## Results

We estimated considerable variability in resilience to wave energy and sea level rise across each shore type (Figure 12). In general, of the seven predominant shore types assessed, large river estuaries and human-modified shore types were projected to be the least resilient to wave energy and sea level rise with respective median WSLRR scores of -0.60 and -0.16. Conversely, barrier beaches, sediment source beaches, and rocky beaches were projected to be the most resilient to wave energy and sea level rise with median WSLRR scores of 0.39, 0.53, and 0.74, respectively. Each shore type exhibited a high degree of variability in WSLRR across the study area (e.g., Figure 13), which was largely dependent on spatial variability in fetch score, geomorphic score, existing human condition based on the percentage of armored shoreline within each GSU, and predicted future conditions based on the percentage of forested habitat within each GSU\_ID (Figures 12-17).

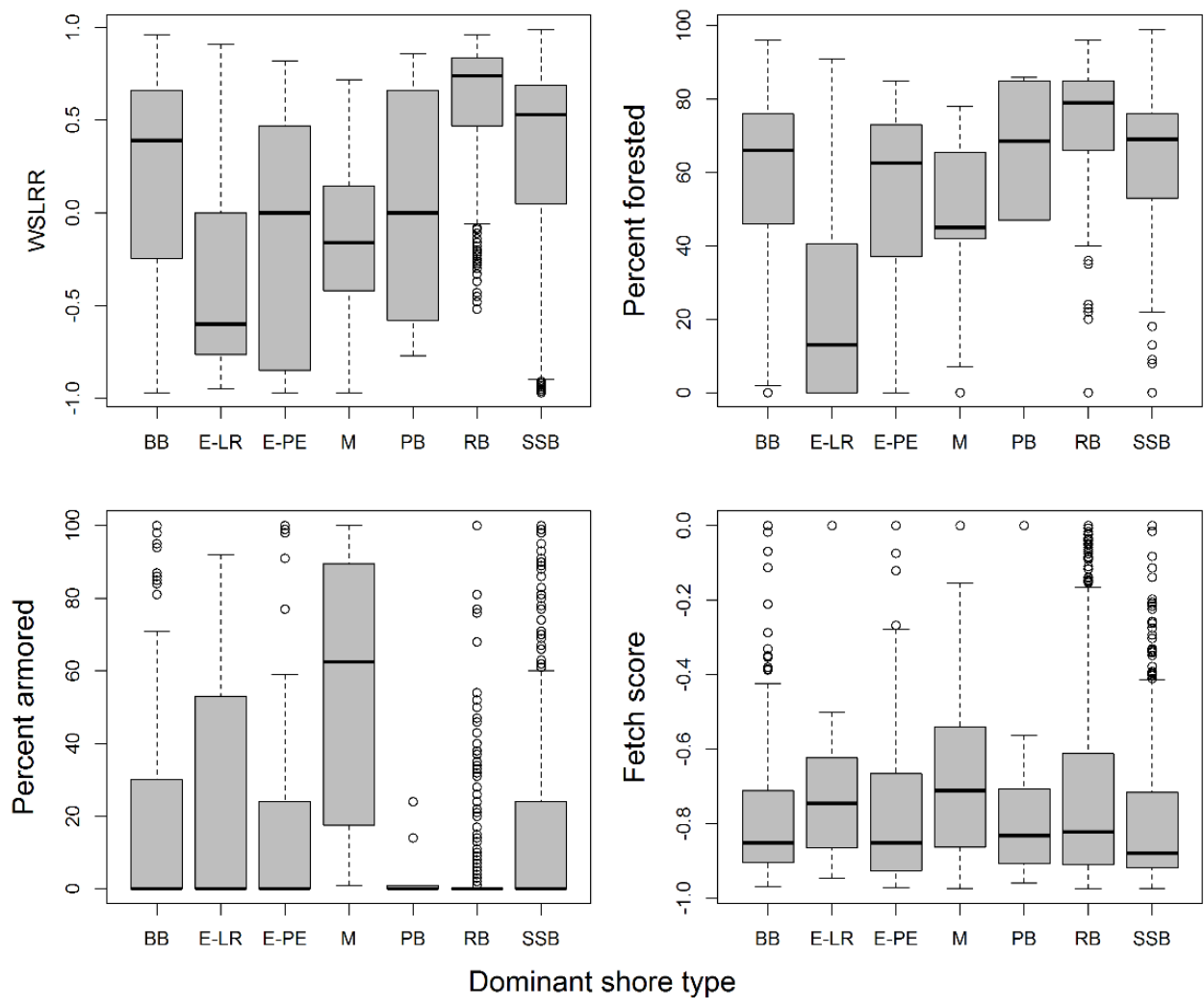


Figure 12. Boxplots of wave and sea level rise resilience (WSLRR) predictions, percent forested habitat, percent armored, and fetch score by shore type. Shore type abbreviations are: BB = barrier beach; E-LR = estuary, large river type; E-PE = estuary, pocket estuary type; PB = pocket beach; RB = rocky beach; SSB = sediment source beach. The resilience score is a qualitative metric with a possible range between -1 and +1 where the most resilient areas have positive scores (but not >1) and the least resilient areas have negative scores (but not <-1)

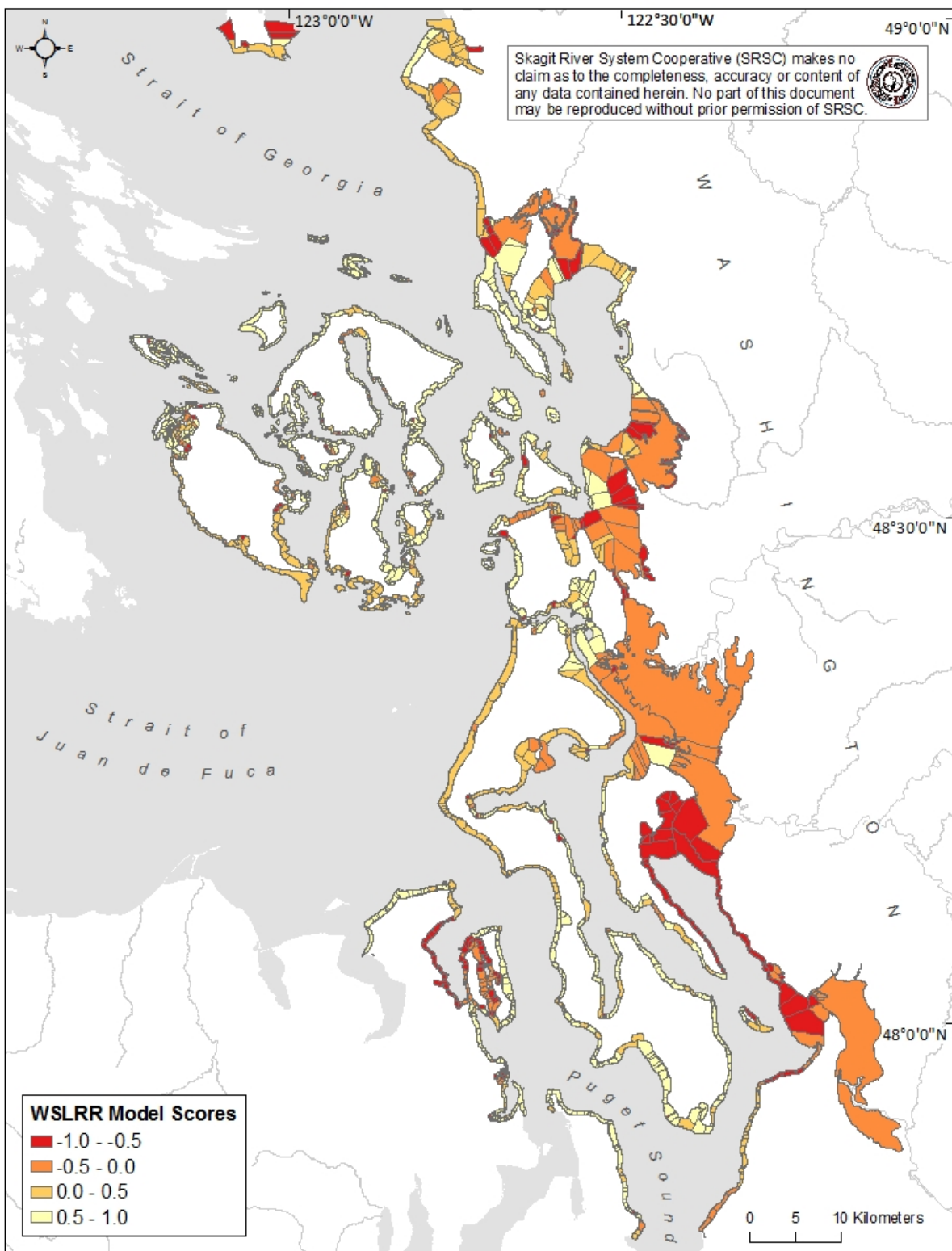


Figure 13. Map of wave and sea level rise resilience (WSLRR) predictions for each GSU in the study area where a value of 1 indicates a highly resilient GSU.

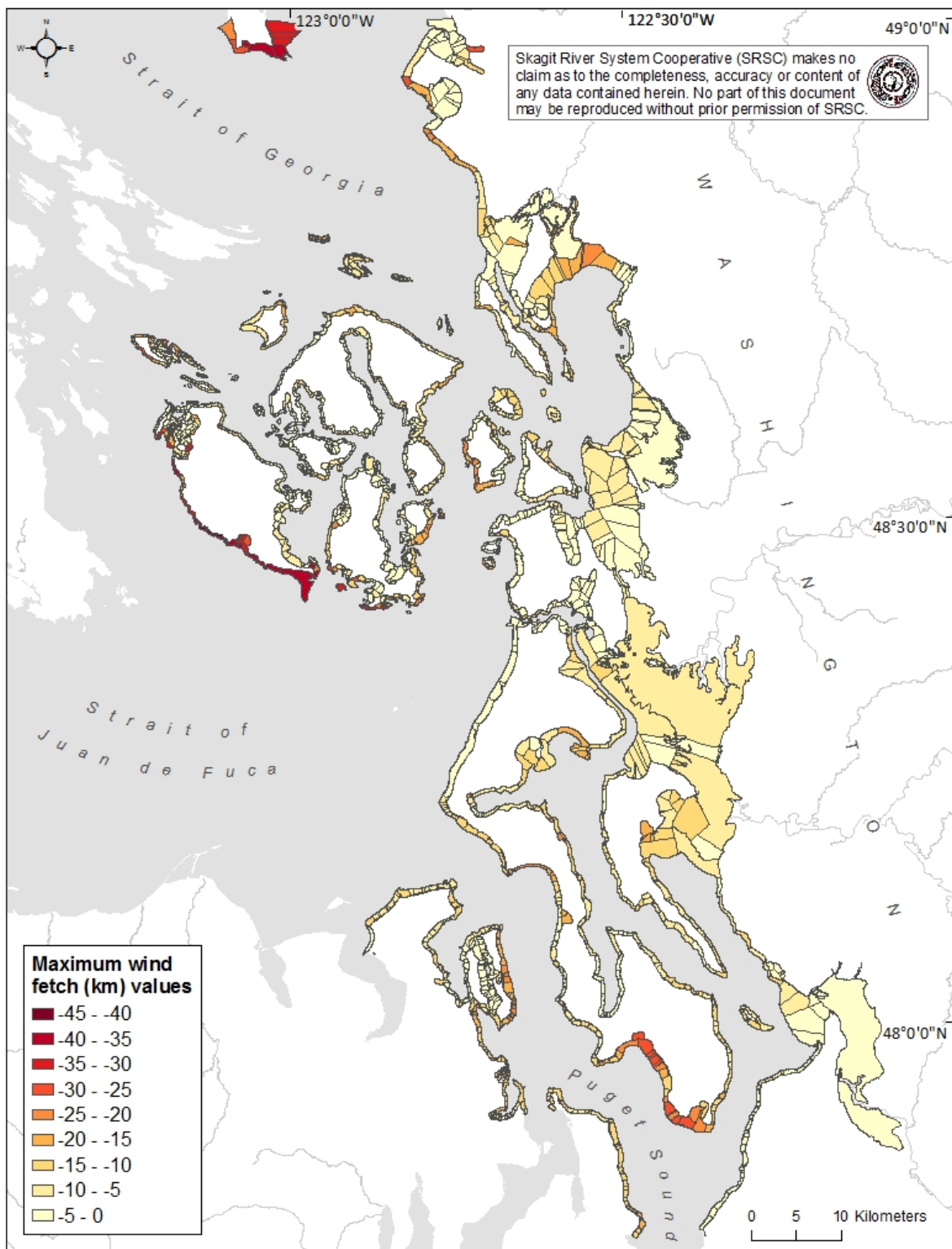


Figure 14. Map of maximum fetch values used for the wave and sea level rise resilience predictions. Values incorporate the maximum distance (km) from four possible wind directions including northeast, east, southeast, and south (see Chapter 2 for detailed information) where a more negative value equals a high maximum fetch.

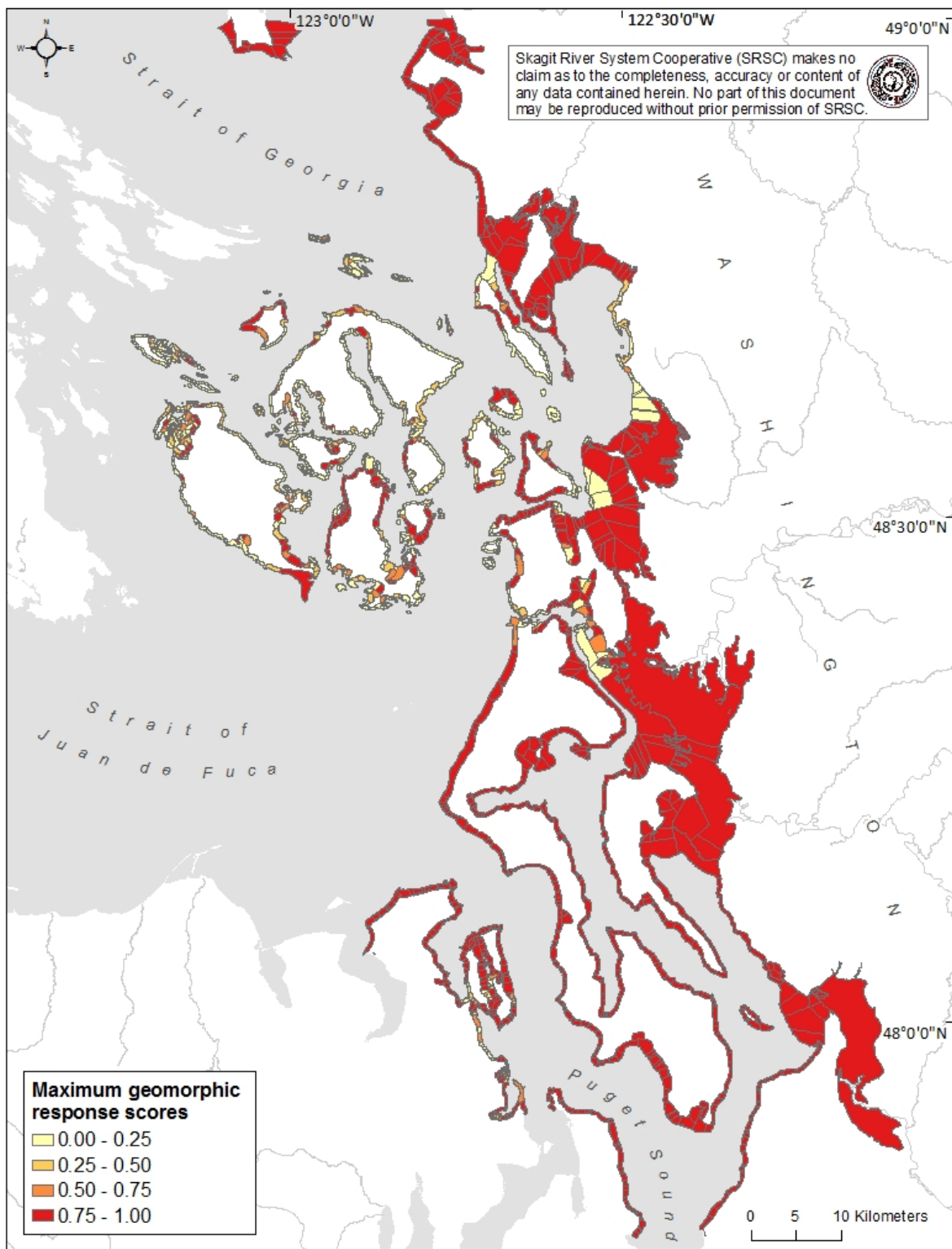


Figure 15. Map of maximum geomorphic response scores ( $G$ ) used for the wave and sea level rise resilience predictions. Values are based on projected geomorphic resistance to wave energy where a value of zero indicates high resistance to erosion.

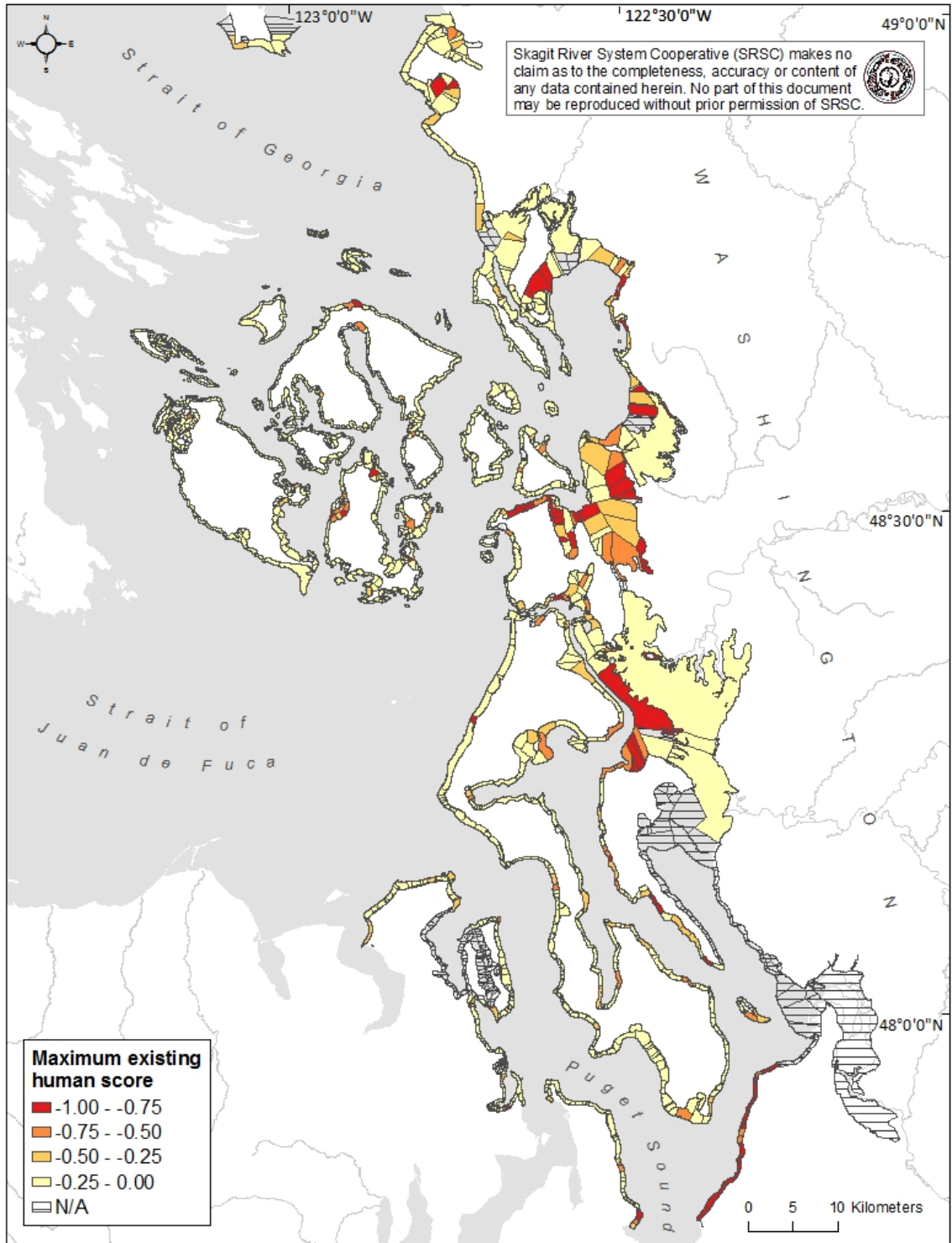


Figure 16. Map of maximum existing human scores used for the wave and sea level rise resilience predictions. Values are based on the percentage of armored shoreline present in each GSU in the 1990s where a score of -1 indicates a high percentage of armored shoreline.

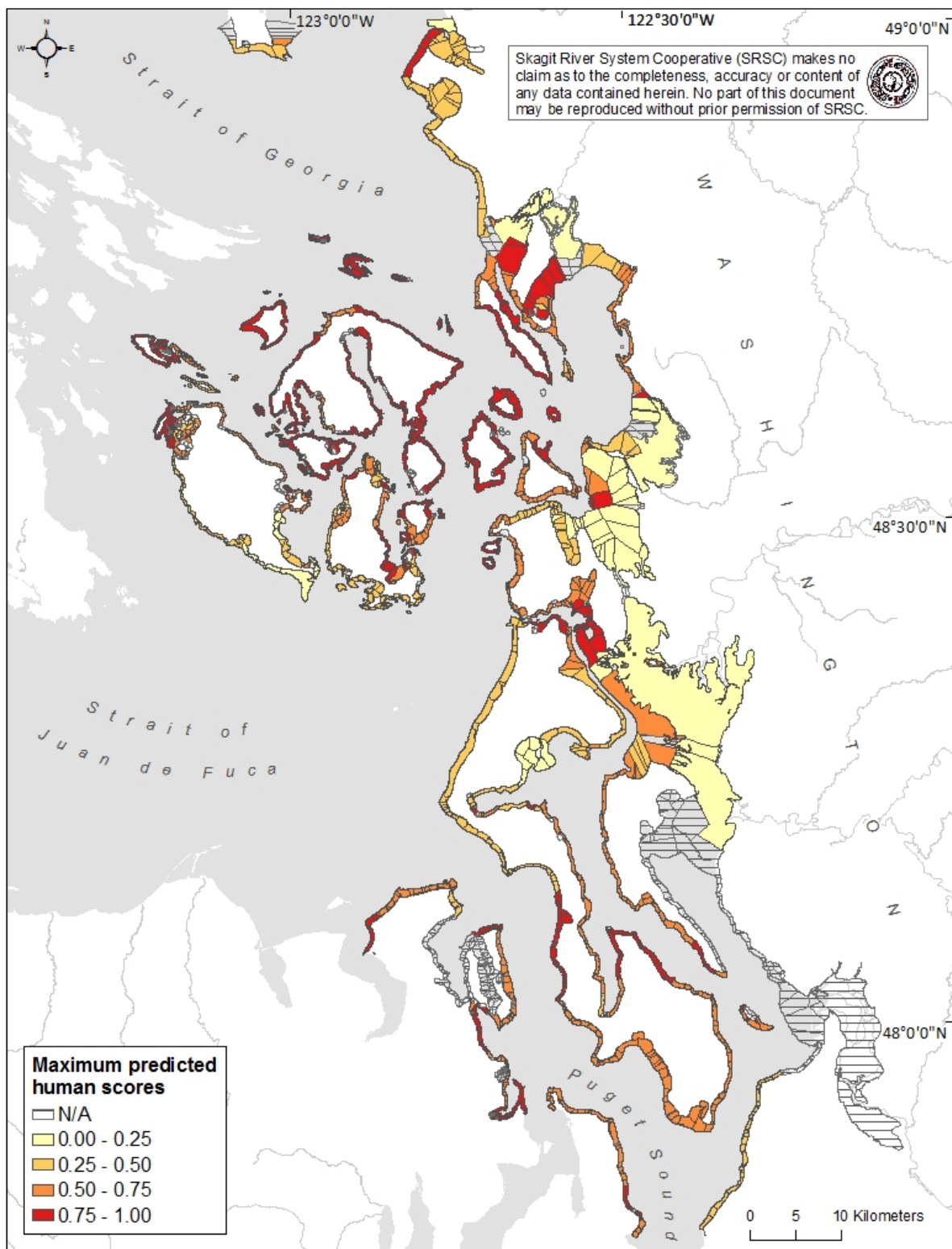


Figure 17. Map of maximum future human scores values based on percent forested area used for the wave and sea level rise resilience predictions. A score of zero equates to lower percentage of forested area in the 1990s.

## Discussion

### Utility of WSLRR framework

The framework presented here provides a tool to assess resilience of estuarine and nearshore habitats to erosional losses due to climate change. Although coarse in nature, this analysis illustrates how a landscape scale assessment of habitat characteristics can be combined with subjective information to provide a spatially explicit projection of risk to habitats throughout the study area. This information can be used to inform prioritization of habitat protection measures across the landscape in combination with future climate change predictions.

The target fish and shellfish species considered in this work (e.g., Chapter 4) require a diversity of habitats throughout the study area to complete their life cycles (Table 2). Projected vulnerability of estuarine or nearshore habitats to climate change may affect species differently depending on the species or life history stage occupying a specific habitat type. In some cases, the effect of habitat vulnerability on an individual species may not correlate well with the assessment of habitat vulnerability. For example, our analysis suggests that large river estuaries within the study area are at the most risk of erosional loss (e.g., large negative WSLRR value) due to increased wave energy and sea level rise under climate change (Figure 12 – Figure 13). For subyearling juvenile Chinook salmon that rear extensively in these habitats prior to initiating their seaward migration (Beamer et al. 2005, Quinn 2005), loss of this habitat may present a significantly higher risk to this species compared to fish and invertebrate species that do not necessarily rely on this habitat type. Conversely, rocky beaches are projected to be the least vulnerable to erosional processes and hence, the most resilient in their extent and structure to increasing wave energy and sea level rise due to climate change. However, fish and invertebrate species that utilize the more wave energy resilient rocky beaches may still be susceptible to the increase wave energy disturbance predicted from climate change even though rocky beach extent and structure is less likely to change compared to large river estuaries. Future spatial analyses could overlay known species distributions throughout the study area on top of habitat vulnerability results from this study to better link species-specific vulnerability to habitat vulnerability considering climate change projections.

Further work is needed to test the validity of this framework in assessing habitat vulnerability to climate change. Specifically, a logical next step should compare results from the WSLRR model with hydrodynamic model results that have been completed for subsets of GSU's within the study area (Yang et al. 2014).

### Limitations of current data and suggested improvements

Within the WSLRR model we used land use and shoreline armoring results from the PSNERP dataset (Simenstad et al. 2011) for the existing human score (EH) and predicted human score (PH). Surprisingly, these were the best available data covering the entire study area at the time of this study's inception. However, many of the results for land use and shoreline armoring are over 20 years old and therefore could bias the WSLRR model results. We suggest future efforts to improve this study utilize two new datasets that will soon be available; links to these data have been provided at the end of Chapter 2.

Additionally, the WSLRR model could be modified to incorporate site-based predictions of relative sea level rise (RSLR) which are now available through University of Washington's Climate Impacts Group at: <https://cig.uw.edu/resources/special-reports/sea-level-rise-in->

washington-state-a-2018-assessment/. The RSLR predictions are provided for a low (RCP 4.5) and a high greenhouse gas scenario (RCP 8.5). Results are presented in a probabilistic format so that their use in a model application can be flexible depending on how much management precautionary principle is being applied to questions addressed by the model.

## **Chapter 4. Nearshore surface water characteristics**

Environmental variability can influence the landscape distribution of fish and invertebrate species by affecting their ability to utilize habitats important for individual growth, survival, and reproduction. Temperature and salinity are two parameters that influence physiological processes critical to the persistence of aquatic species including metabolism and osmoregulation (Reed 1969, Numaguchi 1998, Webster & Dill 2006). The species considered in this report have known thermal and salinity ranges for different life stages beyond which individuals begin to experience deleterious physiological effects that may directly or indirectly lead to increased mortality (see Table 10). Adding to this complexity, species may require the use of specific habitats or shore types to successfully complete their lifecycle. For example, Dungeness crab larvae are pelagic while juvenile and adult Dungeness crab utilize sediment source beaches, barrier beaches, estuarine deltas, pocket estuaries, and low-energy bays. These shore types vary naturally in temperature and salinity and are likely to be impacted differently by climate change and other anthropogenic drivers. Therefore, to better understand how these species may respond to projected changes in SST and salinity, it is necessary to 1) evaluate factors that influence these parameters at the landscape scale so all relevant shore types are assessed, and 2) examine both current and projected conditions to understand changes in habitat suitability.

In this chapter we quantified relationships between current instantaneous observations of SST and salinity, landscape variables that account for landscape position, and shore type (Table 3). We then used the resulting models to generate predictions of SST and salinity throughout the study area. To illustrate how this tool could be used to assess species-specific vulnerability to increased thermal stress due to climate change, we used the resulting spatial map of SST to estimate the percentage of existing habitat suitable for target species (juvenile Chinook salmon, larval cockle clams, and postlarval and juvenile Dungeness crab) under current conditions and a projected climate change scenario of a 2.2°C increase in SST. Results from this study present a preliminary approach to identifying vulnerability of aquatic species to climate change across different habitat and shore types and may help inform prioritization of adaptive management actions to conserve species (e.g., Stein et al. 2013).

### **Methods**

We examined 6,672 observations of both SST and salinity collected over a 15-year period (2001-2015) from 169 sites located throughout Whidbey Basin, Bellingham and Samish Bays, and the San Juan Islands (detailed site descriptions provided in Beamer et al. 2006, 2007 & 2016, Beamer & Fresh 2012). The number of sites by shore type was barrier beach (30), large river estuary (48), pocket estuary (26), pocket beach (30), rocky beach (7), and sediment source beach (28). Additionally, six (6) modified shore sites were analyzed based on their current functional shore type; three were considered pocket estuaries and three were considered pocket beaches. Natural geomorphic shore types could not be assigned to the remaining modified sites because they did

not have uniform geomorphic characteristics and were therefore excluded from the analysis. Data from the 175 sites were used to complete the following three steps:

1. *Create a dataset of observed nearshore SST and salinity.* This step empirically creates nearshore SST and salinity results for our study area that are spatially and geomorphically explicit.
2. *Develop predictive models for nearshore SST and salinity.* This step develops predictive models of SST and salinity throughout our study area based on geomorphic (i.e., shore type) and landscape attributes, and
3. *Complete nearshore vulnerability analysis.* This step applies the most supported predictive models for nearshore SST and salinity to conduct a fisheries vulnerability analysis for the entire study area.

The dataset from step 1 created a baseline of current nearshore surface conditions in the study area that are spatially and geomorphically explicit. Predictive models were then developed based on geomorphic and landscape attributes to assess changes in SST and salinity for various shore types under projected climate change scenarios. We then compared the predicted changes in SST and salinity in the study area to known values of thermal and salinity tolerance/preference of target species to identify specific nearshore areas that are vulnerable to climate change.

### **GIS datasets**

We hypothesized that geomorphic and landscape variation (e.g., proximity to the source of fresh and saltwater) within the study area influences nearshore SST and salinity (Moore et al. 2008). Thus, we used the previously described (see Chapter 2) attributes for shore type, water depth adjacent to the nearshore (*MeanGSU\_Depth*), distance from nearest large river (*N\_LgRivKm*), and distance from the entrance of the Strait of Juan de Fuca (*DistSjfKm*; represents distance to ocean). These attributes were associated with each GSU\_ID polygon within the study area.

### **Sea surface temperature and salinity observations**

Following a literature review, we determined SST and salinity levels that were likely to cause some type of stress on fishes and shellfish (Table 10). For our analysis, we then utilized SST from the time of year where fish and shellfish may be most likely to experience metabolic stress due to high SST.

**Sea surface temperature:** Instantaneous observations of SST show a clear seasonal pattern and high degree of variability across shore types (Figure 18). Specifically, SST increases from late winter to July or August and then declines. There are apparent differences in SST between shore types that may be explained by landscape attributes such as the location of a specific shoreline relative to the source of warm or cold water (Figure 19A-C).

In order to quantify the warmest time of year, which reflects conditions fishes and shellfish experience during the summer, we averaged SST across July and August (*Tmean*). We also selected the maximum SST value observed between July and August for each site with adequate data (*Tmax*) (see Figure 18 for summary of all available SST data).

**Salinity:** Salinity and other water properties within our study area are influenced by the seasonal patterns of river flows entering the study area and Strait of Juan de Fuca salinity variability (Babson et al. 2006, Banas et al. 2015). The freshwater inputs within our study area include numerous small

ephemeral and year-round streams as well as several large rivers. The rivers within, or adjacent to, our study area include the Fraser, Nooksack, Skagit, Stillaguamish, and Snohomish rivers. There are apparent differences in salinity between shore types, but many of the differences may be explained by landscape attributes such as the location of a specific shoreline relative to the source of freshwater or seawater (Figure 19 D-F).

To create nearshore surface water salinity metrics reflecting the conditions fishes and shellfish experience annually, we calculated mean salinity (*Smean*), maximum salinity (*Smax*), and minimum salinity (*Smin*). The salinity observations were gleaned from fish monitoring studies which generally had two different monthly sampling regimes based on the expected period of juvenile Chinook salmon: 1) February through August for large river estuaries and pocket estuaries, and 2) February through October for all other shore types (see Figure C1 for summary of all available salinity data).

### **Analytical methods**

In this section we describe the analytical methods used to create prediction models of nearshore SST and salinity for use throughout our study area based on geomorphic (i.e., shore type) and landscape attributes.

#### **Data transformation**

For the SST models we used untransformed and natural log-transformed landscape variables. To account for the non-linear relationship between landscape variables and salinity metrics, we used natural log-transformed landscape variables prior to fitting models to the salinity metrics.

#### **ANOVA models**

We used analysis of variance (ANOVA) to assess the effect of shore type and landscape variables on SST and salinity. Modified shore type was excluded as an option for the factor “shore type” in our model because modified shore types do not have uniform geomorphic characteristics across the group. Specifically, we evaluated the following global model for SST (*Tmean* and *Tmax*) and salinity (*Smean*, *Smax*, and *Smin*).

$$f(Tmean, Tmax, Smean, Smax, Smin) = intercept + a \times Shore\ type + b \times MeanGSU\_Depth + c \times N\_LgRivKm + d \times DistSjfKm$$

where parameters *a* – *d* are the model coefficients for each covariate.

We used the Akaike information criterion corrected for small sample sizes (AICc; Burnham & Anderson 2002) to select the most parsimonious models that could be used for predicting nearshore SST and salinity metrics throughout the study area.

## **Results**

### **Mean July – August sea surface temperature (*Tmean*)**

The best model for mean SST included shore type and two log-transformed landscape variables: log-transformed mean water depth adjacent to the nearshore (*LnMeanGSU\_Depth*) and distance from the entrance of the Strait of Juan de Fuca (*DistSjfKm*) ( $R^2$  of 0.43,  $n=169$ , Table 7).

Pairwise analysis revealed that pocket estuaries are over 2.5°C warmer than all other shore types after controlling for landscape covariates (Table 8, Figure 18). Model coefficients for each shore type (relative to sediment source beaches) were:

- Barrier beach = -0.263
- Estuary, large river type = -0.389
- Estuary, pocket estuary type = 2.269
- Pocket beach = -0.540
- Rocky beach = -0.597
- Sediment source beach = 0.000
- Constant = 3.551

The numerical importance of the two landscape covariates in influencing mean SST is shown in Table 9 (and visually in Figure 19A-C). Deeper water adjacent to the nearshore yields colder nearshore surface water. Shorelines more distant from the entrance to the Strait of Juan de Fuca are warmer than shorelines closer to this source of ocean water. However, these relationships appear to vary significantly across shore types suggesting that some shore types may be more susceptible to future warming under climate change (Figure 19A-C). Inclusion of the landscape covariates within the model explained an additional 17% of the dataset's variation in mean SST (i.e.,  $R^2$  increased from 0.26 to 0.43).

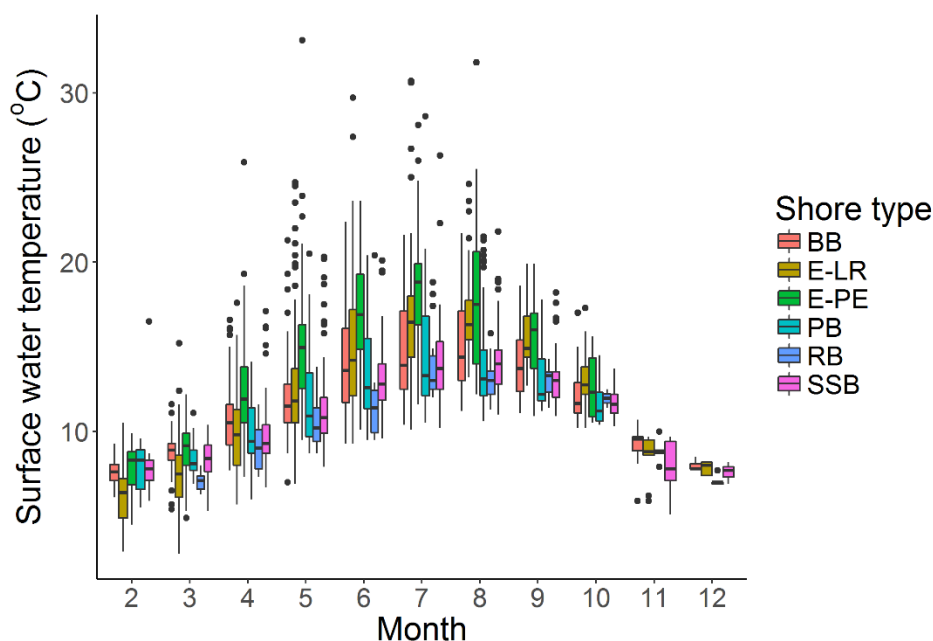


Figure 18. Boxplots of sea surface temperature (C°) by month and geomorphic shore type (excluding human-modified beaches). Data are from 6,872 observation collected at 173 sites across Whidbey Basin, Bellingham and Samish Bays, and the San Juan Islands. Shore type abbreviations are: BB = barrier beach; E-LR = estuary, large river type; E-PE = estuary, pocket estuary type; PB = pocket beach; RB = rocky beach; SSB = sediment source beach. Boxes show median, 25th and 75th percentiles. Whiskers show the 5th and 95th percentiles, circles are outliers.

Table 7. Performance of nearshore mean sea surface temperature models. All models shown, along with the included factors and/or covariates, are significant ( $p < 0.05$ ). The presence of an 'x, t, or u' means that a factor or covariate was included in the model. The presence of a 't' or 'u' denotes the covariate was natural log-transformed or untransformed, respectively. The best model has the lowest AICc value and is in bold font.

Shore type	Water depth adjacent to the nearshore	Distance to nearest large river	Distance to Strait of Juan de Fuca entrance	R <sup>2</sup>	AICc	ΔAICc
<b>x</b>	<b>t</b>		<b>u</b>	<b>0.43</b>	<b>742.70</b>	<b>0.00</b>
x			u	0.42	744.59	1.89
x	t		t	0.42	745.86	3.16
x	u		u	0.44	746.26	3.56
x			t	0.41	747.86	5.16
	t		t	0.30	768.47	25.77
	u		u	0.29	771.35	28.64
x		u		0.31	773.20	30.49
			u	0.26	774.18	31.48
x	u	u		0.31	775.07	32.37
x	t	t		0.30	777.95	35.25
			t	0.24	778.26	35.55
x		t		0.29	778.98	36.28
x	t			0.28	782.41	39.71
x				0.26	783.74	41.04
x				0.26	783.74	41.04
x	u			0.26	785.78	43.07
	t	t		0.15	798.09	55.39
	t			0.14	799.60	56.90
	u	u		0.15	801.60	58.89
		u		0.12	805.33	62.62
		t		0.09	810.23	67.53
	u			0.08	812.21	69.51

Table 8. Pairwise testing of mean sea surface temperature by shore type using Tukey's Honestly-Significant-Difference Test using least squares means from the model results with a MSE of 4.446 with 161 df. Pairs with p-values < 0.05 are bolded.

SHORE_TYPE(i)	SHORE_TYPE(j)	Difference	p-value	Lower 95% CI	Upper 95% CI
BB	E-LR	0.126	1	-1.3	1.524
<b>BB</b>	<b>E-PE</b>	<b>-2.532</b>	<b>&lt;0.001</b>	<b>-4.1</b>	<b>-0.922</b>
BB	PB	0.277	0.997	-1.3	1.828
BB	RB	0.334	0.999	-2.2	2.857
BB	SSB	0.216	0.999	-1.4	1.795
<b>E-LR</b>	<b>E-PE</b>	<b>-2.658</b>	<b>&lt;0.001</b>	<b>-4.1</b>	<b>-1.195</b>
E-LR	PB	0.151	1	-1.2	1.55
E-LR	RB	0.209	1	-2.2	2.64
E-LR	SSB	0.09	1	-1.3	1.519
<b>E-PE</b>	<b>PB</b>	<b>2.809</b>	<b>&lt;0.001</b>	<b>1.2</b>	<b>4.419</b>
<b>E-PE</b>	<b>RB</b>	<b>2.866</b>	<b>0.029</b>	<b>0.31</b>	<b>5.425</b>
<b>E-PE</b>	<b>SSB</b>	<b>2.748</b>	<b>&lt;0.001</b>	<b>1.11</b>	<b>4.385</b>
PB	RB	0.058	1	-2.5	2.58
PB	SSB	-0.061	1	-1.6	1.518
RB	SSB	-0.118	1	-2.7	2.421

Table 9. Summary of landscape coefficients estimated from the ANOVA model for mean sea surface temperature (*Tmean*) for all shore types. P-values significant at the 0.05 level are bolded.

Variable type	Variable	Coefficient	p-value
Covariate	<i>LnMeanGSU_DEPTH</i>	-0.301	<b>0.048</b>
	<i>DistSjfkKm</i>	0.074	<b>&lt;0.001</b>

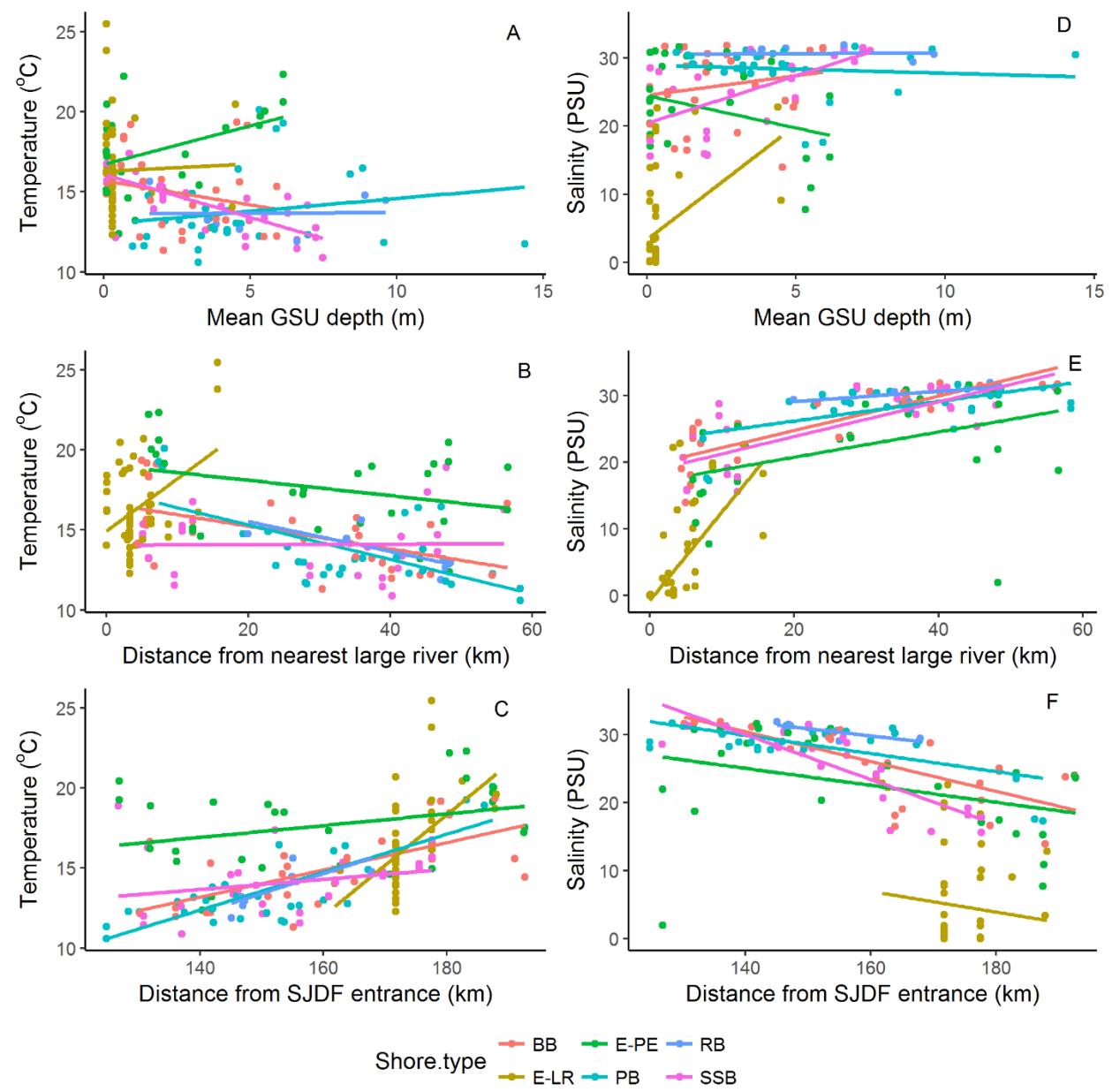


Figure 19. Relationships between observed mean sea surface temperature and salinity and three continuous landscape variables including mean geomorphic scaling unit depth (*MeanGSU\_Depth*), distance from the nearest large river (*N\_LgRivKm*), and distance from the entrance to the Strait of Juan de Fuca (*DistSjfKm*). Lines depict smoothed linear relationships estimated separately for each shore type.

## Additional sea surface temperature and salinity results

In the next section of this report we apply mean summer SST (*T<sub>mean</sub>*) predictions of the study area to biotic threshold relationships for three aquatic species to map habitat suitability and link climate change predictions for SST to future habitat suitability. We do not, however, provide the same habitat suitability applications for other nearshore SST values or any salinity values for two reasons:

1. Additional SST values were not applied mainly to keep the length of the report smaller. While anomalously high SST readings may affect younger life stages of species disproportionately, we felt the mean summer SST applications for multiple biota was adequate to illustrate the utility of the study's spatial dataset for climate change vulnerability analysis of the study area. Additionally, the prediction capability of the best maximum SST model was much poorer than the best mean SST model, making the utility for the application of *T<sub>max</sub>* more limited.
2. We do not currently have tools to link climate change predictions directly to any nearshore salinity value within our study area because climate changes predictions are for precipitation, snowpack, and streamflow change (Table 1), which in turn may influence nearshore salinity conditions within the study area.

Additional nearshore SST metrics that may be applicable to understanding physiological constraints of selected fish and shellfish include maximum, minimum, or the magnitude of SST anomalies depending on what life stage and species is being evaluated.

The same application to biotic threshold relationships is true for salinity values. However, for this report, we only explored whether we could create statistically significant models for additional SST and salinity metrics using shore type and landscape. Documentation of this pilot work is found in Appendix C. Additionally, models linking predicted changes in river streamflow to nearshore salinity metrics is a gap in knowledge and an important next generation of this study's framework.

The results of work described in Appendix C suggest that models can be developed that predict *T<sub>max</sub>* and the mean, maximum, and minimum values for salinity. Additionally, it is likely predictions can be made seasonally (i.e., not just annual estimates or estimates for the warmest/coldest and wettest/driest time of the year). Such models are needed to link climate change predictions for precipitation, snowpack, and streamflow (Table 1) to biotic response related to salinity change of nearshore biota (Table 10).

## **Application of prediction results to biotic thresholds**

Empirically established physiological thresholds specific to SST and salinity for selected fish and shellfish species can be useful linking understanding of species-specific life history to environmental conditions across the study area (Table 10). In this section we compare model predictions of nearshore SST across the study area to values presented in the scientific literature of thermal tolerance for specific life stages of target fish and shellfish species including juvenile Chinook salmon, larval cockle clams, and postlarval and juvenile Dungeness crab. We used the results to generate habitat suitability maps for each target species under current conditions and a 2.2°C increase in SST. These species-specific maps provide a landscape-scale climate change vulnerability assessment that identifies changes in habitat availability due to rising SST. Salinity model prediction results can be found in Appendix C but no biota-specific habitat suitability maps were created for salinity predictions as part of this study.

Table 10. Generalized threshold relationships for specific physical environmental parameters for selected fish and shellfish species utilizing nearshore habitats in the study area. ND = no known data source or thresholds not well understood relative to our predictive models, SST = sea surface temperature.

Species	Life stage	Salinity	SST (°C)	Dissolved oxygen	pH	References	
<i>Oncorhynchus tshawytscha</i>	Chinook salmon	Fry (<60 mm)	ND	Optimal 11 – 14; < Optimal 14.1 – 16; Stressful 16.1 – 20; Negative growth ≥ 20.1	ND	ND	(Hanson et al. 1997, Fresh 2006, Webster & Dill 2006, Beauchamp & Duffy 2011)
		Parr (60-150 mm)	Preference >15 but at 27 energy spent on internal regulation				
<i>Metacarcinus magister</i>	Dungeness crab	Larvae	Optimal 25-30	Megalopae only: Optimal 10-14; Optimal < 15-21; Extremely stressful >22	High	Suboptimal <7.1	(Reed 1969, Pauley et al. 1986, Sulkin & McKeen 1989, Sulkin et al. 1996, Holsman et al. 2003, Curtis & McGaw 2008, Curtis & McGaw 2012, Rasmuson 2013, Miller 2015)
		Juveniles (instars)	ND	High mortality >22	High	ND	
		Adults	Optimal 25-33, Suboptimal 16-24, Intolerable <16	Optimal 7-15, Suboptimal 16-20, Extremely stressful >20	High	ND	
<i>Panopea generosa</i>	Geoduck	Larvae	27-32	Optimal 6-16	High	ND	(Goodwin & Pease 1989)
		Juveniles	Saline	ND	High	ND	
		Adults	Optimal > 25; Tolerant 5-35	Spawn < 16	High	ND	
<i>Leukoma staminea</i>	Native littleneck clam	Larvae	Optimal 27-32	Optimal 10-15	High	ND	(Strathmann 1987)
		Juveniles	Saline	ND	High	ND	
		Adults	Optimal 24-31; Tolerant 20	Optimal 12-18	High	ND	
<i>Saxidomus gigantea</i>	Butter clam	Larvae	Optimal 20-29	Optimal 15	High	ND	(Quayle & Bourne 1972)
		Juveniles	Slow growth 5-15	ND	High	ND	
		Adults		Stressful <5 and >25	High	ND	

Table 10 continued.

Species	Life stage	Salinity	SST (°C)	Dissolved oxygen	pH	References		
<i>Clinocardium nuttallii</i>	Cockle	Larvae	ND	Optimal 10-22; Lethal >26	High	ND	(Gallucci & Gallucci 1982, Strathmann 1987, Liu et al. 2010 & 2011, Hiebert 2015)	
		Juveniles	ND	ND	High			ND
		Adults	ND	Lethal >26	High			ND
<i>Tresus sp.</i>	Horse clam	Larvae	Optimal 27-29	Lethal >20	High	ND	(Bourne & Smith 1972, Strathmann 1987, Harbo 1997, Coan et al. 2000, Hiebert 2015)	
		Juveniles	ND	ND	High	ND		
		Adults	ND	ND	High	ND		
<i>Ruditapes philippinarum</i>	Manila clam	Larvae	Optimal >10	>14	High	ND	(Bardach et al. 1972, Numaguchi 1998)	
		Juveniles	ND	ND	High	ND		
		Adults	Optimal 24-32	Optimal 13-21; Spawn >14	High	ND		
<i>Ostrea lurida</i>	Olympia oyster	Larvae	No growth or development ≤15	Vulnerable to high SST	High	Reduced shell growth, metamorphosis 7.8	(Strathmann 1987, Hettinger et al. 2012 & 2013, Cheng et al. 2015, Rippington 2015, Barber et al. 2016, Gray & Langdon 2018, Hollarsmith et al. 2020)	
		Juveniles	High mortality <10 when exposed ≥5 days	Vulnerable to high SST	High	Reduced shell growth <8.0		
		Adults	Feeding ceases <10; Feeding effects 10-20; Optimum >25	Brood >10.5; Decreased survival >14	High	ND		

## Climate change scenarios for sea surface temperature

Across the North Pacific, SST increased by 0.1 °C/yr to 0.3 °C/yr from 1950 to 2009 with continued SST warming anticipated for the entire North Pacific over the next century (Poloczanska et al. 2013). Relative to mean conditions from 1956 to 2000, projected SST increases for 2050 to 2099 range from a 1.4 °C to 2.2 °C increase under climate change prediction RCP 4.5 (Barange et al. 2018). The RCP 4.5 scenario assumes greenhouse gas emissions will peak in year 2040 (IPCC 2014) and, therefore, may be on the lower bound of potential changes to our global climate (i.e., this represents a less extreme, more optimistic on the greenhouse gas reduction timeline). Thus, some of these results may be considered conservative in light of the current lack of global political will to reduce greenhouse gas emissions. For the purpose of illustrating the utility of the dataset and analytical framework we applied the upper limit of the IPCC's RCP 4.5 prediction of increased SST for the North Pacific Ocean (2.2 °C) to our mean SST dataset.

## Vulnerability results for sea surface temperature

We applied the regression equations described earlier in Chapter 4 to the GSU\_ID dataset to estimate nearshore SST metrics for all GSU\_IDs within the study area. Because individual GSU\_IDs may have more than one shore type present, we applied the dominant shore type by shoreline length to each model. Forty-four of 1,742 GSU\_IDs are dominated by the modified shore type classification. Modified shore type GSU\_IDs were modeled based on their current functional shore type. For example, three GSU\_IDs in the urbanized Bellingham Bay shoreline (Whatcom Waterway, I & J St. Waterway, and Squalicum Harbor) were all modeled as pocket estuaries due to their high degree of shoreline enclosure and localized freshwater inputs. The 44 modified shore type GSU\_IDs were modeled as barrier beaches (13), pocket estuaries (23), sediment source beaches (7), and rocky beach (1).

The role of this report is not to provide exhaustive fish and shellfish nearshore habitat vulnerability predictions but rather to present a dataset and framework to conduct such analyses as part of an ongoing program. Here we demonstrate how this framework can be used to predict the vulnerability of target species under current SST regimes and a future SST regime based on the RCP 4.5 scenario of a 2.2°C increase in SST.

We used the regression results from the best mean SST model to predict SST for each GSU\_ID. The equations by shore type were:

- $T_{mean}$  (Barrier beaches) =  $-0.263 + \ln(\text{MeanGSU\_Depth}) \times -0.301 + \text{DistSjfKm} \times 0.074 + 3.551$
- $T_{mean}$  (Estuary, large river type) =  $-0.389 + \ln(\text{MeanGSU\_Depth}) \times 0.301 + \text{DistSjfKm} \times 0.074 + 3.551$
- $T_{mean}$  (Estuary, pocket estuary type) =  $2.269 + \ln(\text{MeanGSU\_Depth}) \times -0.301 + \text{DistSjfKm} \times 0.074 + 3.551$
- $T_{mean}$  (Pocket beach) =  $-0.54 + \ln(\text{MeanGSU\_Depth}) \times -0.301 + \text{DistSjfKm} \times 0.074 + 3.551$
- $T_{mean}$  (Rocky beach) =  $-0.597 + \ln(\text{MeanGSU\_Depth}) \times -0.301 + \text{DistSjfKm} \times 0.074 + 3.551$
- $T_{mean}$  (Sediment source beach) =  $\ln(\text{MeanGSU\_Depth}) \times -0.301 + \text{DistSjfKm} \times 0.074 + 3.551$

To improve the accuracy of SST predictions for pocket estuaries and large river estuary areas that are cutoff from direct river flow, we applied an adjustment to the mean SST predictions based on the presence/absence of local freshwater (FW) inputs to the nearshore. There was no statistically significant relationship between mean SST and the presence/absence of a FW input in our dataset ( $p = 0.339$ ) (Figure 20). However, the result is likely an artifact caused by a small sample size and imbalance in observations ( $n = 5$  for no FW input;  $n = 21$  for FW input). On average, estuaries with a FW input had SSTs that were  $1.3^{\circ}\text{C}$  warmer than those without FW input. We suggest the small surface FW inputs flowing into the nearshore have a higher mean SST than the adjacent sea surface water. In the semi-enclosed environment of pocket estuaries these small surface FW flows are likely to lead to warmer SSTs. Thus, to improve the mean SST prediction for each GSU\_ID we added  $1.3^{\circ}\text{C}$  to model predictions of SSTs for pocket estuaries with known FW inputs. GSU\_IDs with FW inputs were derived from the SSHIAP geomorphic layer (i.e., McBride et. al 2009) where presence of a FW input is a data category.

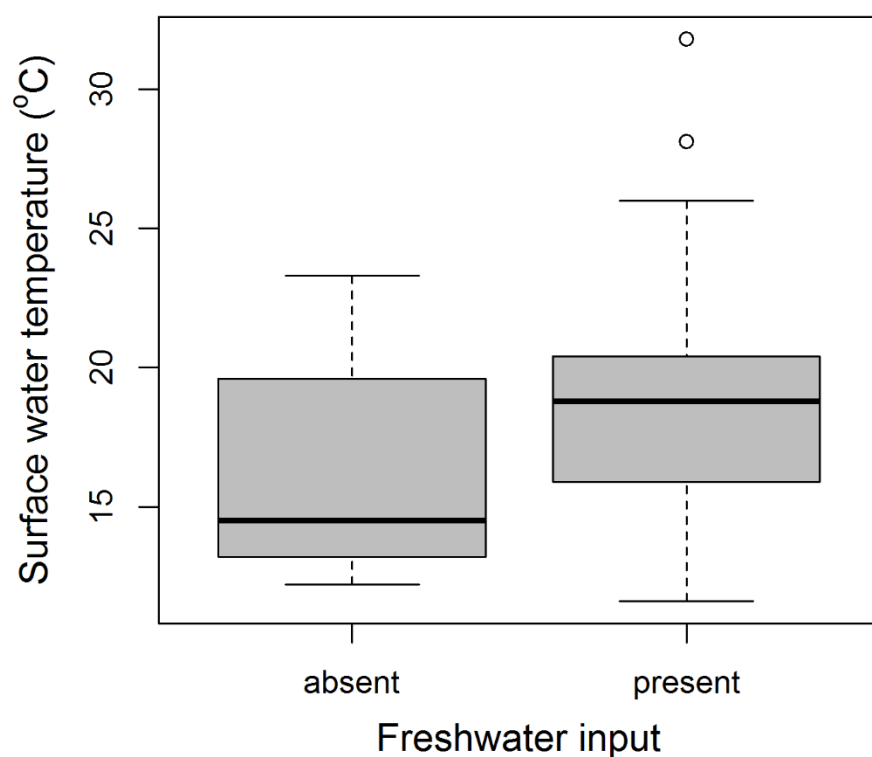


Figure 20. Boxplot showing the distribution nearshore sea surface temperature ( $^{\circ}\text{C}$ ) in July/August in pocket estuaries with ( $n = 21$ ) or without ( $n = 5$ ) direct freshwater sources. Boxes show median, 25th and 75th percentiles. Whiskers show the 5th and 95th percentiles and circles are outliers.

***Predictions of mean sea surface temperature***

Our estimates of mean nearshore SST during the summer under current conditions ranged from 10.9 to 23.2°C throughout the study area with the coldest areas located on the west side of San Juan Island and the warmest areas located within isolated parts of large river estuaries and pocket estuaries (Figure 21). Categorically applying a 2.2°C increase in North Pacific Ocean SST to the study area resulted in mean nearshore SSTs ranging from 13.1 to 25.4°C (Figure 22).

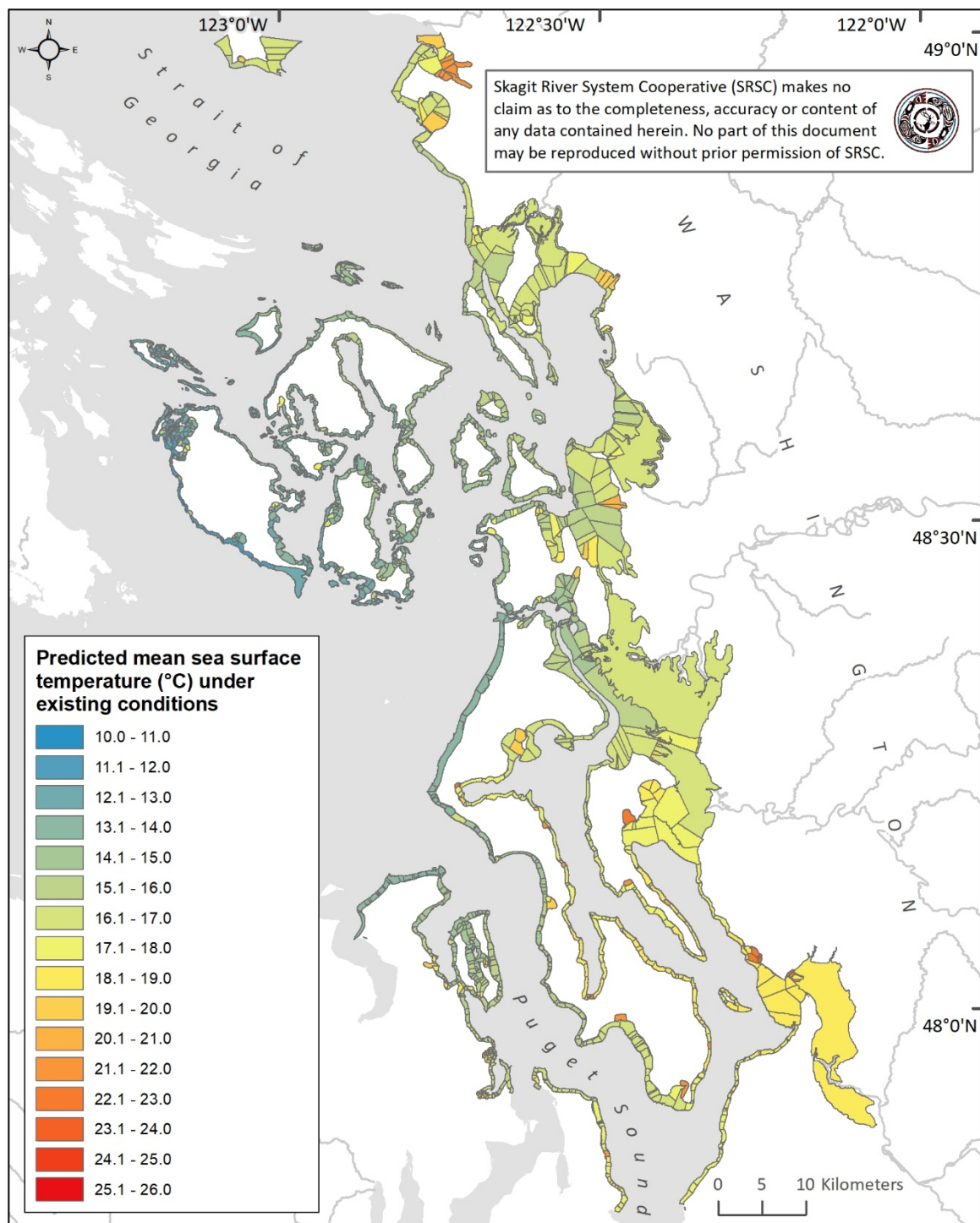


Figure 21. Spatial distribution of mean July/August sea surface temperature under existing conditions.

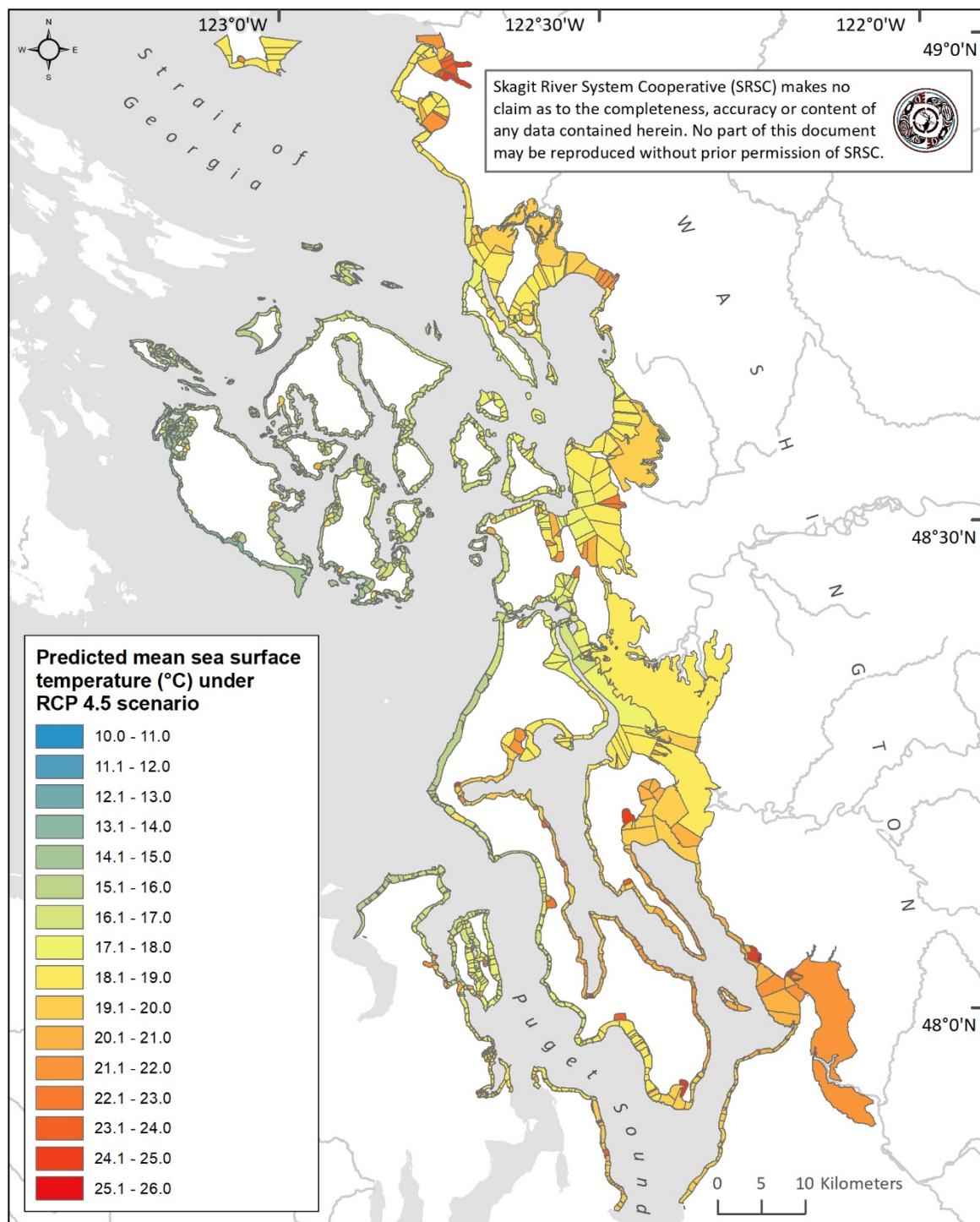


Figure 22. Spatial distribution of mean July/August sea surface temperature under a future climate change scenario of a 2.2°C rise in sea surface temperature.

### ***Juvenile Chinook salmon growth under current and future sea surface temperature regimes***

We applied known thresholds for juvenile Chinook salmon growth to the study area's summer mean nearshore SST under current conditions and a 2.2°C SST climate change scenario (Table 10). Instead of using a single threshold metric for SST and juvenile Chinook growth, we translated temperature-influenced growth curves previously developed for Chinook salmon into four growth bins (Beauchamp & Duffy 2011). The optimal temperature range for juvenile Chinook salmon growth is 11 – 14°C, beyond which growth rates begin to decline. Growth can become negative when food is less abundant at 16°C (~50 % of a full ration) so we assigned growth as '< optimal' for SSTs between 14.1 - 16°C and 'stressful' for SSTs between 16.1 - 20°C. At SSTs  $\geq$  20°C, the metabolic deficit results in negative growth rates, even with abundant food (Beauchamp & Duffy 2011).

Under current July/August SST conditions, the non-estuary shore types within the study area generally have growth conditions considered metabolically favorable for juvenile Chinook salmon (Figure 23 & Figure 24). In contrast, July/August SSTs within all the large river and pocket estuarine habitats exceeded those that would be considered metabolically favorable for juvenile Chinook salmon. These results suggest that growth opportunity for juvenile Chinook salmon is dependent on an individual's ability to time their rearing and migration behavior such that they utilize each habitat type when temperature and food availability are optimal. Based on our prior observations of rearing and migration patterns of juvenile Chinook salmon originating from the Skagit River, fish appear to be adapted to transition from large river estuaries to nearshore habitats as temperatures begin to exceed optimal metabolic thresholds (Figure 25). Specifically, in the Skagit River estuary, Chinook fry reach peak densities between March and May, after which they move to the nearshore marine habitats of Skagit Bay where temperatures are more favorable for growth (Beamer et al. 2005).

Under the climate change scenario of a 2.2°C increase in July/August SST, we predicted a major reduction in the percentage of nearshore habitat within the study area that would be considered metabolically favorable for juvenile Chinook salmon. Specifically, only a small percentage of rocky beach shore types remain optimal for Chinook salmon growth based on the SST threshold of 11-14°C. In general, the nearshore habitats most conducive to Chinook growth under the climate change scenario are pocket and rocky beach shore types along with some sediment source beaches or barrier beaches, particularly those located further from rivers such as within the San Juan Islands or along the western Whidbey Island shore (Figure 23 & Figure 26).

As the spatial and temporal window for optimal growth potential in critical rearing habitats, such as estuaries, is constrained under future climate change, juvenile Chinook salmon may be forced to move prematurely to more favorable SSTs in nearshore habitats at the expense of increased predation risk. Indeed, juvenile Chinook salmon tend to experience higher marine survival rates if they spend more time rearing in estuaries, maximizing their growth prior to moving to nearshore/open water. Except for shore types in the western San Juan Islands, juvenile Chinook salmon may be required to transition from the nearshore to offshore habitats (neritic) by July/August if SSTs increase by the predicted 2.2°C. That movement translates to an approximately two-month earlier shift in the timing of offshore migration by juvenile Chinook (Figure 25). Unless these fish can achieve sufficient growth prior to moving offshore, marine survival may be reduced in the future.

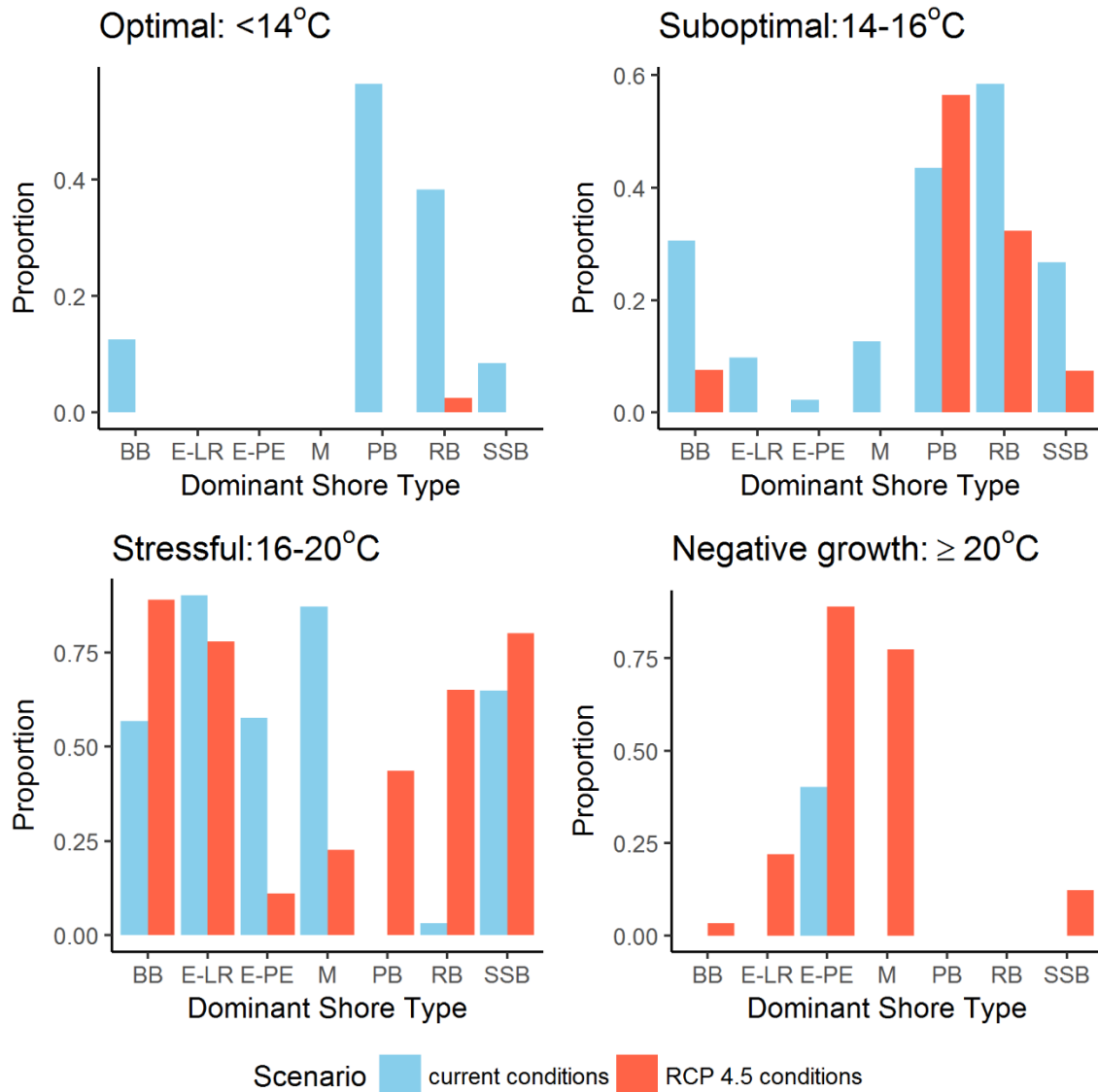


Figure 23. Percent distribution of each shore type across the study area overlapping sea surface temperature (SST)-dependent growth categories for juvenile Chinook salmon based on mean SST in July/August under existing conditions and a future climate change scenario of a 2.2°C increase in SST. BB = barrier beach, E-LR = large river estuary, E-PE = pocket estuary, M = modified, PB = pocket beach, RB = rocky beach, SSB = sediment source beach.

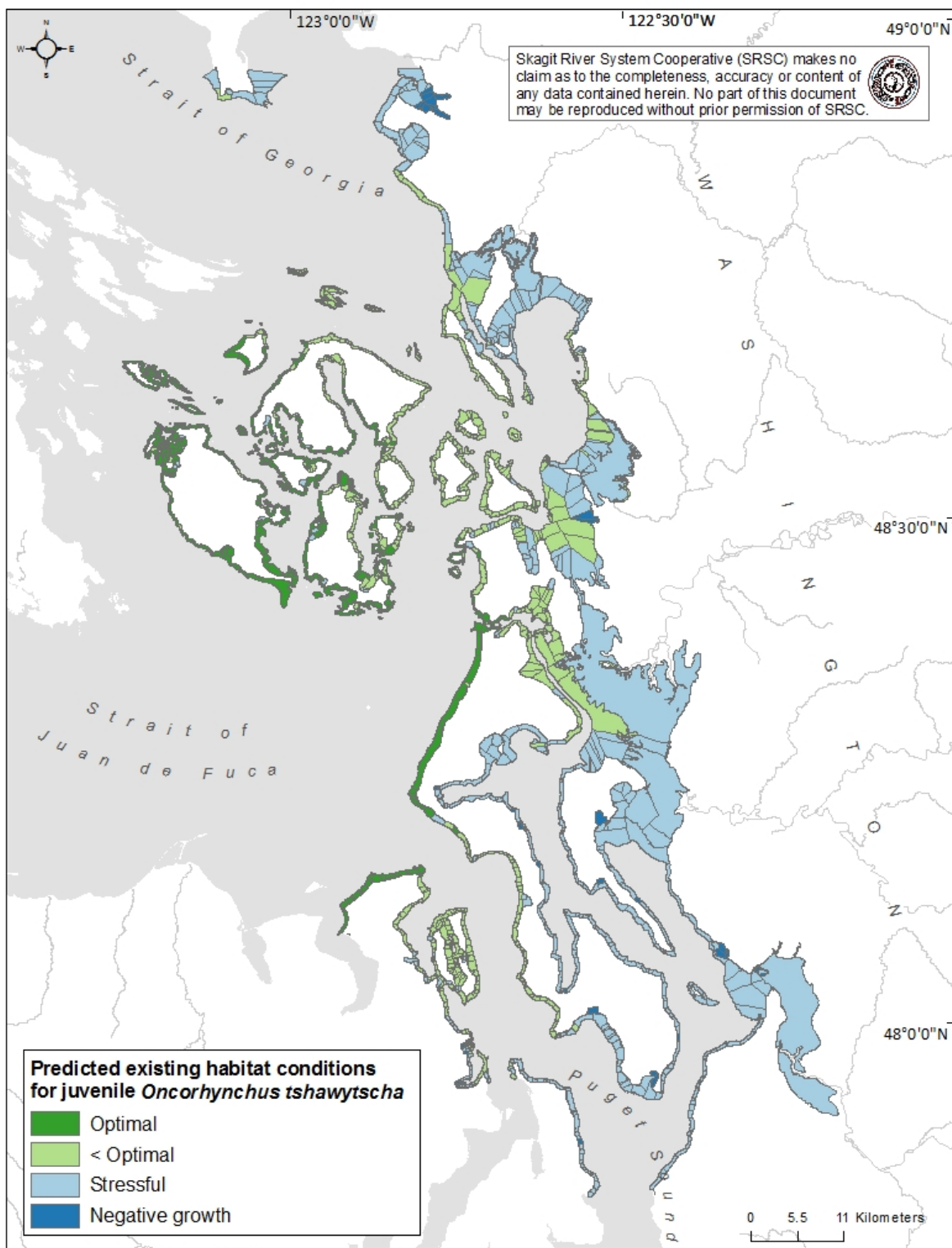


Figure 24. Spatial distribution of optimal growth ranges for juvenile Chinook based on mean water temperature in July/August under existing conditions. Optimal growth = 11°C – 14°C; < optimal = 14.1°C – 16°C; stressful = 16.1°C – 20°C; negative growth is  $\geq 20.1^\circ\text{C}$ .

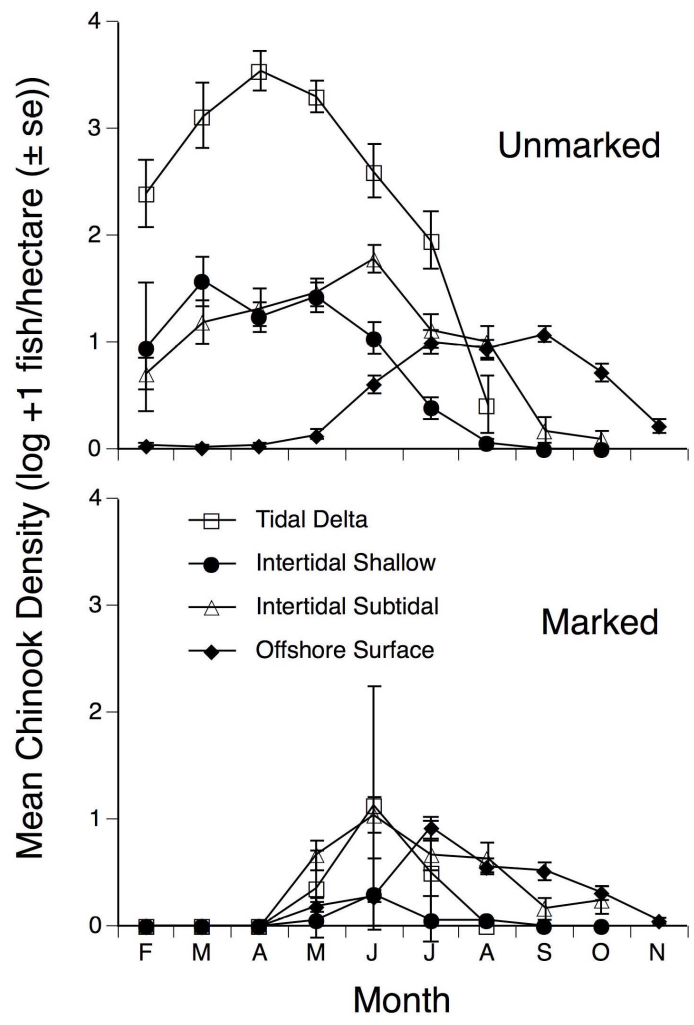


Figure 25. Mean density of marked (hatchery origin) and unmarked (natural origin) juvenile Chinook salmon by habitat type and month in the Skagit River estuary and Skagit Bay (Figure 2.1 from Beamer et al. 2005).

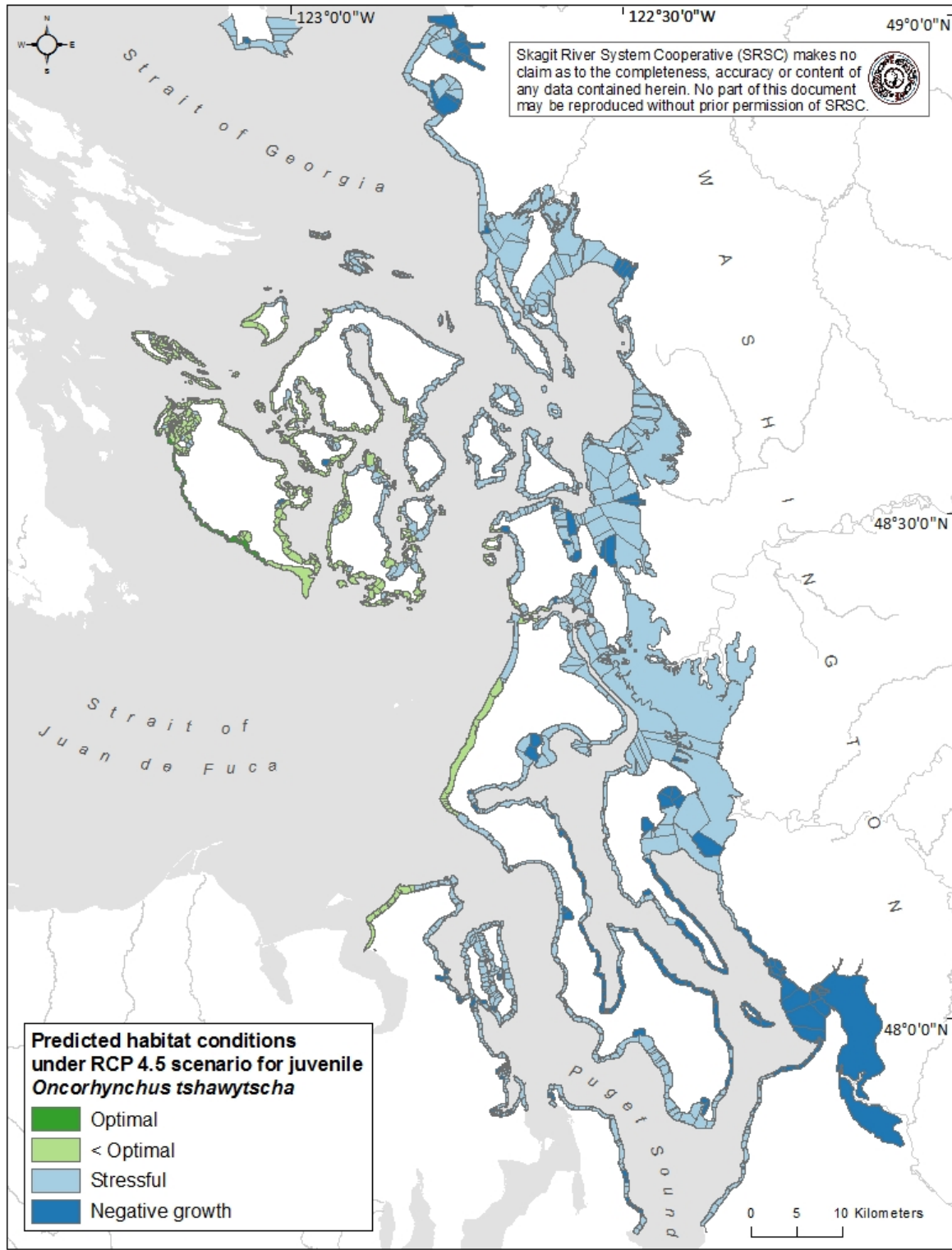


Figure 26. Spatial distribution of optimal growth ranges for juvenile Chinook based on mean water temperature in July/August under a climate change scenario where sea surface temperatures rise by 2.2°C. Optimal growth = 11°C – 14°C; < optimal = 14.1°C – 16°C; stressful = 16.1°C – 20°C; negative growth is ≥ 20.1°C.

### **Cockle larvae survival under current and future sea surface temperature regimes**

The basket cockle, *Clinocardium nuttallii*, is a native intertidal clam species harvested year-round by SITC and other Coast Salish tribes. *C. nuttallii* inhabit the low intertidal to shallow subtidal zones and can be found from Alaska to California on tidal flats comprised of fine to medium sand and in eelgrass beds. Unlike most bivalves, *C. nuttallii* do not burrow into the sediment as they grow. Instead they reside on or just below the surface of the beach where fluctuations in parameters such as SST and weather extremes can result in high mortality (Gallucci & Gallucci 1982, Harbo 1997, Coan et al. 2000).

For cockles, as well as other bivalves, temperature can affect growth, reproduction, and recruitment which influences population dynamics (Pörtner 2002). In early-life history stages, individuals can exhibit a range of effects from elevated temperature including enhanced growth and reduced size, increased metabolic stress, or mortality (Byrne & Przeslawski 2013). Because cockles within the study area spawn from April-November, changes in mean summer SST can greatly impact successful recruitment. In a laboratory setting, Liu et al. (2010) found optimal temperatures for cockle larval growth and survival ranged from 10-22°C and temperatures above 26°C were lethal (Table 10). Thus, we applied two thresholds (optimal 10-22°C and < optimal 23-25°C) to the study area's mean SST estimates under current conditions and a projected increase of 2.2°C SST to assess larval survival potential.

Under current conditions, we predicted habitat across all shore types within the study area would have SSTs that were cooler than the suboptimal SST threshold for cockle larvae with the exception that a small percentage of pocket estuaries (<10%, 281 of nearly 3,000 hectares) exceeded 22°C (Figure 27). Under the climate change scenario of a 2.2°C increase in SST, we predicted that all shore type habitats within the study area would remain within the optimal SST range except pocket estuaries where the percent under suboptimal conditions increased to 45% (1340 of nearly 3,000 hectares; Figure 28).

These results suggest minimal impacts on habitat availability for cockle larvae due to a projected increase in SST, however, they should be interpreted with caution and should not be extrapolated to different life history stages for cockles or other clam species. Species sensitivity to increased SST varies depending on life stage and life history. Additional research on thermal tolerances and biological performance of bivalve species would provide more robust results.

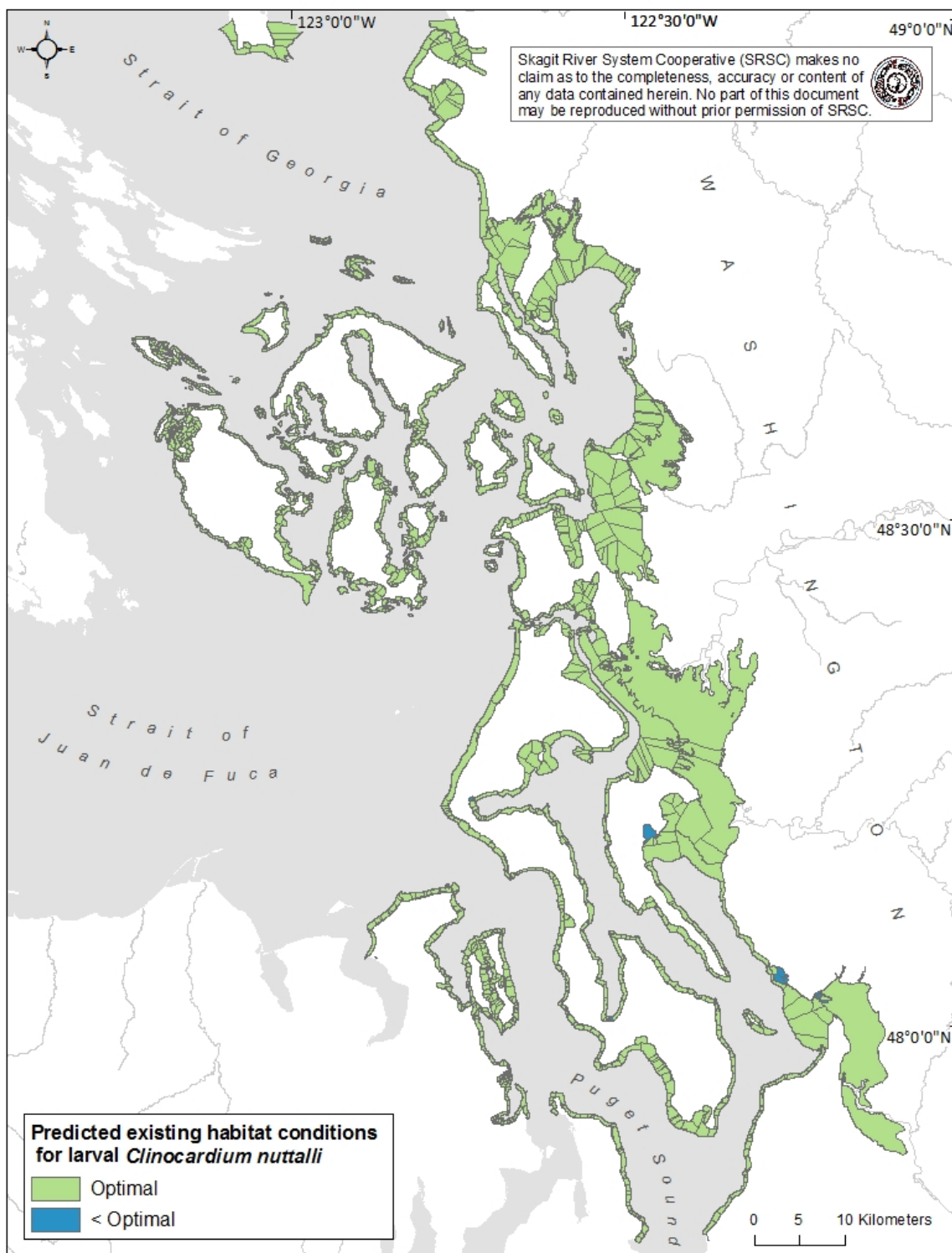


Figure 27. Spatial distribution of larval basket cockle, *Clinocardium nuttalli*, survival potential based on mean water temperature July/August under existing conditions. Optimal survival = 10-22°C; < optimal = 23-25°C.

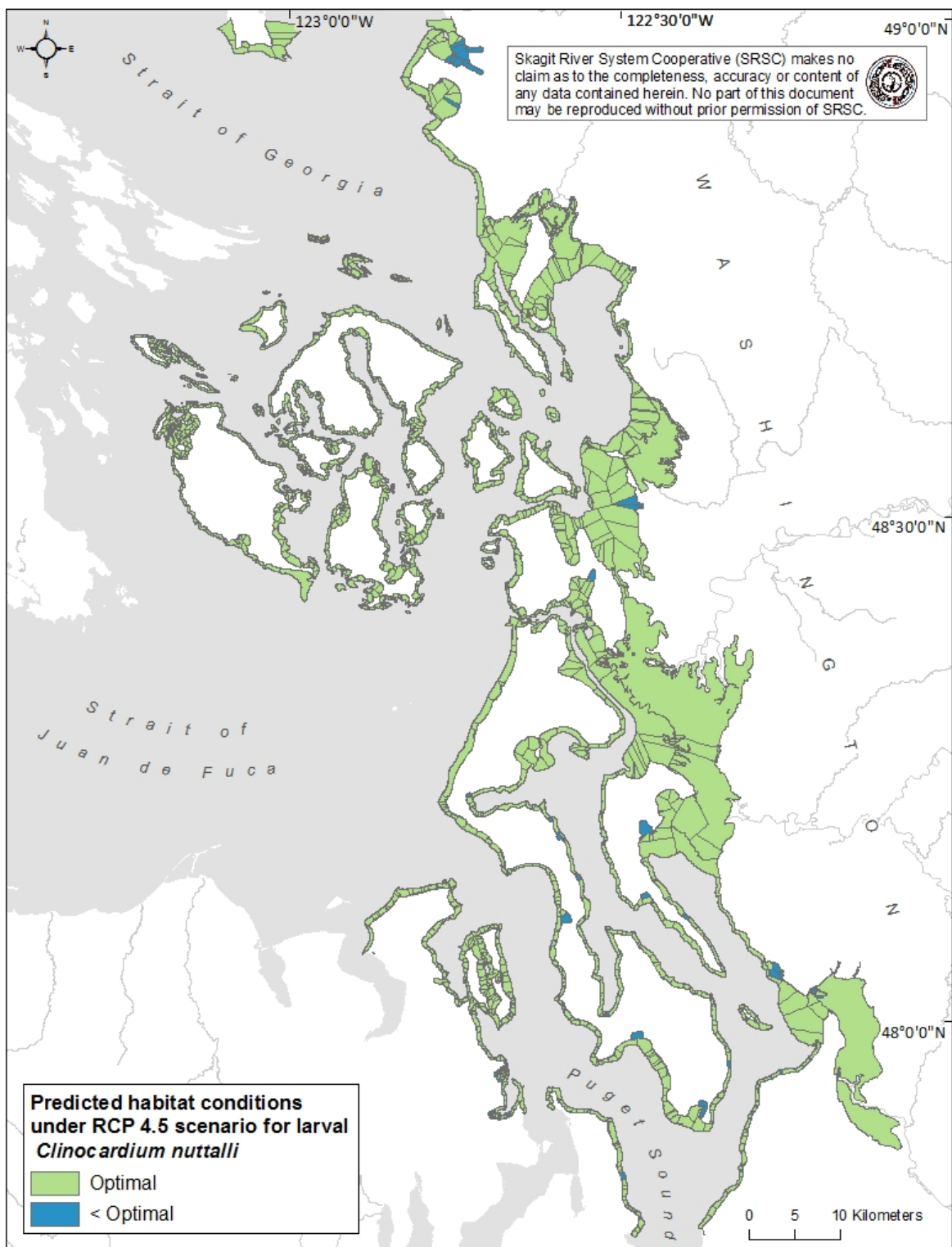


Figure 28. Spatial distribution of larval basket cockle, *Clinocardium nuttalli*, survival potential based on mean water temperature in July/August under a climate change scenario where sea surface temperatures rise by 2.2°C. Optimal survival = 10-22°C; < optimal = 23-25°C.

### **Postlarval and juvenile Dungeness crab survival under current and future sea surface temperature regimes**

The Dungeness crab, *Metacarcinus magister*, not only serves a culturally-important role for Indigenous tribes, but the species is also the source of a multimillion-dollar fishery along the northeastern Pacific coast (Suttles 1974, Losey et al. 2004, PSMFC 2014). *Metacarcinus magister* is also a substantial predator and prey item, thus playing a valuable role in marine food web health (as reviewed in Rasmuson 2013). Despite the obvious importance of this species, however, Dungeness crab face many potential human-caused threats including ocean acidification and warming sea surface temperatures (Ekstrom et al. 2015, Marshall et al. 2017). As these threats intensify, scientists and managers will need to develop adaptive responses to sustain this species.

*Metacarcinus magister* ranges from the Pribilof Islands, Alaska to Santa Barbara, California and is capable of occupying open ocean habitat as well as the estuarine habitats of inland fjords (Rasmuson 2013). Due to the extensive range of this species, *M. magister* biology can vary dramatically by latitude and oceanographic system (e.g., in California larvae are released in the winter but larvae from Alaskan Dungeness crab are released in the summer). Larval and postlarval phases last ~four months and consist of five zoeal and one postlarval megalopal stage (Rasmuson 2013). For the purposes of this report, the term “larvae” will refer to both larval and postlarval stages and “postlarvae” refers solely to megalopae, unless otherwise noted. Megalopae found in the coastal and inland waters of Washington State typically settle and metamorphosize into benthic instars (juveniles) from spring to the end of summer (Dinnel et al. 1993). We opted to focus our work on postlarval and juvenile Dungeness crab life stages because they are slightly better understood in our region than zoeal stages and because we know they are located in our nearshore waters. Most interestingly, within Washington’s inland waters, multiple recruitment cohorts of Dungeness crab are known to exist with some cohorts presumably originating from within Puget Sound or Hood Canal populations and a smaller proportion of recruits possibly originating from oceanic stocks in some years (Dinnel et al. 1993). The timing of settlement and metamorphosis of megalopae to phenotypically-distinct instars generally ranges from May to August; with the cohort that may be originating from the oceanic population settling in late spring and the cohort believed to be originating within Puget Sound settling in mid-summer (Dinnel et al. 1993).

Sulkin et al. (1996) found that if *M. magister* could reach the megalopal stage, the megalopae could tolerate laboratory water temperatures up to 22°C. Water temperatures ranging from 15-22°C are considered suboptimal for megalopae, as studies have shown that while larval duration may be shortened in higher temperatures, subsequent mortality rates of benthic instars may increase at higher temperatures (Sulkin et al. 1996, Rasmuson 2013). Therefore, to assess survival potential for Dungeness crab postlarval and juvenile phases under existing conditions and a 2.2°C SST climate change scenario, we assigned water temperatures for survival potential as optimal (10-14°C), suboptimal (15-21°C), or extremely stressful (>22°C). For this study, we did not assign a lethal temperature range because it is likely to be 25°C or higher and because crab could conceivably move out of some stressful conditions.

Under current conditions, most nearshore habitats preferred by early life stage crab within the study area (sediment source beaches, barrier beaches, and estuaries) have SSTs that are less than optimal for postlarval or juvenile survival by July/August (Figure 29 & Figure 30). Exceptions to this pattern are the pocket and rocky beach shore types, particularly those located further from rivers; these still provide optimal growth conditions for early life stages of Dungeness crab. Under

the climate change scenario of a 2.2°C rise in SST, we predicted virtually all shore type habitats within the study area would have suboptimal temperatures for crab postlarvae and juveniles (Figure 29 & Figure 31).

Our analysis suggests that preferred crab habitats are the most susceptible to increases in SST relative to Chinook salmon and cockles. The predicted spatial shift in optimal thermal habitats supporting postlarval and juvenile crab growth under climate change may not only result in reduced cohort survival due to thermal tolerance mismatch but may result in density dependent processes, such as increased cannibalism. Importantly, if the presumed Puget Sound larval cohort is identified as a genetically-distinct population, this cohort is likely to be exposed to higher late summer temperatures during the critical time period of postlarval settlement to the benthos. Differential impacts to cohorts could affect how this fishery needs to be managed in the future. Our study results also can be hypothetically linked to effects on other species because the survival of one species may impact the survival of others. For example, because Dungeness crab larvae are an important prey resource to juvenile Chinook salmon, variability in crab survival may also influence the survival of juvenile Chinook salmon (Duffy & Beauchamp 2011).

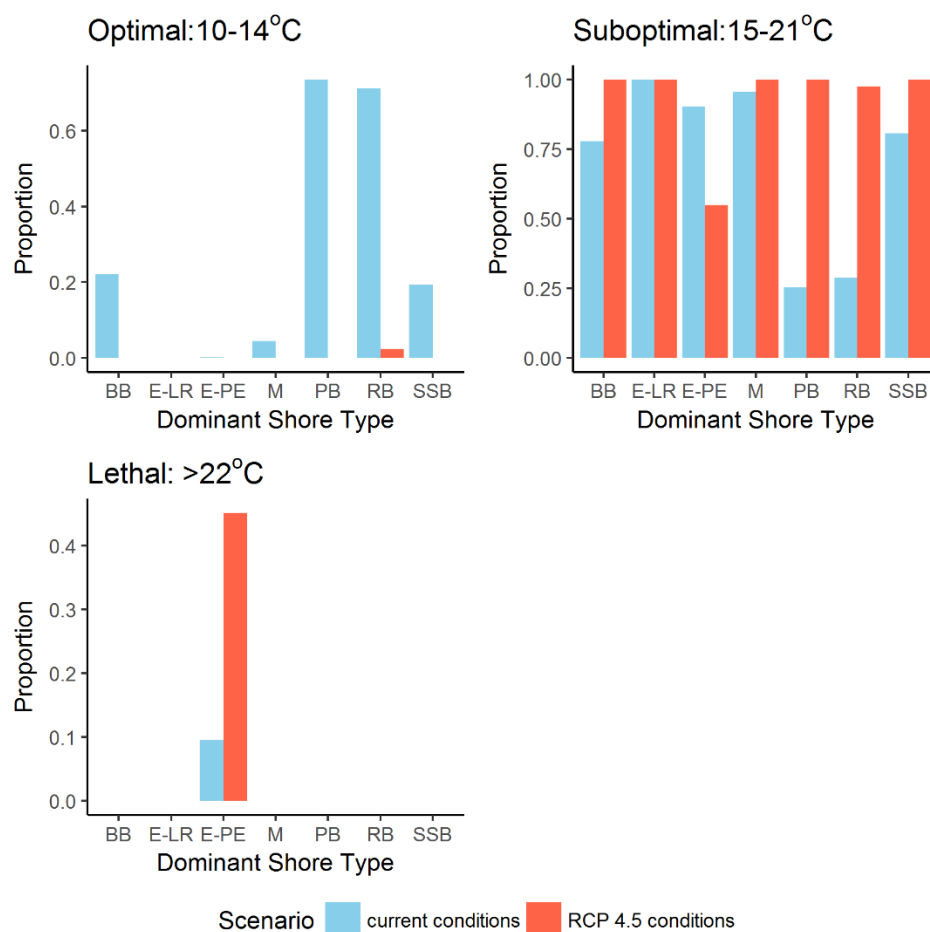


Figure 29. Percent distribution of each shore type across the study area and megalopae and juvenile Dungeness crab survival potential in July/August under existing sea surface temperature conditions and future climate change scenario of a 2.2°C increase in sea surface temperature. BB = barrier beach, E-LR = large river estuary, E-PE = pocket estuary, M = modified, PB = pocket beach, RB = rocky beach, SSB = sediment source beach.

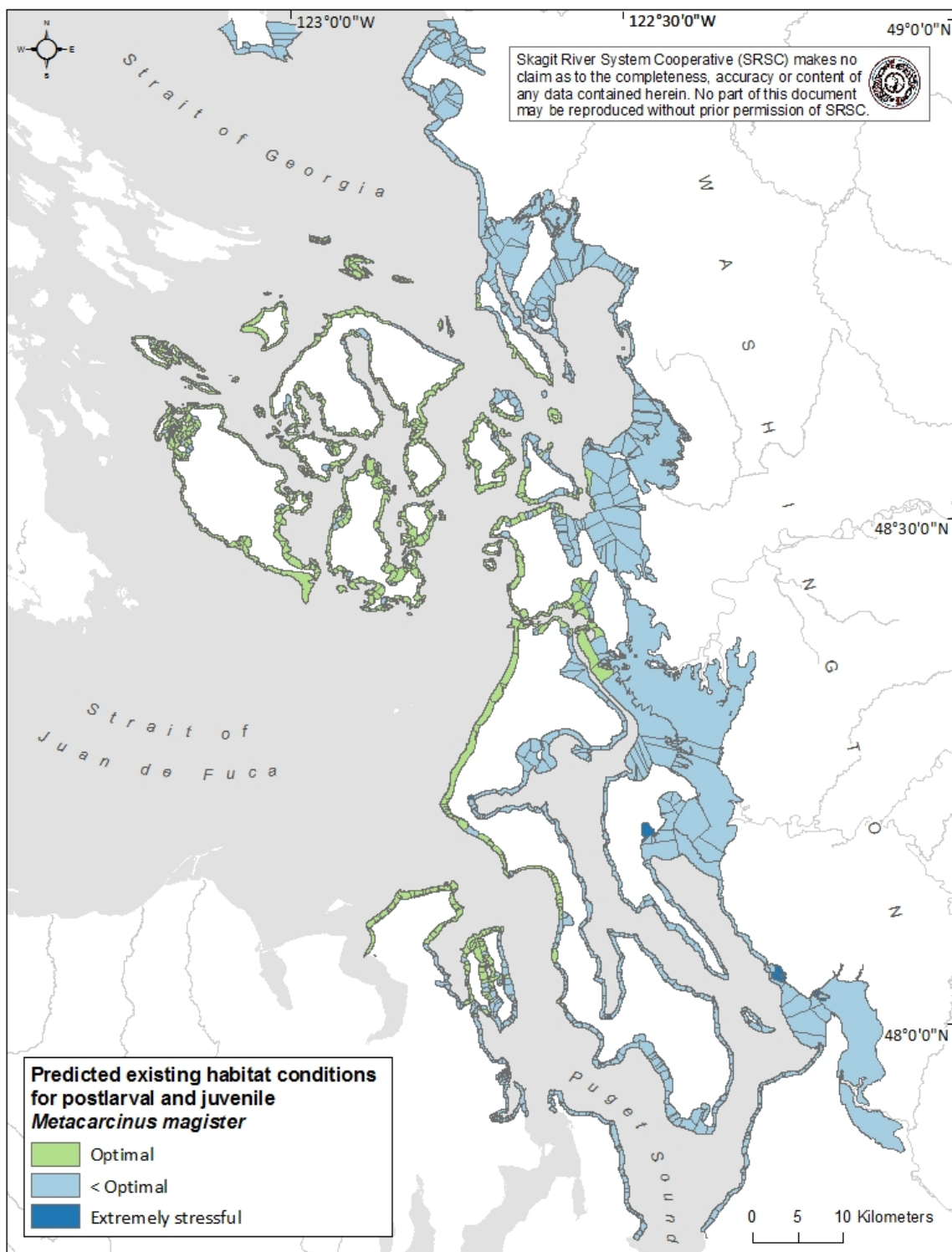


Figure 30. Spatial distribution of postlarval and juvenile Dungeness crab survival potential in July/August under existing conditions. Optimal survival = 10-14°C; < optimal = 15-21°C; extremely stressful = > 22°C.

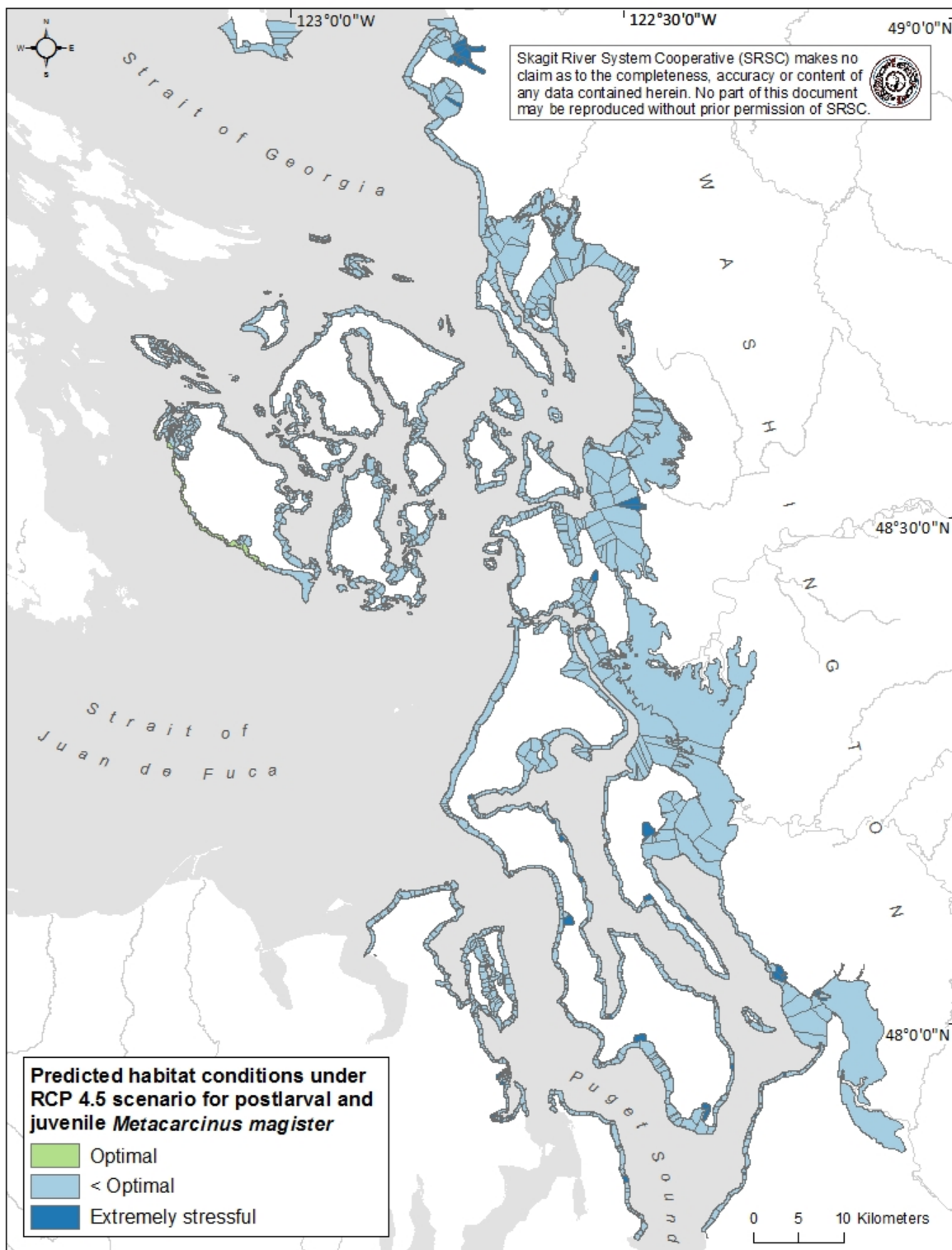


Figure 31. Spatial distribution of postlarval and juvenile Dungeness crab survival potential in July/August under a climate change scenario where sea surface temperatures rise by 2.2°C. Optimal survival = 10-14°C; < optimal = 15-21°C; extremely stressful = > 22°C.

## Discussion

### Utility of framework

The utility of this analysis is the transparent and repeatable way to develop and test specific hypotheses regarding nearshore habitats that may be at risk of developing more stressful physical conditions for target fish and shellfish resources under future climate change. Results generated from this project were developed based on a mechanistic understanding of physiological constraints for target species. Therefore, incremental learning about nearshore habitat dynamics, species-specific preferences/tolerances, or climate change projections can easily be incorporated as new information becomes available from future studies.

The framework to assess species-specific habitat vulnerability to climate change presented here demonstrates the need for more robust monitoring programs to develop empirical relationships between abiotic factors known to regulate key physiological processes (e.g., SST and salinity) and landscape-scale attributes. This information can be combined with phenological data as well as spatial and temporal species distribution, to help resource managers better understand how species are currently distributed and utilize different habitat types that may be influenced by climate change. Furthermore, our models suggest that variability in these abiotic factors are influenced by landscape-scale attributes (e.g., distance from the mouth of the Strait of Juan de Fuca or nearest large river) across different shore types. Therefore, some nearshore habitats may be less vulnerable to SST or salinity changes due to climate change.

The utility of this framework could ultimately be improved upon as more species-specific life history information becomes available for lesser-studied species (relative to Pacific salmon) such as clams and inland water Dungeness crab. Although more robust quantitative frameworks have been developed to understand fish community level responses to climate change (e.g., Molinos et al. 2015), our framework provides a simplistic approach to understanding habitat and species-specific vulnerability to climate change that can be adapted with additional data. Additionally, other landscape-scale metrics could be incorporated into our model such as Puget Sound-wide distributions of seagrass, kelp, shoreline armoring, overwater structures, and land cover change coupled with human population density.

In this analysis we proved we could use observations of nearshore SST and salinity (Appendix C) with landscape and shore type data to explicitly predict spatially distinct means and extremes of nearshore SST and salinity throughout the study area. We demonstrated how current and future climate change patterns of mean summer SST could structure habitat availability for juvenile Chinook salmon, larval cockle clams, and postlarval and juvenile Dungeness crab. Specifically, we predicted that increases in SST, due to climate change, are likely to expand geographic regions with suboptimal rearing conditions for postlarval and juvenile Dungeness crab and juvenile Chinook salmon but not larval cockles. However, these results should be interpreted with some caution due to a number of factors including: 1) oversimplified relationships between biota and environmental thresholds (i.e., an inadequate Table 10), 2) gaps between climate change predictions and biotic environmental thresholds, and 3) accuracy and precision in model predictions.

### Oversimplified relationships between biota and environmental thresholds

Applying environmental thresholds to biota has value for large scale and longer-term planning which is the intended purpose of this report. What this simplistic approach does not account for

are the nuances of complex ecology, including adaptive responses by biota at the individual or population level. Obviously, many animals can move away from suboptimal environments into more suitable environments. Additionally, the duration of exposure to a stressful environment may be equally as important as an environmental threshold value. We provide three examples where two of our modeled species (Dungeness crabs, Chinook salmon) show adaptive responses.

1. Low salinity is known to be stressful to Dungeness crabs (e.g., Reed 1969) but low salinity periods in estuaries often occur when prey abundance is high. Dungeness crab, thus, behaviorally overcome the low salinity limitation by synchronizing foraging times with tidally-driven fluctuations in salinity (Curtis & McGaw 2008).
2. Juvenile Chinook salmon are known to be stressed when SST exceed 16°C and prefer a salinity of 15 PSU (Fresh 2006, Webster & Dill 2006). However, several abiotic and biotic characteristics (e.g., depth, amount and type of food, predation) influence the tolerance of juvenile Chinook salmon to SST or salinities outside this optimal range. Webster and Dill (2006) experimentally showed how smolt-sized Chinook salmon passively organized themselves in response to different combinations of temperature, salinity, depth, and food availability.
3. Skagit Chinook salmon spawn timing has shifted later as water temperature during spawning has increased (Austin et al. in review). The shift appears to be an adaptive response at the population level that maintains fry emergence timing from shifting to earlier in the year when freshwater and estuarine fry rearing conditions would be less favorable.

Thus, the simplistic application of Table 10 thresholds does not capture the complexities of real ecology. We acknowledge the limitations of Table 10 but the deficiencies elucidate where new knowledge could fill gaps and thus improve analyses and management. Additionally, we argue a lack of full understanding and modeling of possible population compensation mechanisms by species to climate change pressure is not necessary to make incremental progress in climate change vulnerability assessments. For example, if climate change pressure reduces habitat options for biota, then their populations have fewer options to compensate with an adaptive response. In this sense, despite the listed data and model limitations, our study framework provides big picture evidence of climate change pressure on our selected species and provides a useful spatially explicit framework to build upon.

### **Gaps between climate change predictions and biotic environmental thresholds**

For sea surface salinity metrics, given the importance of geographic position relative to the nearest large river, the value of instantaneous flow metrics in explaining variability in sea surface salinity should be evaluated. This additional evaluation would allow for fine-scale projections of future hydrologic change to be more easily incorporated into the model and create a more useful tool to project future changes in sea surface salinity due to climate change (e.g., Lee et al. 2016).

Our analysis revealed a substantial data gap between readily available climate change predictions (Table 1) and important biotic relationships with environmental conditions (Table 10). In some cases, thresholds can be too general for some species and non-existent for others, especially depending upon specific life-history stages (e.g., in some species adult habitat use may be better understood than juvenile habitat use). Further work is needed to improve understanding of the effects of environmental variability on the ecology of individual species.

Additionally, many species are hypothesized to be sensitive to salinity change. However, we do not currently have tools to link climate change predictions to any nearshore salinity value within our study area because climate changes predictions are for precipitation, snowpack, and streamflow change, which in turn will influence nearshore salinity conditions within the study area. Thus, models linking predicted changes in streamflow to nearshore salinity metrics are lacking and new information can provide for an important next generation of this study.

### **Accuracy and precision in model predictions**

The spatial datasets of SST (this chapter) and salinity (see Appendix C) and resulting predictive models created for this project should be considered dynamic products that can be updated as new information becomes available. Specifically, given the observed variation in the effects of landscape position on SST and salinity across shore types, additional models that include interaction terms accounting for this variation should be evaluated. As new information becomes available on physiological constraints for target species and life stages, this information can be used to update vulnerability assessments for target species.

We compared the predictions of mean SST to the original observations (Figure 32) and found that, the SST model tended to over predict lower SST (10-12°C) by up to 3°C and under predict higher (>22°C) SST by a similar amount. Specifically, for predicted SSTs of 16.2 & 17.0°C, a wide range of SSTs were observed. This lack of precise resolution was likely caused by the use of two geographically large GSU\_ID polygons (i.e., Nooksack estuary = 1,384 hectares; Skagit estuary = 11,269 hectares). In reality, these areas have very diverse habitat conditions and much more diverse landscape characteristics than could feasibly be detected from the averaged conditions across large polygons. Although the mean size of all GSU\_ID polygons may not present a significant issue (mean GSU\_ID size = 54.3 hectares), the resolution of the landscape data influenced our prediction capability for SST. To improve model predictions, we recommend that the largest GSU-ID polygons be divided into smaller parts to better reflect their landscape variability.

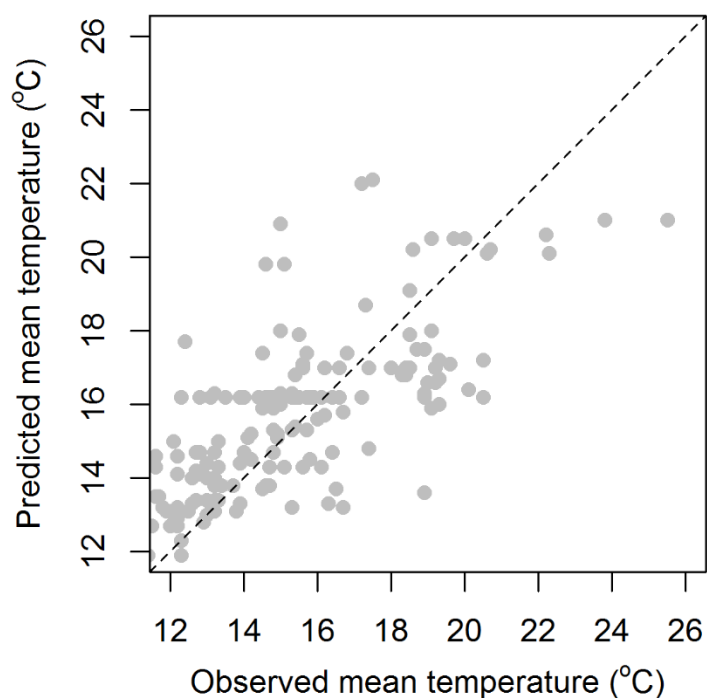


Figure 32. Relationship between observed and predicted mean sea surface temperature for 169 nearshore surface water sites located throughout the Whidbey Basin, Bellingham and Samish Bays, and the San Juan Islands.

Additionally, the SST model utilized data spanning 15 years (2001-2015) from four different studies to assemble the spatially-extensive dataset. Two disadvantages to this data acquisition method are: 1) temporal autocorrelation may exist because SST may have significantly increased over the 15-year period and 2) imbalance in the number of shore types sampled. We recommend future versions of the model be refit with year as a covariate to account for the potential effect of temporal autocorrelation. Additionally, further exploration of available data should be completed to rectify any imbalance of samples by shore type. Future model versions could also explore using error structures that better address influences of autocorrelation.

## References

- Abatzoglou JT, Brown TJ (2012) A comparison of statistical downscaling methods suited for wildfire applications. *Int J Climatol* 32:772-780
- Austin CS, Essington TE, Quinn TP (in review) Long-term responses of Pacific salmon spawning timing under climate change and hatchery propagation.
- Babson A, Kawase M, MacCready P (2006) Seasonal and interannual variability in the circulation of Puget Sound, Washington: a box model study. *Atmos Ocean* 44:29-45
- Bamber RN (1990) The effects of acidic seawater on three species of lamellibranch mollusc. *J Exp Mar Bio Ecol* 143:181-191
- Banas N, Conway-Cranos L, Sutherland D, MacCready P, Kiffney P, Plummer M (2015) Patterns of river influence and connectivity among subbasins of Puget Sound, with application to bacterial and nutrient loading. *Estuar Coast* 38:735-753
- Barange M, Bahri T, Beveridge MC, Cochrane KL, Funge-Smith S, Poulain F (2018) Impacts of climate change on fisheries and aquaculture: Synthesis of current knowledge, adaptation and mitigation options. FAO, Rome
- Barber J, Dexter J, Grossman S, Greiner C, McArdle J (2016) Low temperature brooding of Olympia oysters in northern Puget Sound. *J Shellfish Res* 35:351-357
- Bardach JE, Ryther JH, McLarney WO (1972) Aquaculture. The farming and husbandry of freshwater and marine organisms. John Wiley & Sons, Inc.
- Bayne B (1965) Growth and the delay of metamorphosis of the larvae of *Mytilus edulis* (L.). *Ophelia* 2:1-47
- Beamer E, Fresh K (2012) Juvenile salmon and forage fish presence and abundance in shoreline habitats of the San Juan Islands, 2008-2009: Map applications for selected fish species. Skagit River System Cooperative, La Conner
- Beamer E, Greene C, Brown E, Wolf K, Rice C, Henderson R (2016) An assessment of juvenile Chinook salmon population structure and dynamics in the Nooksack estuary and Bellingham Bay shoreline, 2003-2015. Skagit River System Cooperative, La Conner
- Beamer E, McBride A, Greene C, Henderson R, Hood G, Wolf K, Larsen K, Rice C, Fresh K (2005) Delta and nearshore restoration for the recovery of wild Skagit River Chinook salmon: Linking estuary restoration to wild Chinook salmon populations. Supplement to Skagit Chinook Recovery Plan, Skagit River System Cooperative, La Conner
- Beamer E, McBride A, Henderson R, Griffith J, Fresh K, Zackey T, Barsh R, Wyllie-Echeverria T, Wolf K (2006) Habitat and fish use of pocket estuaries in the Whidbey Basin and north Skagit County bays, 2004 and 2005. Skagit River System Cooperative, La Conner
- Beamer E, Rice C, Henderson R, Fresh K, Rowse M (2007) Taxonomic composition of fish assemblages, and density and size of juvenile Chinook salmon in the greater Skagit River estuary: Field sampling and data summary report. Skagit River System Cooperative, La Conner
- Beauchamp DA, Duffy EJ (2011) Stage-specific growth and survival during early marine life of Puget Sound Chinook salmon in the context of temporal-spatial environmental conditions and trophic interactions. Final report to the Pacific Salmon Commission, Pacific Salmon Commission
- Beechie T, Steel E, Roni P, Quimby E (2003) Ecosystem recovery planning for listed salmon: an integrated assessment approach for salmon habitat. U.S. Dept. Commerce, NOAA
- Beechie TJ, Sear DA, Olden JD, Pess GR, Buffington JM, Moir H, Roni P, Pollock MM (2010) Process-based principles for restoring river ecosystems. *Bioscience* 60:209-222

- Bourne N, Smith D (1972) The effect of temperature on the larval development of the horse clam, *Tresus capax* (Gould). Proc Nat Shellfish Assoc 62: 35-38
- Burnham KP, Anderson DR (2002) Model selection and multimodel inference. Springer New York
- Byrne M, Przeslawski R (2013) Multistressor impacts of warming and acidification of the ocean on marine invertebrates' life histories. Integr Comp Biol 53:582-596
- Cheng BS, Bible JM, Chang AL, Ferner MC, Wasson K, Zabin CJ, Latta M et al. (2015) Testing local and global stressor impacts on a coastal foundation species using an ecologically realistic framework. Glob Change Biol 21:2488–2499
- Coan E, Scott P, Bernard F (2000) Bivalve seashells of Western North America: Santa Barbara Museum of Natural History Monographs. Studies in Biodiversity 2:764
- Cowardin LM (1979) Classification of wetlands and deepwater habitats of the United States. Book FWS/OBS-97-31. Fish and Wildlife Service, U.S. Dept. of the Interior, Biological Services Program
- Curtis DL, McGaw IJ (2008) A year in the life of a Dungeness crab: Methodology for determining microhabitat conditions experienced by large decapod crustaceans in estuaries. J Zool 274:375-385
- Curtis DL, McGaw IJ (2012) Salinity and thermal preference of Dungeness crabs in the lab and in the field: Effects of food availability and starvation. J Exp Mar Bio Ecol 413:113-120
- Deutsch C, Ferrel A, Seibel B, Pörtner H-O, Huey RB (2015) Climate change tightens a metabolic constraint on marine habitats. Science 348:1132-1135
- Dinnel P, Armstrong D, McMillan R (1993) Evidence for multiple recruitment-cohorts of Puget Sound Dungeness crab, *Cancer magister*. Mar Biol 115:53-63
- Doney SC, Ruckelshaus M, Duffy JE, Barry JP, Chan F, English CA, Galindo HM, Grebmeier JM, Hollowed AB, Knowlton N, Polovina J, Rabalais NN, Sydeman WJ, Talley LD (2012) Climate change impacts on marine ecosystems. Ann Rev Mar Sci 4:11-37
- Duffy EJ, Beauchamp DA (2011) Rapid growth in the early marine period improves the marine survival of Chinook salmon (*Oncorhynchus tshawytscha*) in Puget Sound, Washington. Can J Fish Aquat Sci 68:232-240
- Ekstrom JA, Suatoni L, Cooley SR, Pendleton LH, Waldbusser GG, Cinner JE, Ritter J, Langdon C, van Hooedonk R, Gledhill D, Wellman K, Beck MW, Brander LM, Rittschof D, Doherty C, Edwards PET, Portela R (2015) Vulnerability and adaptation of US shellfisheries to ocean acidification. Nat Clim Chang 5:207-214
- ESRI (2017) Creating the Least-Cost Path. Accessed December 11. <https://desktop.arcgis.com/en/analytics/case-studies/cost-lesson-3-desktop-creating-a-least-cost-path.htm>
- Free CM, Thorson JT, Pinsky ML, Oken KL, Wiedenmann J, Jensen OP (2019) Impacts of historical warming on marine fisheries production. Science 363:979-983
- Fresh K (2006) Juvenile Pacific salmon and the nearshore ecosystem of Puget Sound. Puget Sound Nearshore Partnership, Olympia
- Gaines SD, Costello C, Owashi B, Mangin T, Bone J, Molinos JG, Burden M, Dennis H, Halpern BS, Kappel CV, Kleisner KM, Ovando D (2018) Improved fisheries management could offset many negative effects of climate change. Sci Adv 4:eaa01378
- Gallucci VF, Gallucci BB (1982) Reproduction and ecology of the hermaphroditic cockle *Clinocardium nuttallii* (Bivalvia: Cardiidae) in Garrison Bay. Mar Ecol Prog Ser 7:137-145

- Gazeau F, Quiblier C, Jansen JM, Gattuso J-P, Middelburg JJ, Heip CHR (2007) Impact of elevated CO<sub>2</sub> on shellfish calcification. *Geophys Res Lett* 34:L07603
- Goodwin C, Pease B (1989) Species profiles: Life histories and environmental requirements of coastal fish and invertebrates (Pacific Northwest) -- Pacific geoduck clam. *US Fish Wildl Serv Biol Rep* 82 (11.120):14
- Gray MW, Langdon CJ (2018) Ecophysiology of the Olympia oyster, *Ostrea lurida*, and Pacific oyster, *Crassostrea gigas*. *Estuar Coast* 41:521-535
- Griffiths C, Griffiths R (1987) *Bivalvia*. Academic Press, New York
- Gruber N (2011) Warming up, turning sour, losing breath: Ocean biogeochemistry under global change. *Philos T R Soc A: Math Phys Eng Sci* 369(1943):1980-1996
- Hanson P, Johnson T, Schindler D, Kitchell J (1997) *Fish Bioenergetics 3.0*. University of Wisconsin Sea Grant Institute, Madison, Wisconsin
- Harbo R (1997) *Shells & shellfish of the Pacific northwest: A field guide*. Harbour Publishing, Madiera Park
- Hettinger A, Sanford E, Hill TM, Lenz EA, Russell AD, Gaylord BJGCB (2013) Larval carry-over effects from ocean acidification persist in the natural environment. *Glob Chang Biol* 19:3317-3326
- Hettinger A, Sanford E, Hill TM, Russell AD, Sato KN, Hoey J, Forsch M, Page HN, Gaylord B (2012) Persistent carry-over effects of planktonic exposure to ocean acidification in the Olympia oyster. *Ecology* 93:2758-2768
- Hiebert T (2015) *Saxidomus giganteus*. In: Hiebert TC BB, Shanks AL (ed) *Oregon estuarine invertebrates: Rudys' illustrated guide to common species*. University of Oregon Libraries and Oregon Institute of Marine Biology, Charleston
- Hiebert T (2016) *Tresus capax*. In: Hiebert TC BB, Shanks AL (ed) *Oregon estuarine invertebrates: Rudys' illustrated guide to common species*. University of Oregon Libraries and Oregon Institute of Marine Biology, Charleston
- Hollarsmith JA, Sadowski JS, Picard MMM, Cheng B, Farlin J, Russell A, Grosholz ED (2020) Effects of seasonal upwelling and runoff on water chemistry and growth and survival of native and commercial oysters. *Limnol Oceanogr* 65:224-235
- Holsman KK, Armstrong DA, Beauchamp DA, Ruesink JL (2003) The necessity for intertidal foraging by estuarine populations of subadult Dungeness crab, *Cancer magister*: Evidence from a bioenergetics model. *Estuaries* 26:1155
- IPCC (2013) *Climate Change 2013: The Physical Science Basis. Contribution of working group I to the fifth assessment report of the Intergovernmental Panel on Climate Change*. In: Stocker TF, D. Qin, G.-K. Plattner, M. Tignor, S.K. Allen, J. Boschung, A. Nauels, Y. Xia, V. Bex and P.M. Midgley (ed), Cambridge, United Kingdom and New York
- IPCC (2014) *Climate Change 2014: Synthesis Report*. In: Contribution of working groups I, II and III to the fifth assessment report of the Intergovernmental Panel on Climate Change (ed), Geneva, Switzerland
- Jamieson G, Phillips A (1993) Megalopal spatial distribution and stock separation in Dungeness crab (*Cancer magister*). *Can J Fish Aquat Sci* 50:416-429
- Liu W, Gurney-Smith H, Beerens A, Pearce CM (2010) Effects of stocking density, algal density, and temperature on growth and survival of larvae of the basket cockle, *Clinocardium nuttallii*. *Aquaculture* 299:99-105

- Liu W, Pearce CM, Alabi AO, Beerens A, Gurney-Smith H (2011) Effects of stocking density, ration, and temperature on growth of early post-settled juveniles of the basket cockle, *Clinocardium nuttallii*. *Aquaculture* 320:129-136
- Losey RJ, Yamada SB, Largaespada L (2004) Late-Holocene Dungeness crab (*Cancer magister*) harvest at an Oregon coast estuary. *J Archaeol Sci* 31:1603-1612
- Marshall KN, Kaplan IC, Hodgson EE, Hermann A, Busch DS, McElhany P, Essington TE, Harvey CJ, Fulton EA (2017) Risks of ocean acidification in the California Current food web and fisheries: ecosystem model projections. *Glob Chang Biol* 23:1525-1539
- Mauger G, Casola J, Morgan H, Strauch R, Jones B, Curry B, Busch-Isaksen T, Binder L, Krosby M, Snover A (2015) State of knowledge: Climate change in Puget Sound. Climate Impacts Group, University of Washington, Seattle
- McBride A, Todd S, Odum O, Koschak M, Beamer E (2009) Developing a geomorphic model for nearshore habitat mapping and analysis. Skagit River System Cooperative, LaConner
- Michaelidis B, Christos O, Andreas P, Hans OP (2005) Effects of long-term moderate hypercapnia on acid-base balance and growth rate in marine mussels *Mytilus galloprovincialis*. *Mar Ecol Prog Ser* 293:109-118
- Miller I, Morgan H, Mauger G, Newton T, Weldon R, Schmidt D, Welch M, Grossman E (2018) Projected sea level rise for Washington State – A 2018 assessment. A collaboration of Washington Sea Grant, University of Washington Climate Impacts Group, University of Oregon, University of Washington, and US Geological Survey. Prepared for the Washington Coastal Resilience Project. updated 07/2019
- Miller J (2015) Effect of low pH on early life stages of the decapod crustacean, Dungeness crab (*Cancer magister*). Master thesis, University of Washington, Seattle
- Molinos JG, Halpern Benjamin S, Schoeman David S, Brown Christopher J, Kiessling W, Moore Pippa J, Pandolfi John M, Poloczanska Elvira S, Richardson Anthony J, Burrows Michael T (2015) Climate velocity and the future global redistribution of marine biodiversity. *Nat Clim Chang* 6:83
- Moore SK, Mantua NJ, Kellogg JP, Newton JA (2008) Local and large-scale climate forcing of Puget Sound oceanographic properties on seasonal to interdecadal timescales. *Limnol Oceanogr* 53:1746-1758
- Mote P, Abatzoglou J, Lettenmaier D, Turner D, Rupp D, Bachelet D, Conklin D (2014) Integrated scenarios of climate, hydrology, and vegetation for the Northwest, Final Report. Pacific Northwest Climate Impacts Research Consortium, College of Earth, Ocean, and Atmospheric Sciences, Oregon State University, Corvallis
- Numaguchi K (1998) Preliminary experiments on the influence of water temperature, salinity and air exposure on the mortality of Manila clam larvae. *Aquac Int* 6:77-81
- Pauley G, Armstrong D, Heun T (1986) Species profiles: Life histories and environmental requirements of coastal fishes and invertebrates (Pacific Northwest)--Dungeness crab. *US Fish Wildl Serv Biol Rep* 82 (11.63)
- Poloczanska ES, Brown CJ, Sydeman WJ, Kiessling W, Schoeman DS, Moore PJ, Brander K, Bruno JF, Buckley LB, Burrows MT, Duarte CM, Halpern BS, Holding J, Kappel CV, O'Connor MI, Pandolfi JM, Parmesan C, Schwing F, Thompson SA, Richardson AJ (2013) Global imprint of climate change on marine life. *Nat Clim Chang* 3:919-925
- Pörtner HO (2002) Climate variations and the physiological basis of temperature dependent biogeography: systemic to molecular hierarchy of thermal tolerance in animals. *Comp Biochem Physiol A: Mol Integr Physiol* 132:739-761

- PSMFC (2014) Dungeness crab report 2014. Pacific States Marine Fisheries Commission:5 pp
- Quayle DB, Bourne N (1972) The clam fisheries of British Columbia. Fish Res Board Canada, Bull 179:85
- Quinn TP (2005) The behavior and ecology of Pacific salmon and trout. University of Washington Press, Seattle
- Rasmuson LK (2013) The biology, ecology and fishery of the Dungeness crab, *Cancer magister*. In: Lesser M (ed) Advances in Marine Biology. Academic Press, Burlington, p 95–148
- Reed PH (1969) Culture methods and effects of temperature and salinity on survival and growth of Dungeness Crab (*Cancer magister*) larvae in the laboratory. J Fish Res Board Can 26:389-397
- Rice CA, Greene CM, Moran P, Teel DJ, Kuligowski DR, Reisenbichler RR, Beamer EM, Karr 1 JR, Fresh KL (2011) Abundance, stock origin, and length of marked and unmarked juvenile Chinook salmon in the surface waters of greater Puget Sound. Trans Am Fish Soc 140:170-189.
- Rippington A (2015) Effects of temperature, salinity and food stress on larval growth and development in the Olympia oyster, *Ostrea lurida*. M.S. thesis. University of Victoria
- Roop HA, Mauger GS, Morgan H, Snover AK, Krosby M (2020) Shifting snowlines and shorelines: The Intergovernmental Panel on Climate Change’s special report on the ocean and cryosphere and implications for Washington State. Briefing paper prepared by the Climate Impacts Group, University of Washington, Seattle
- Scavia D, Field JC, Boesch DF, Buddemeier RW, Burkett V, Cayan DR, Fogarty M, Harwell MA, Howarth RW, Mason C (2002) Climate change impacts on US coastal and marine ecosystems. Estuaries 25:149-164
- Shipman H (2008) A geomorphic classification of Puget Sound nearshore landforms. Puget Sound Nearshore Partnership Report No. 2008-01. Published by Seattle District, US Army Corps of Engineers, Seattle
- Simenstad C (1983) The ecology of estuarine channels of the Pacific Northwest coast: A community profile. University of Washington Fisheries Research Institute, Seattle
- Simenstad C, Ramirez M, Burke J, Logsdon M, Shipman H, Tanner C, Toft J, Craig B, Davis C, Fung J, Bloch P, Fresh K, Campbell S, Myers D, Iverson E, Bailey A, Schlenger P, Kiblinger C, Myre P, Gertsel W, MacLennan A (2011) Historical change of Puget Sound shorelines: Puget Sound nearshore ecosystem project change analysis. Puget Sound Nearshore Report No. 2011-01. Published by Washington Department of Fish and Wildlife, Olympia, Washington, and U.S. Army Corps of Engineers, Seattle, Washington
- Stein BA, Staudt A, Cross MS, Dubois NS, Enquist C, Griffis R, Hansen LJ, Hellmann JJ, Lawler JJ, Nelson EJ, Paris A (2013) Preparing for and managing change: Climate adaptation for biodiversity and ecosystems. Front Ecol Environ 11:502-510
- Strathmann MF (1987) Reproduction and development of marine invertebrates of the northern Pacific coast: Data and methods for the study of eggs, embryos, and larvae. University of Washington Press, Seattle
- Sulkin S, McKeen G (1989) Laboratory study of survival and duration of individual zoeal stages as a function of temperature in the brachyuran crab *Cancer magister*. Mar Biol 103:31-37
- Sulkin SD, Mojica E, McKeen GL (1996) Elevated summer temperature effects on megalopal and early juvenile development in the Dungeness crab, *Cancer magister*. Can J Fish Aquat Sci 53:2076-2079

- Suttles W (1974) Coast Salish and Western Washington Indians: The economic life of the Coast Salish of Haro and Rosario Straits. Garland Publishing Inc., New York
- van Vuuren DP, Edmonds J, Kainuma M, Riahi K, Thomson A, Hibbard K, Hurtt GC, Kram T, Krey V, Lamarque JF, Masui T (2011) The representative concentration pathways: an overview. *Clim Change* 109:5-31.
- Webster SJ, Dill LM (2006) The energetic equivalence of changing salinity and temperature to juvenile salmon. *Funct Ecol* 20:621-629
- Yang Z, Wang T, Cline D, Williams B (2014) Hydrodynamic Modeling Analysis to Support Nearshore Restoration Projects in a Changing Climate. *J Mar Sci Eng* 2:18-32

## **Appendix A. Geographic distribution of common shore types throughout the study area**

Appendix A contains figures of the geographic distribution of common shore types throughout the study area including: barrier beaches, estuary - large river type, estuary - pocket estuary, human-modified beaches, pocket beaches, rocky beaches, and sediment source beaches.

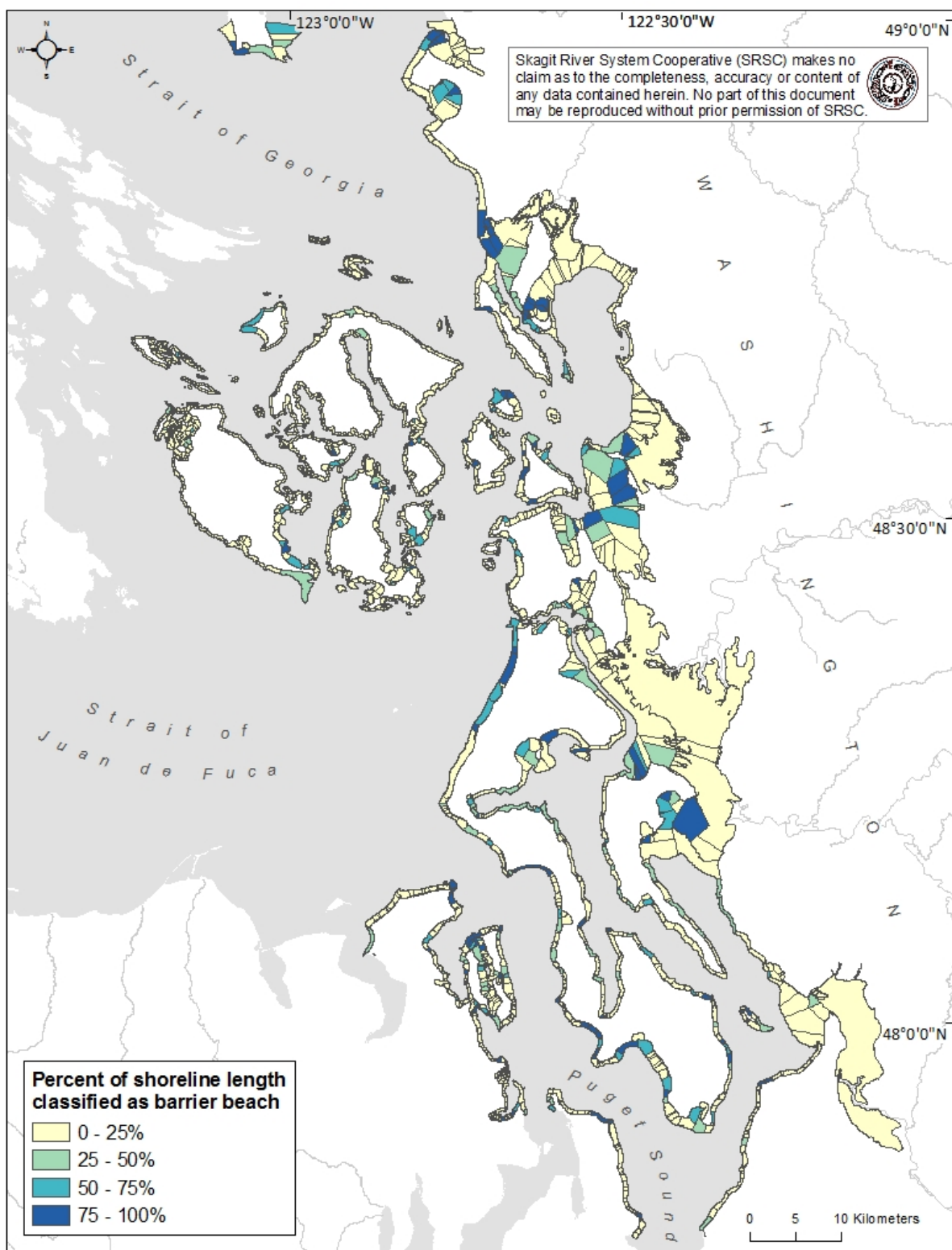


Figure A1. Percent of shoreline length within each GSU\_ID polygon that is the barrier beach shore type.

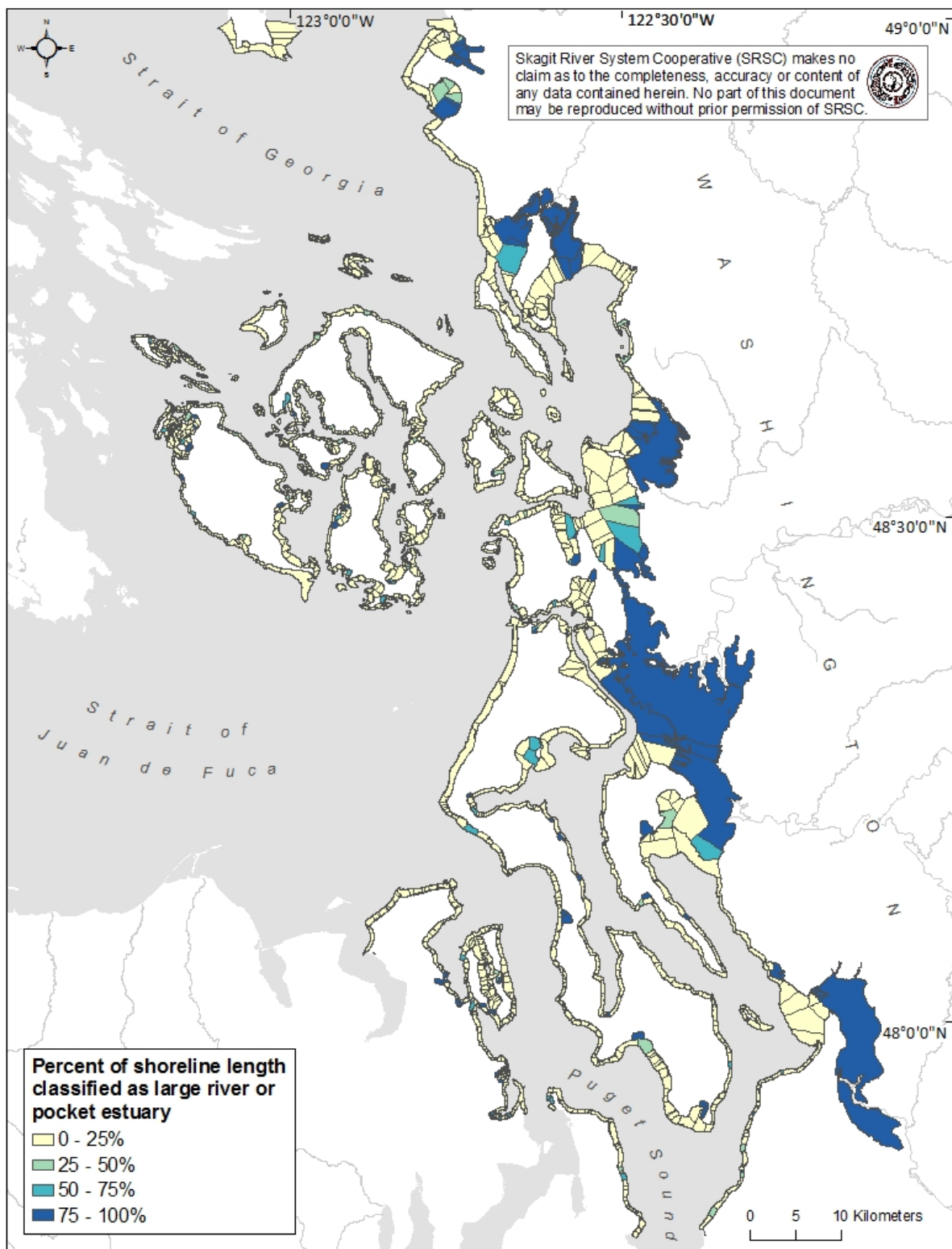


Figure A2. Percent of shoreline length within each GSU\_ID polygon that is the pocket estuary or large river estuary shore type.

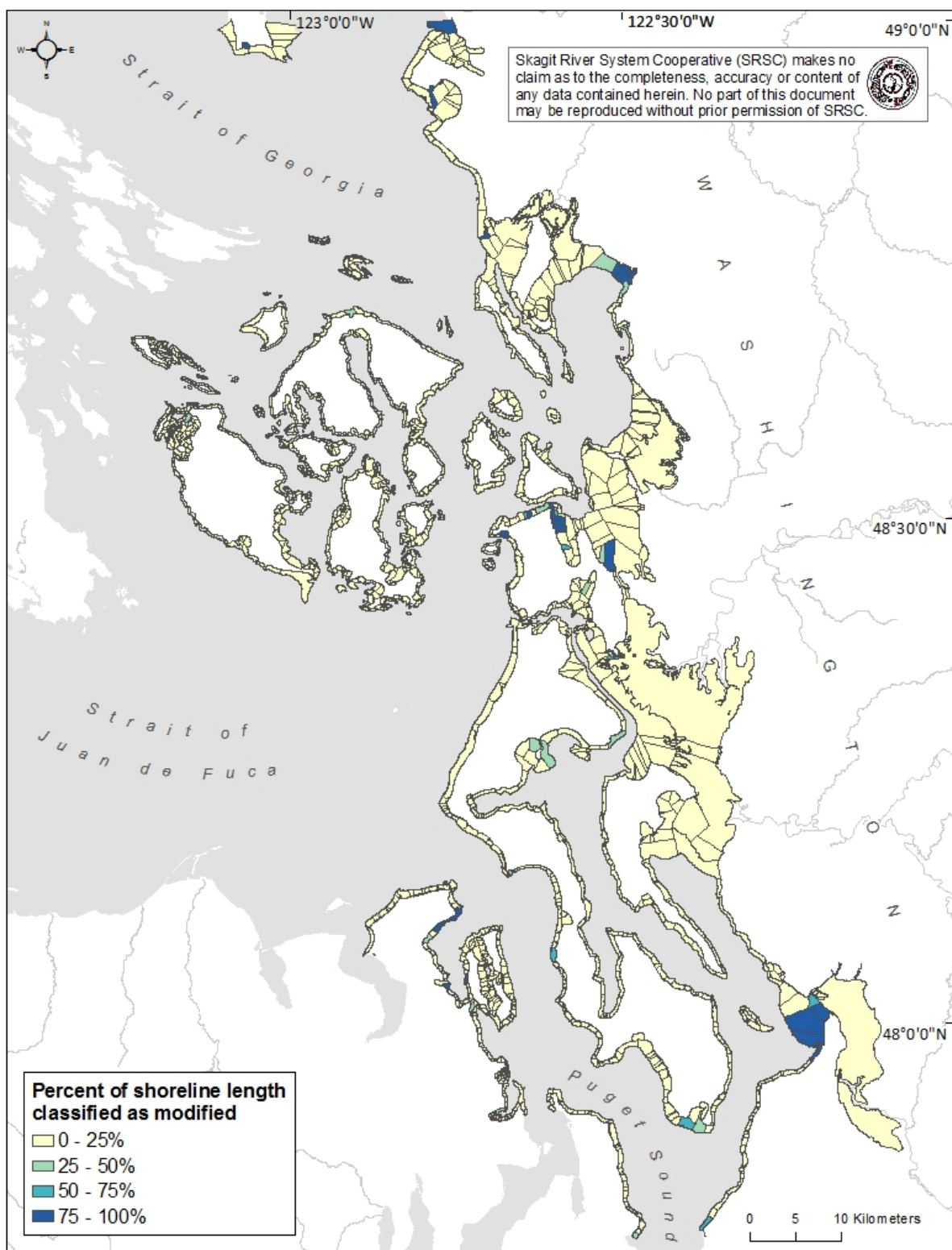


Figure A3. Percent of shoreline length within each GSU\_ID polygon that is the human-modified shore type during the mid-1990s.

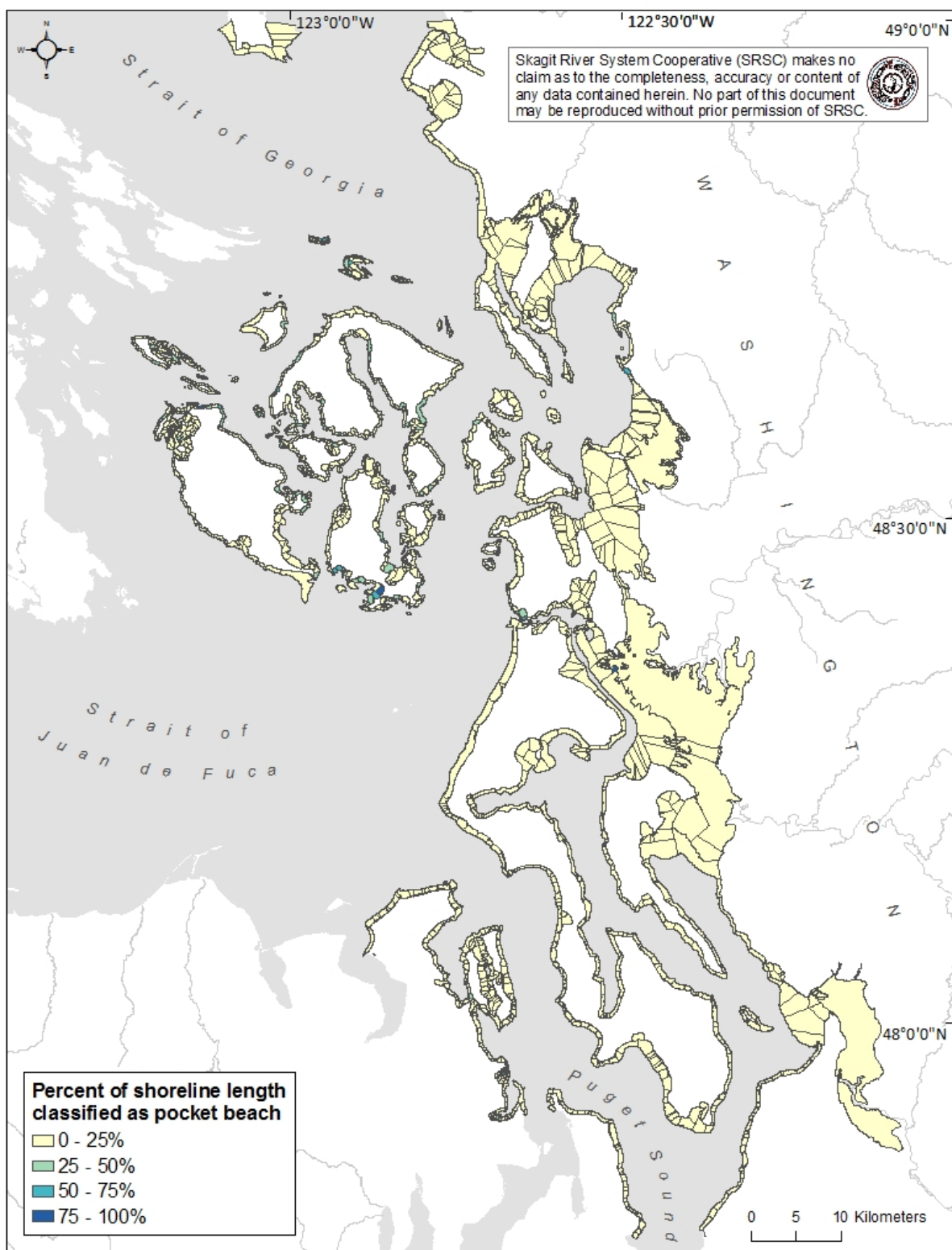


Figure A4. Percent of shoreline length within each GSU\_ID polygon that is the pocket beach shore type.

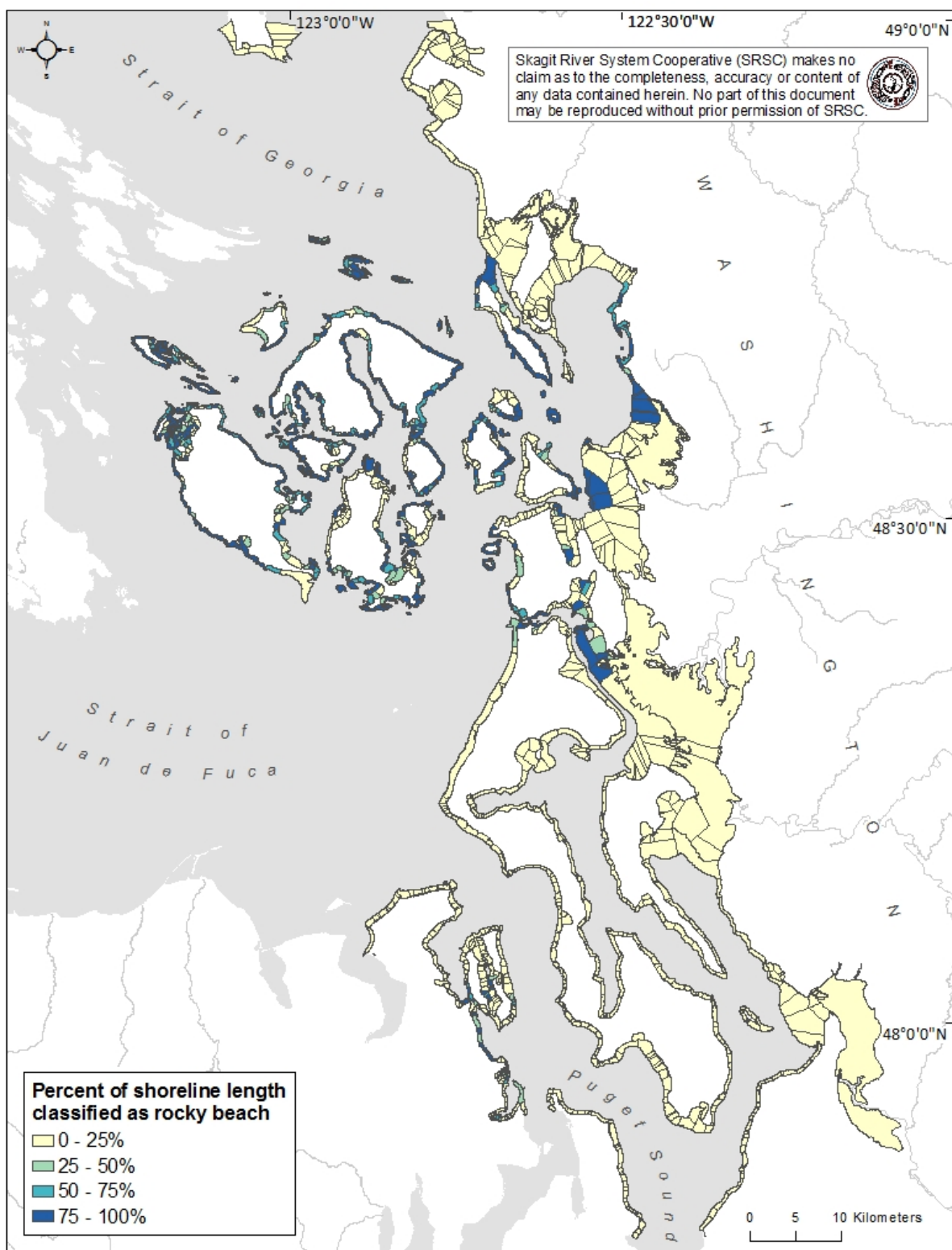


Figure A5. Percent of shoreline length within each GSU\_ID polygon that is the rocky beach shore type.

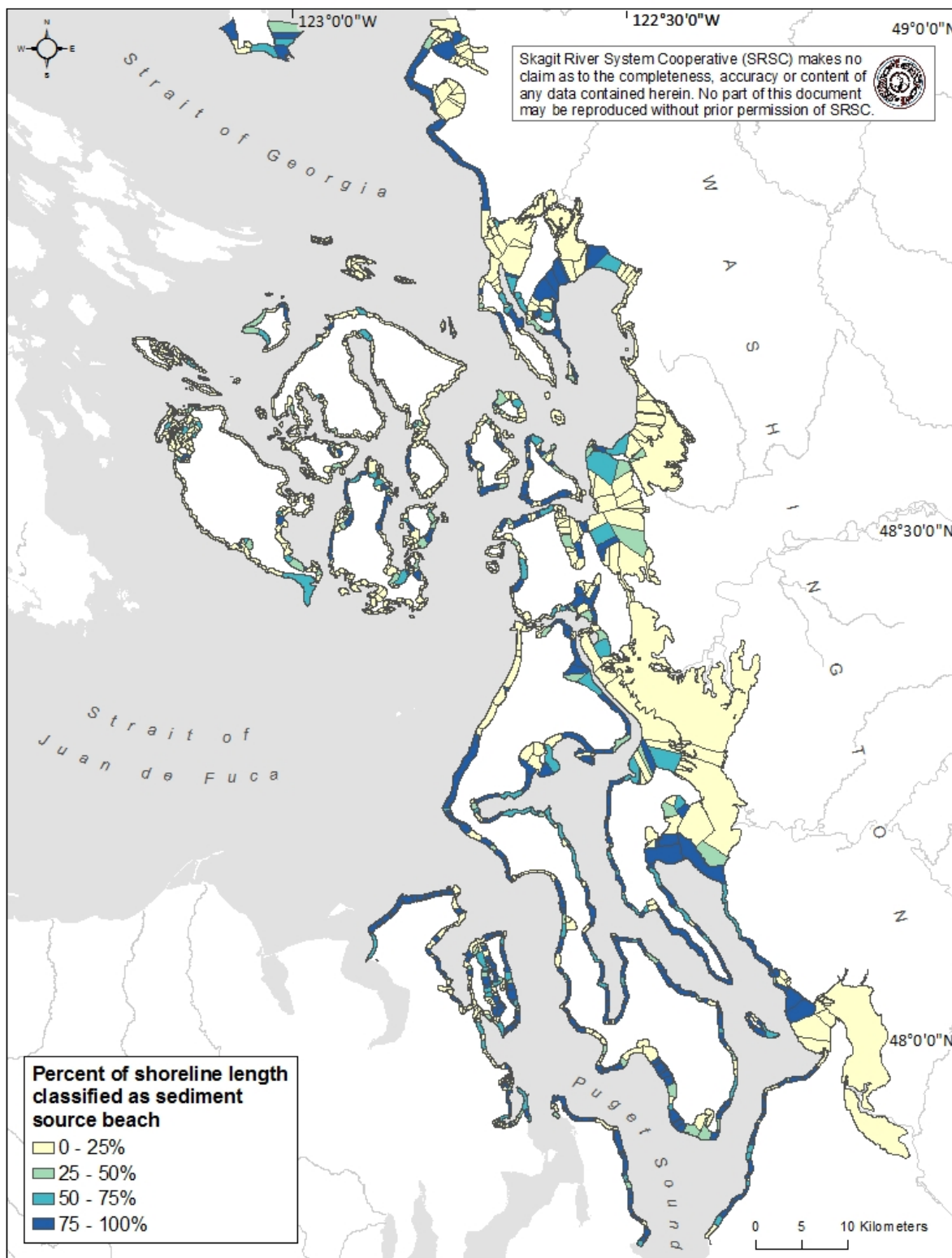


Figure A6. Percent of shoreline length within each GSU\_ID polygon that is the sediment source beach shore type.

## **Appendix B. Geographic distribution of landscape characteristics assessed throughout the study area**

Appendix B contains figures of the geographic distribution of landscape characteristics assessed throughout the study area including: fetch, depth of adjacent marine water, distance from nearest large river, distance from the entrance of the strait of Juan de Fuca, and human land use (percent forested and percent shoreline armored).

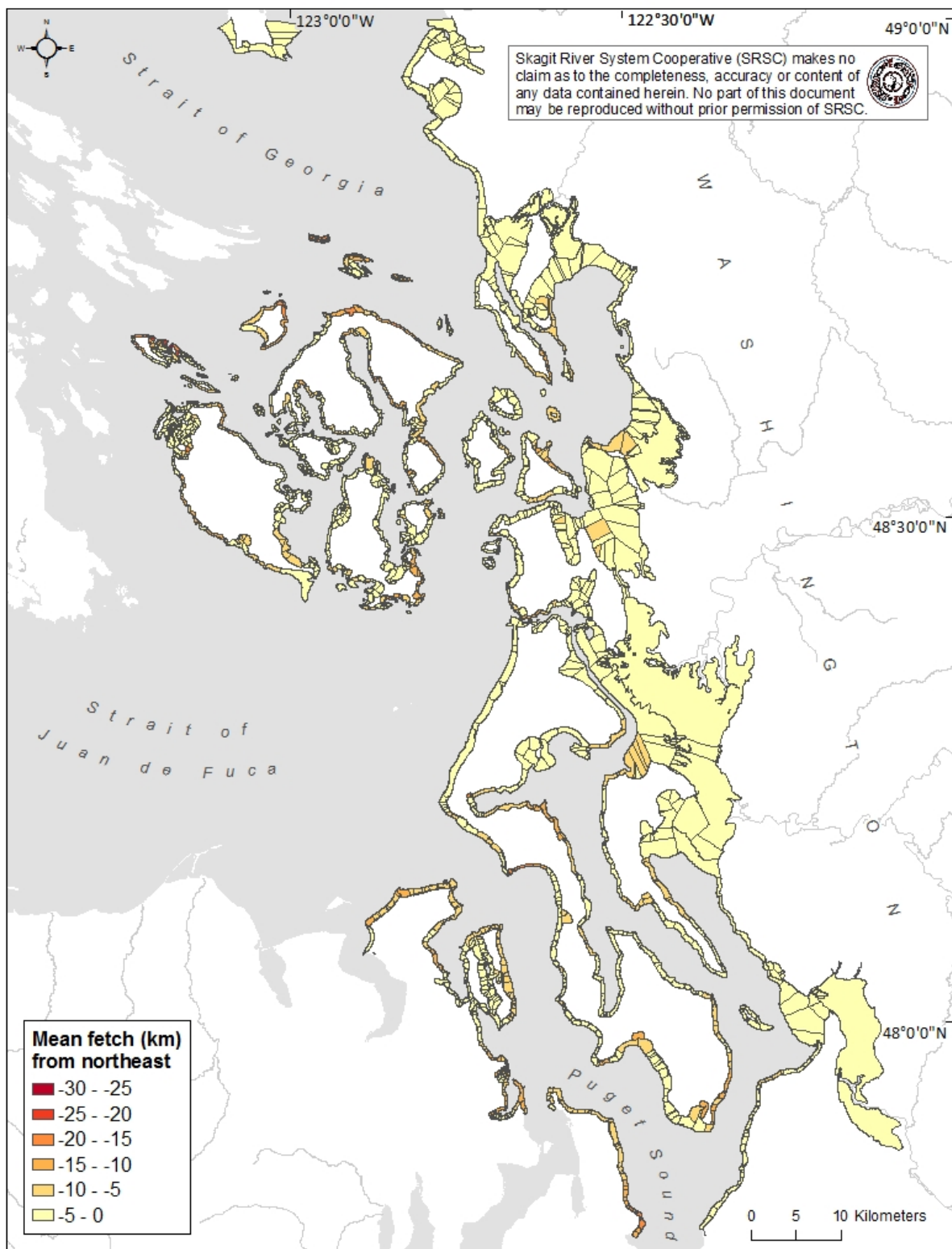


Figure B1. Average fetch in kilometers for winds blowing from the northeast direction by GSU\_ID. Shorelines with larger fetch lengths are more negative than sheltered shorelines

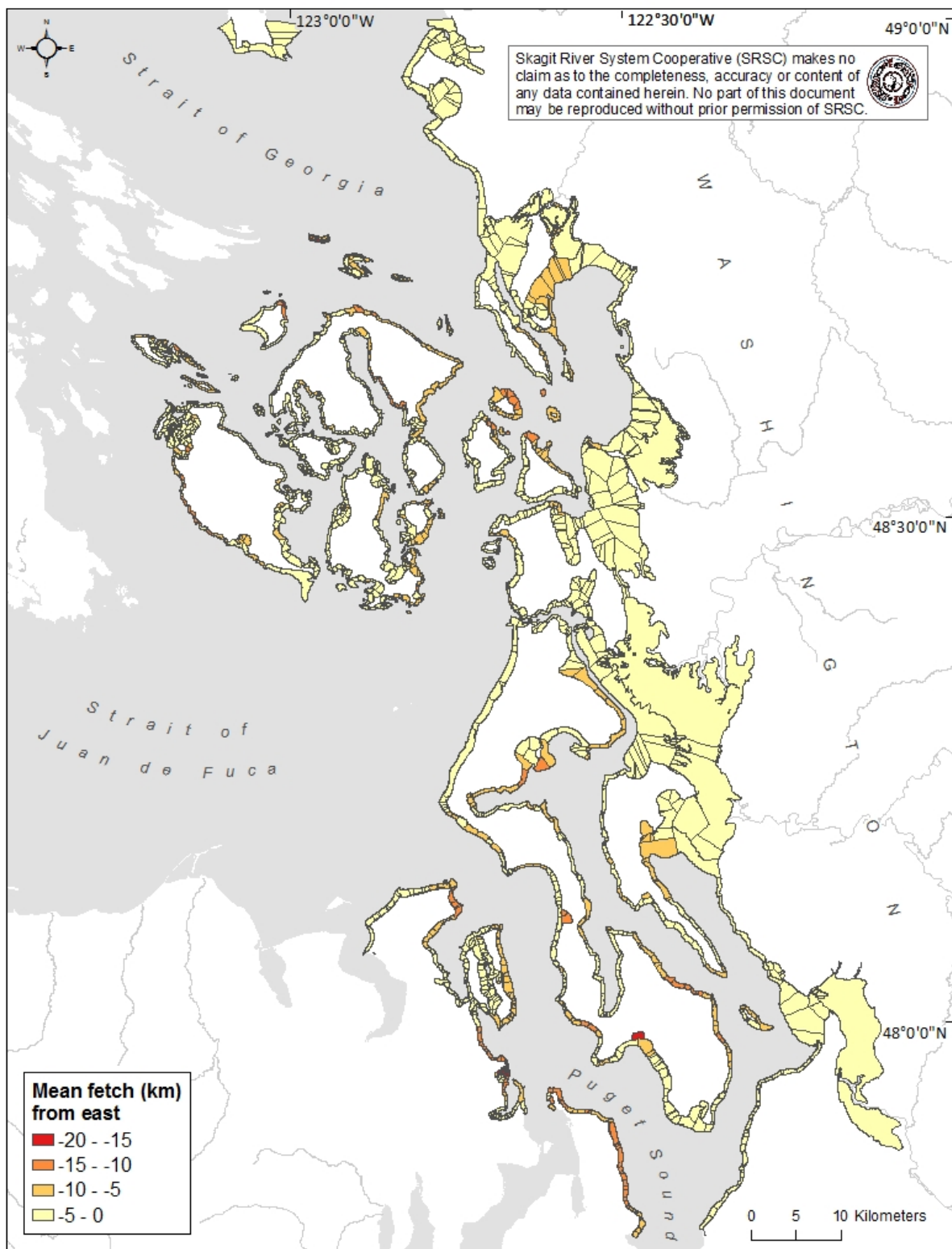


Figure B2. Average fetch in kilometers for winds blowing from the east direction by GSU\_ID. Shorelines with larger fetch lengths are more negative than sheltered shorelines.

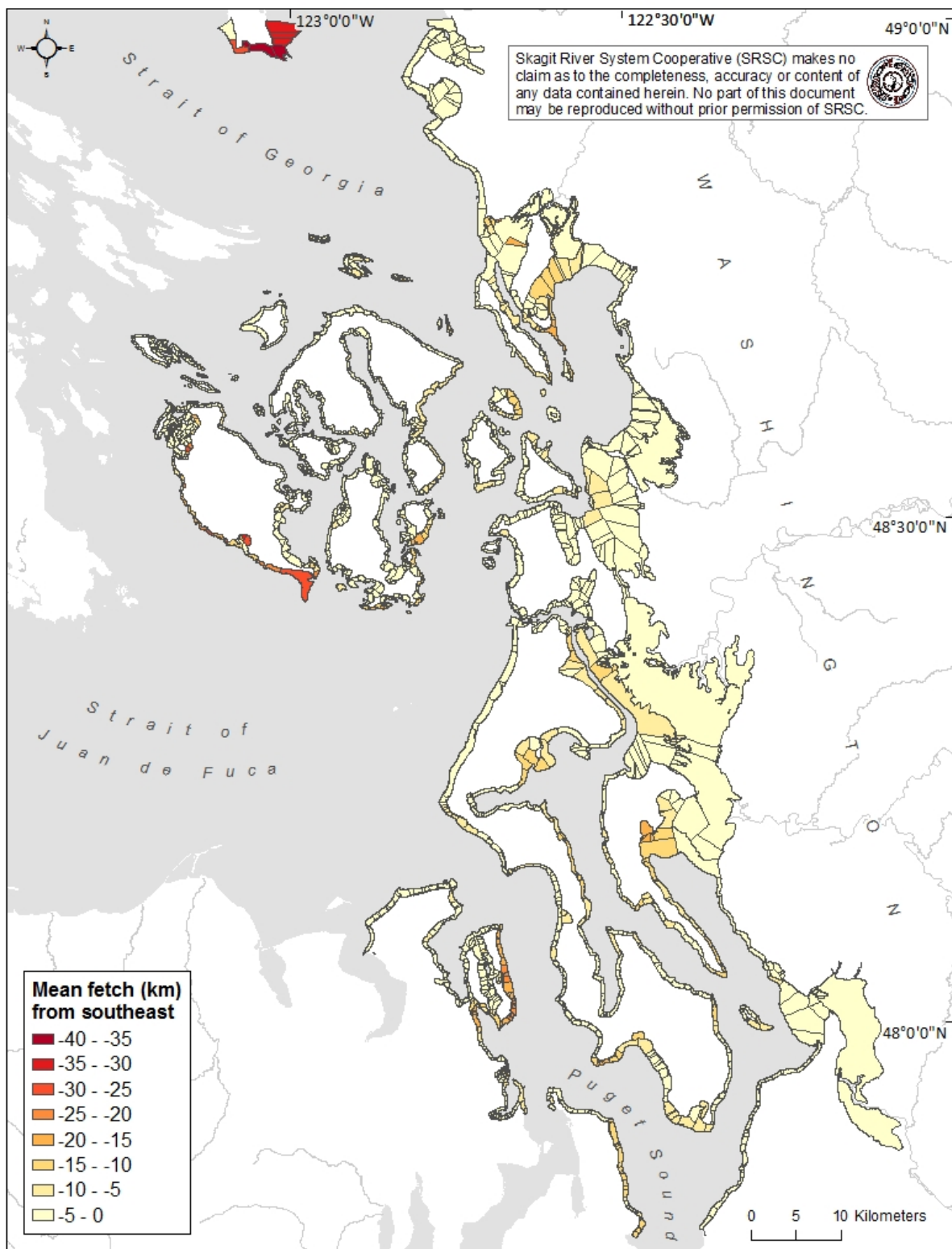


Figure B3. Average fetch in kilometers for winds blowing from the southeast direction by GSU\_ID. Shorelines with larger fetch lengths are more negative than sheltered shorelines.

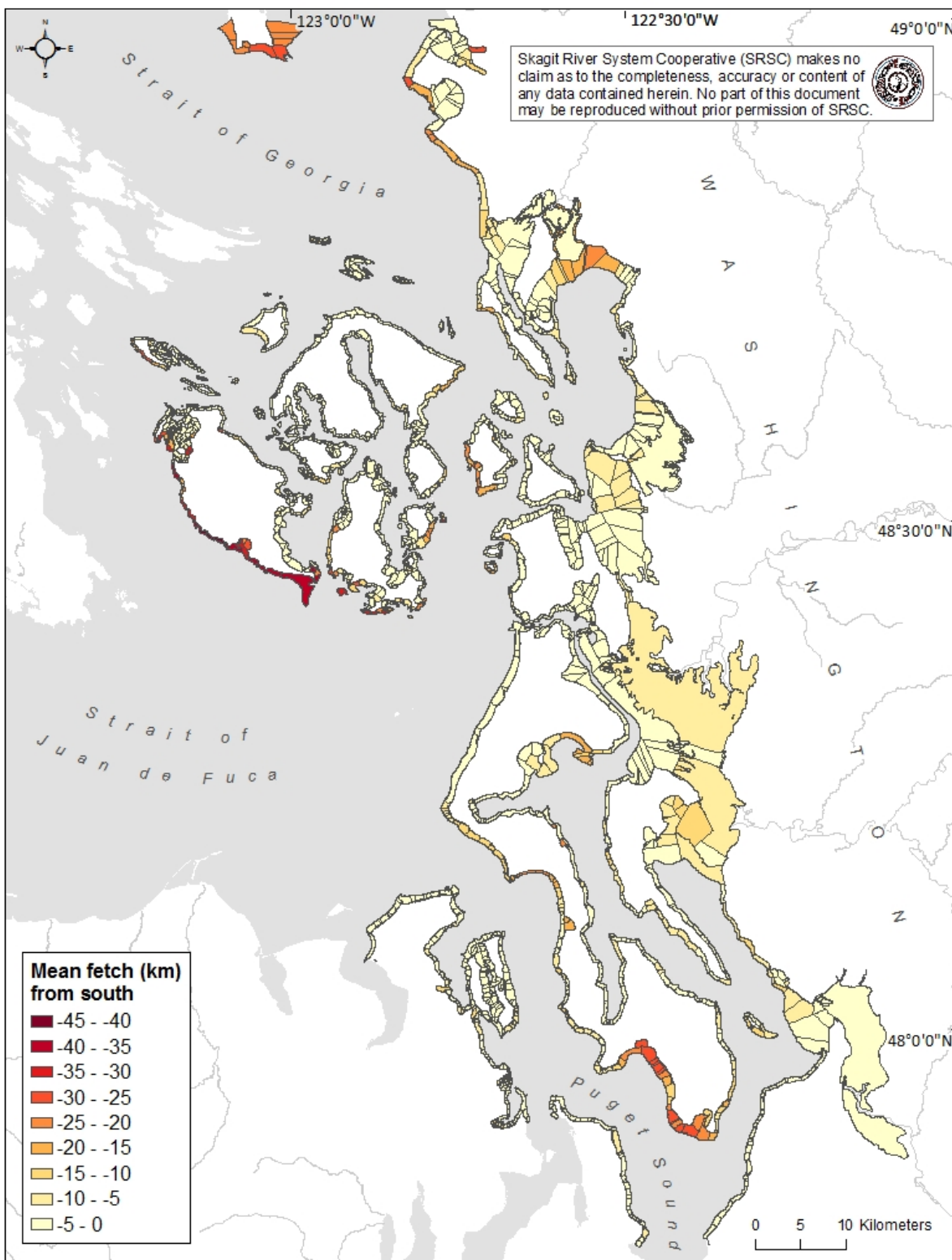


Figure B4. Average fetch in kilometers for winds blowing from the south direction by GSU\_ID. Shorelines with larger fetch lengths are more negative than sheltered shorelines.

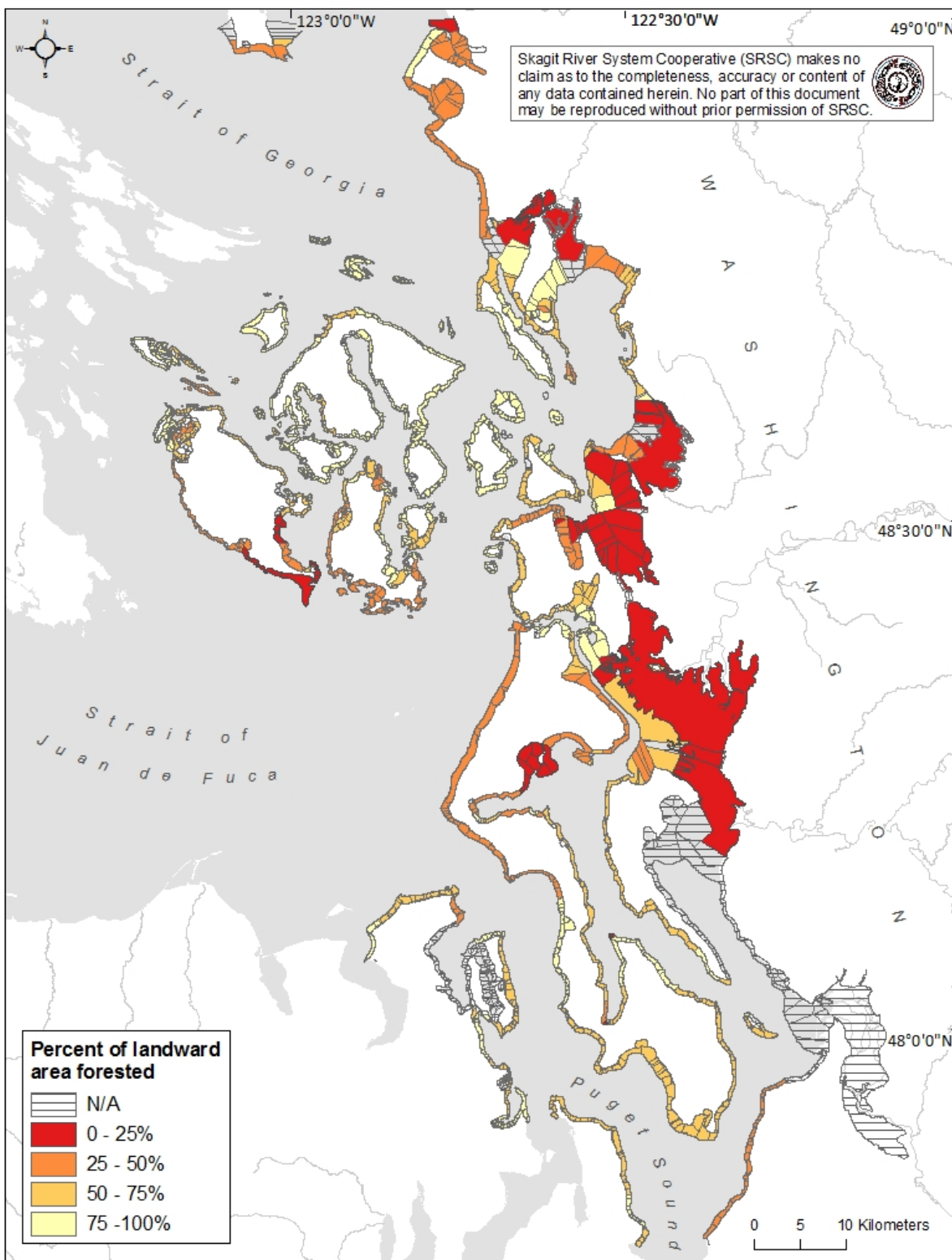


Figure B5. Percent of landward areas (i.e., within 200-meters of the shoreline) that is forested for each GSU\_ID polygon. N/A = no data.

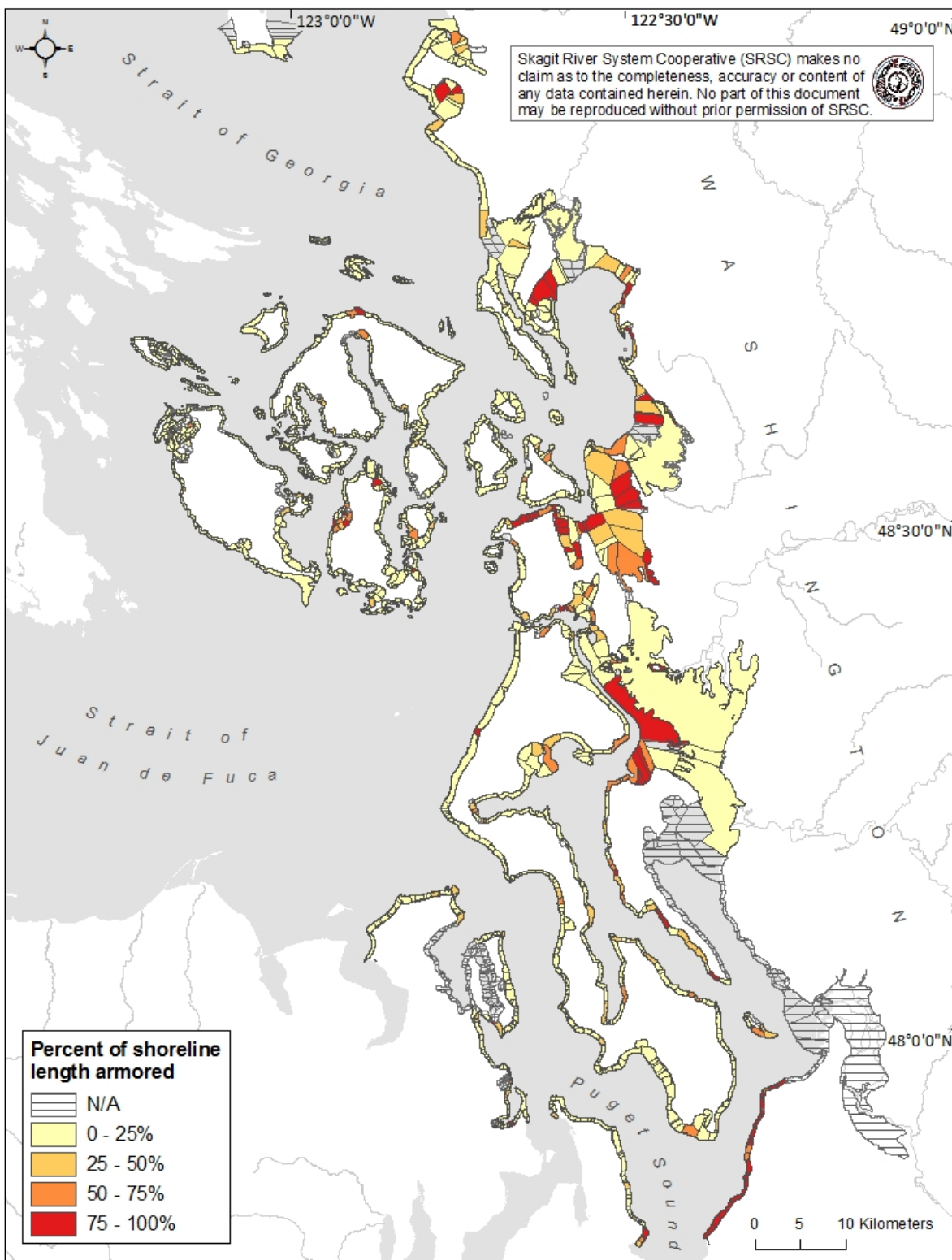


Figure B6. Percent of shoreline length within each GSU\_ID polygon that is armored. N/A = no data.

## Appendix C. Additional temperature and salinity models

In this section we report our exploratory effort to develop predictive models for maximum July – August sea surface temperature (SST) ( $T_{max}$ ) and three nearshore surface salinity models ( $S_{mean}$ ,  $S_{max}$ ,  $S_{min}$ ) using shore type and landscape data.

### Maximum July – August sea surface temperature ( $T_{max}$ )

The best model for maximum SST for all shore types includes significant covariates for shore type and landscape variables including log-transformed water depth adjacent to the nearshore ( $LnMeanGSU\_depth$ ) and distance from the entrance to the Strait of Juan de Fuca ( $DistSjfKm$ ) ( $R^2 = 0.29$ ,  $n = 169$ ). However, the predictive power of the best model was poor so we did not utilize  $T_{max}$  results for the habitat vulnerability analysis in this report. Because SST metrics are usually correlated, an alternative approach to estimating  $T_{max}$  would be to use  $T_{mean}$  as the predictor variable. For our dataset, mean SST and maximum SST are positively correlated ( $R^2 = 0.78$ ,  $p < 0.001$ ,  $n = 169$ ) where  $T_{max} = (1.264 * T_{mean}) - 1.916$ .

### Mean salinity ( $S_{mean}$ )

The best model for mean salinity included significant covariates for shore type and two landscape variables including log-transformed water depth adjacent to the nearshore ( $LnMeanGSU\_depth$ ) and log-transformed distance from nearest large river ( $LnN\_LgRivKm$ ) ( $R^2 = 0.82$ ,  $n = 169$ , Table C1)

Pairwise analysis revealed that large river estuaries are over nine PSU fresher than all other shore types after controlling for landscape covariates (Table C2). Model coefficients for each shore type (relative to sediment source beaches) were:

- Barrier beach = 2.754
- Estuary, large river type = -9.786
- Estuary, pocket estuary type = -0.702
- Pocket beach = 2.384
- Rocky beach = 3.673
- Sediment source beach = 0.000
- Constant = 12.460

Mean salinity was positively correlated with large river estuaries and water depth adjacent to the nearshore (Table C3, Figure 19D-F). Deeper water adjacent to the shoreline yields saltier nearshore surface water. Shorelines more distant from their nearest large river were also saltier than shorelines closer to their nearest large river. Similar to SST, these relationships appear to vary significantly across shore types suggesting that some shore types may be more susceptible changes in freshwater inputs under future climate change (Figure 19D-F).

We used the regression results from the best model to predict mean salinity for each  $GSU\_ID$ . The equations by shore type are:

- Barrier beaches =  $2.754 + LnMeanGSU\_depth \times 0.934 + LnN\_LgRivKm \times 3.573 + 12.460$
- Estuary, large river type =  $-9.786 + LnMeanGSU\_depth \times 0.934 + LnN\_LgRivKm \times 3.573 + 12.460$

- Estuary, pocket estuary type =  $-0.702 + LnMeanGSU\_depth \times 0.934 + LnN\_LgRivKm \times 3.573 + 12.460$
- Pocket beach =  $2.384 + LnMeanGSU\_depth \times 0.934 + LnN\_LgRivKm \times 3.573 + 12.460$
- Rocky beach =  $3.673 + LnMeanGSU\_depth \times 0.934 + LnN\_LgRivKm \times 3.573 + 12.460$
- Sediment source beach =  $0 + LnMeanGSU\_depth \times 0.934 + LnN\_LgRivKm \times 3.573 + 12.460$

There was a significant difference in *Smean* between pocket estuaries with or without direct freshwater sources ( $p = 0.008$ ). Pocket estuaries with direct freshwater inputs were on average 9.9 PSU lower in salinity than pocket estuaries without direct freshwater inputs (Figure C2). Therefore, we applied an adjustment to the mean salinity predictions based on the presence of local freshwater inputs to the nearshore to improve mean salinity accuracy for pocket estuaries. Specifically, we subtracted 9.9 from the mean salinity prediction for pocket estuaries with freshwater inputs. GSU\_IDs with freshwater inputs were derived from the SSHIAP geomorphic layer (i.e., McBride et al. 2009) where presence of a freshwater input was a data category.

Table C1. Performance of nearshore mean salinity models. All models shown, along with the included factors and/or covariates, are significant ( $p < 0.05$ ). The presence of an ‘x, t, or u’ means that a factor or covariate was included in the model. The presence of a ‘t’ or ‘u’ denotes the covariate was natural log-transformed or untransformed, respectively. The best model has the lowest AICc value and is in bold font.

Shore type	Water depth adjacent to the nearshore	Distance of nearest large river	Distance to Strait of Juan de Fuca entrance	R <sup>2</sup>	AICc	ΔAICc
<b>x</b>	<b>t</b>	<b>t</b>		<b>0.8</b>	<b>1032</b>	<b>0</b>
x		t		0.81	1037.3	4.862
x	t		t	0.89	1061.9	29.478
x			t	0.78	1067.2	34.775
	t	t		0.74	1085.6	53.193
x	t			0.77	1097.4	64.997
x				0.72	1101.5	69.053
		t		0.66	1125.8	93.401
	t		t	0.58	1167.1	134.667
	t			0.39	1226.1	193.653
			t	0.38	1229.5	197.062

Table C2. Pairwise testing of mean salinity (*Smean*) by shore type using Tukey's Honestly-Significant-Difference Test using least squares means from the model results with a MSE of 24.689 with 161 df. Pairs with p-values < 0.05 are bolded.

SHORE_TYPE(i)	SHORE_TYPE(j)	Difference	p-value	Lower 95% CI	Upper 95%CI
<b>BB</b>	<b>E-LR</b>	<b>12.541</b>	<b>0</b>	<b>9.2</b>	<b>15.84</b>
BB	E-PE	3.456	0.119	-0.3	7.25
BB	PB	0.37	1	-3.3	4.026
BB	RB	-0.919	0.998	-6.9	5.024
BB	SSB	1.078	0.963	-2.6	4.799
<b>E-LR</b>	<b>E-PE</b>	<b>-9.085</b>	<b>0</b>	<b>-13</b>	<b>-5.637</b>
<b>E-LR</b>	<b>PB</b>	<b>-12.17</b>	<b>0</b>	<b>-15</b>	<b>-8.875</b>
<b>E-LR</b>	<b>RB</b>	<b>-13.46</b>	<b>0</b>	<b>-19</b>	<b>-7.731</b>
<b>E-LR</b>	<b>SSB</b>	<b>-11.463</b>	<b>0</b>	<b>-15</b>	<b>-8.095</b>
E-PE	PB	-3.086	0.283	-6.9	0.708
E-PE	RB	-4.375	0.363	-10	1.654
E-PE	SSB	-2.378	0.547	-6.2	1.478
PB	RB	-1.289	0.99	-7.2	4.654
PB	SSB	0.708	0.995	-3	4.428
RB	SSB	1.997	0.937	-4	7.98

Table C3. ANOVA landscape covariate results for *Smean* for all shore types. P-values significant at the 0.05 level are bolded.

Variable type	Variable	Coefficient	p-value
	<b>LnMeanGSU_DEPTH</b>	<b>0.934</b>	<b>0.009</b>
Covariate	<i>LnN_LgRivKm</i>	<b>3.573</b>	<b>&lt;0.001</b>

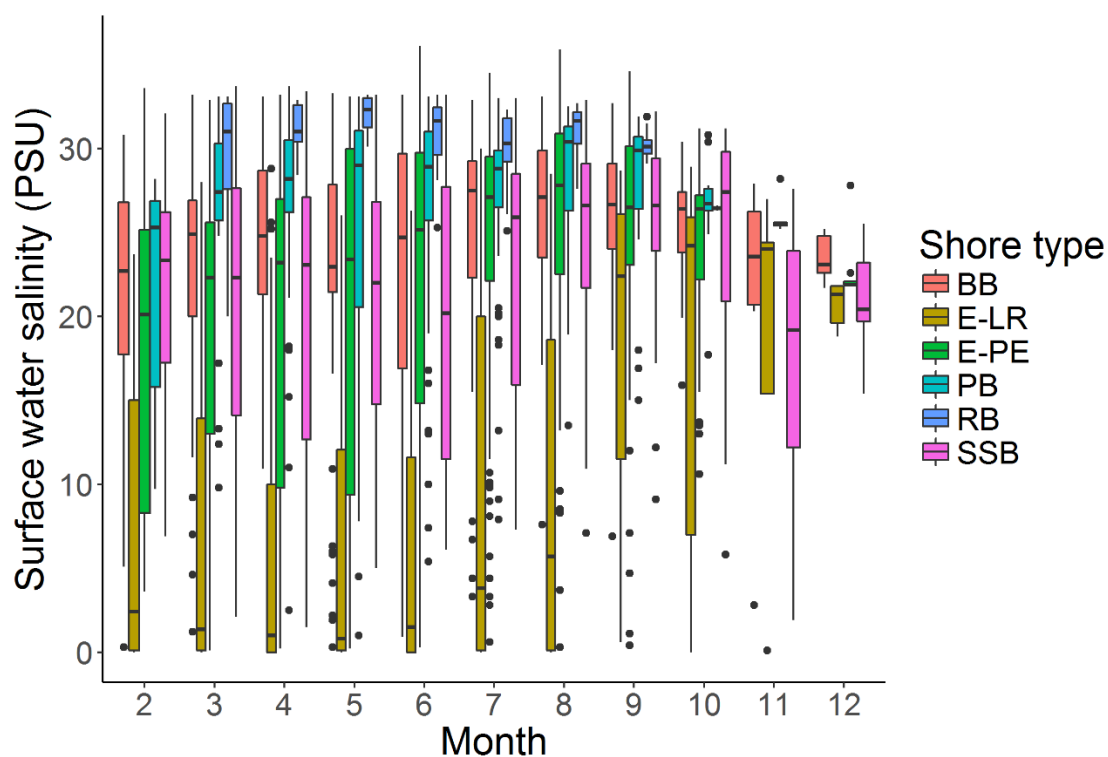


Figure C1. Boxplots of surface water salinity (PSU) by month and geomorphic shore type. Data are from 6,872 observations collected at 173 sites across Whidbey Basin, Bellingham and Samish Bays, and the San Juan Islands. Shore type abbreviations are: BB = barrier beach; E-LR = estuary, large river type; E-PE = estuary, pocket estuary type; PB = pocket beach; RB = rocky beach; SSB = sediment source beach. Boxes show median, 25th and 75th percentiles. Whiskers show the 5th and 95th percentiles, circles are outliers.

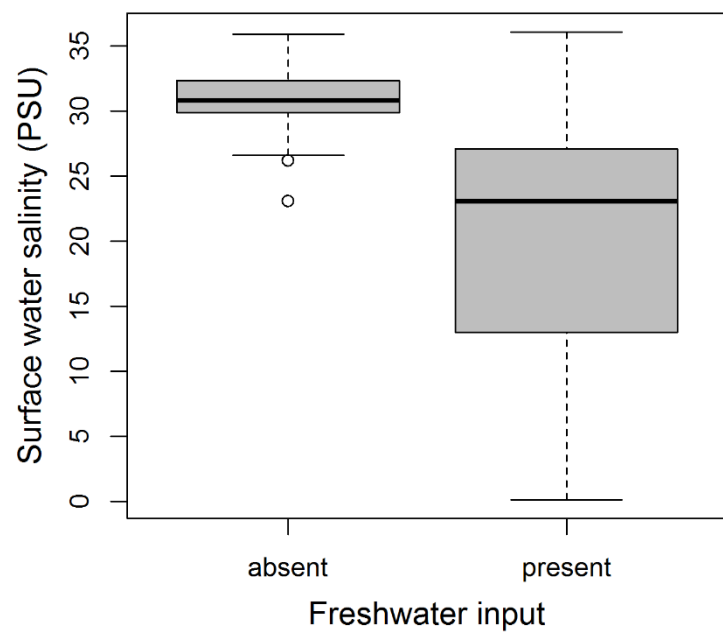


Figure C2. Boxplot of annual nearshore surface water salinity (*S<sub>mean</sub>*) in PSU by pocket estuaries with or without direct freshwater sources. Boxes show median, 25th and 75th percentiles. Whiskers show the 5th and 95th percentiles, circles are outliers.

### Maximum seasonal salinity (*S<sub>max</sub>*)

The best model for maximum salinity for all shore types included covariates for shore type and landscape variables including log-transformed water depth adjacent to the nearshore (*LnMeanGSU\_depth*) and log-transformed distance from nearest large river (*LnN\_LgRivKm*) ( $R^2 = 0.75$ ,  $n = 169$ , Table C4).

Table C4. Performance of nearshore maximum salinity models. The presence of an 'x, t, or u' means that a factor or covariate was included in the model. The presence of a 't' or 'u' denotes the covariate was natural log-transformed or untransformed, respectively. The best model has the lowest AICc value and is in bold font.

Shore type	Water depth adjacent to the nearshore	Distance to nearest large river	Distance to Strait of Juan de Fuca entrance	$R^2$	AICc	$\Delta AICc$
<b>x</b>	<b>t</b>	<b>t</b>		<b>0.750</b>	<b>1092.005</b>	0.000
x		t		0.744	1093.217	1.212
x	t		t	0.690	1127.870	35.865
x			t	0.684	1129.289	37.284
x	t			0.682	1130.029	38.024
x				0.675	1131.443	39.438
	t	t		0.648	1138.772	46.767
		t		0.592	1160.414	68.409
	t		t	0.414	1224.914	132.909
	t			0.321	1247.549	155.544
			t	0.227	1269.506	177.501

### Minimum seasonal salinity (*S<sub>min</sub>*)

The best model for minimum salinity for all shore types included the factor ‘shore type’ and two significant landscape variables including log-transformed water depth adjacent to the nearshore (*LnMeanGSU\_depth*) and log-transformed distance from the entrance to the Strait of Juan de Fuca (*LnDistSjfkKm*) ( $R^2 = 0.66$ ,  $n = 169$ , Table C5).

Table C 5. Performance of nearshore minimum salinity models. All models shown, along with the included factors and/or covariates, are significant ( $p < 0.05$ ). The presence of an ‘x, t, or u’ means that a factor or covariate was included in the model. The presence of a ‘t’ or ‘u’ denotes the covariate was natural log-transformed or untransformed, respectively. The best model has the lowest AICc value and is in bold font.

Shore type	Water depth adjacent to the nearshore	Distance to nearest large river	Distance to Strait of Juan de Fuca entrance	R <sup>2</sup>	AICc	ΔAICc
<b>x</b>	<b>t</b>		<b>t</b>	<b>0.663</b>	<b>1138.797</b>	0.000
x			t	0.651	1142.254	3.457
x	t	t		0.650	1144.918	6.121
x		t		0.641	1147.059	8.262
	t	t		0.602	1155.733	16.936
	t		t	0.569	1169.317	30.520
		t		0.535	1179.967	41.170
x	t			0.538	1189.853	51.056
x				0.525	1192.025	53.228
			t	0.428	1215.046	76.249
	t			0.329	1242.101	103.304

### Limitations in sea surface salinity predictions

We compared the predictions of mean sea surface salinity to the original observations (Figure C3). The predictive power of sea surface salinity models was somewhat limited. Specifically, the sea surface salinity model predicted the upper ( $> 28$  PSU) and lower ( $< 1$  PSU) range of observed salinities well but under-predicted approximately 1/3 of the observed salinities within 15-25 PSU range by approximately 10 PSU, suggesting that additional processes not captured in our model (e.g., instantaneous flow) may affect sea surface salinity. To improve salinity predictions, we recommend the following to improve future models: 1) break the largest GSU-ID polygons into smaller polygons to better reflect landscape variability (see temperature model prediction discussion) and 2) include daily or seasonal discharge of the nearest large river as an independent variable.

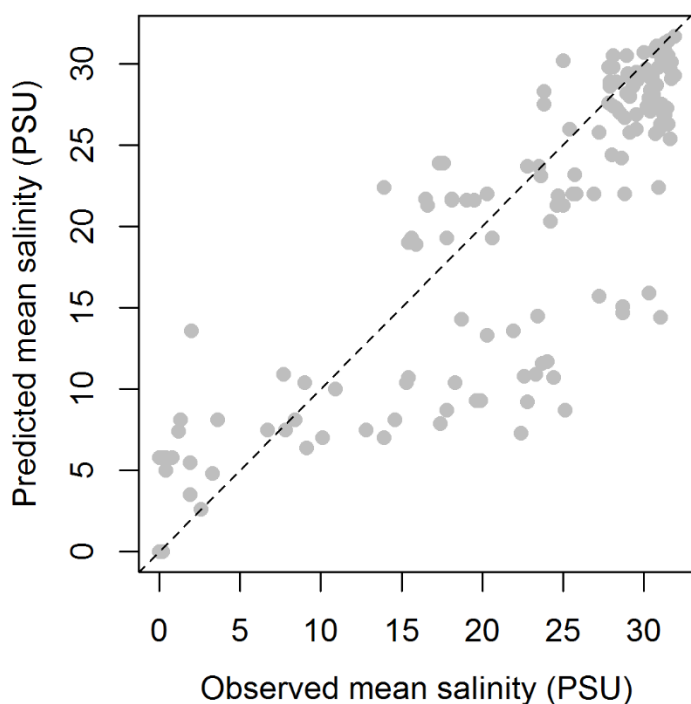


Figure C3. Relationship between observed and predicted mean sea surface sea surface salinity for 169 nearshore surface water sites located throughout the Whidbey Basin, Bellingham and Samish Bays, and the San Juan Islands.

### Future model applications

Our results show that the proximity of a site to large rivers influences mean salinity for all shore types and that the presence of direct freshwater inputs to the pocket estuary shore type results in significantly reduced salinity (see earlier sections of Appendix C). But we were also interested in determining if we could describe predictors for various salinity metrics beyond using mean or maximum salinity values. If we could describe plausible predictors, we could address broader questions about our ability to link climate change predictions to changes in nearshore salinity in ways that are likely to be biologically-relevant to fish and shellfish species. Using data from an area located in Skagit Bay with three shore types, we tested our ability to predict landscape-scale nearshore salinity beyond annual mean or maximum value (E. Beamer, unpublished data). We found that model predictions may be possible by linking the shore type and landscape variables with daily or seasonal values for hydrology. Results such as this should be informative in linking climate change predictions for stream flow to changes in nearshore salinity in such a way to be biologically-relevant to fish and shellfish species (e.g. useful applications for Table 10).